DISSERTATION

EARLY PERIPHERAL IMMUNOLOGICAL EVENTS DICTATE CHRONIC WASTING DISEASE

Submitted by

Brady Michel

Department of Microbiology, Immunology, and Pathology

In the partial fulfillment of the requirements

For the degree of Doctor of Philosophy

Colorado State University

Fort Collins, Colorado

Spring 2013

Doctoral Committee:

Advisor: Mark Zabel

Ed Hoover
Steve Dow
Eric Ross

ABSTRACT

EARLY PERIPHERAL IMMUNOLOGICAL EVENTS DICTATE CHRONIC WASTING DISEASE

Chronic wasting disease (CWD) is an emerging prion disease of captive and free-ranging cervid populations that, like scrapie, has been shown to involve the immune system, which most likely contributes to their relatively proficient horizontal and environmental transmission. While CWD prions probably interact with the innate immune system immediately following peripheral exposure, little is known about this initial encounter. In the first chapter of this dissertation we examined initial events in lymphotropic and intranodal prion trafficking by tracking highly enriched, fluorescent CWD prions from infection sites to draining lymph nodes. We observed biphasic lymphotropic transport of prions from the initial entry site upon peripheral prion inoculation. CWD prions rapidly reached draining lymph nodes in a cell autonomous manner within two hours of intraperitoneal administration. Monocytes and dendritic cells (DCs) showed a strong dependence on Complement for optimal prion delivery to lymph nodes hours later in a second wave of prion trafficking. B cells comprised the majority of prion-bearing cells in the mediastinal lymph node by six hours. As most B cells are mainly located in the follicles, acquisition of prions by these cells most likely occurred through interaction with resident DCs, subcapsulary sinus macrophages, or directly from the follicular conduit system. These data highlight a novel mechanism of cell autonomous prion transport, and a vital role for B cells in intranodal prion trafficking.

Upon entry into the draining lymph nodes, prion accumulation and replication on follicular dendrtic cells (FDCs) is greatly facilitated by the complement system. Complete

elimination of CD21/35 significantly delays splenic prion accumulation and terminal prion disease in mice inoculated intraperitoneally with mouse-adapted scrapie prions. In the second chapter of this thesis we show that mice overexpressing the cervid prion protein and susceptible to CWD (Tg(cerPrP)5037 mice) but lack CD21/35 expression completely resist clinical CWD upon peripheral infection. Ablation of complement receptors CD21/35 greatly diminished splenic prion accumulation and replication throughout the course of disease, similar to CD21/35 deficient murine PrP mice infected with mouse scrapie. Mice with deficiencies in CD21/35 showed a reduction in severity of neuropathology and deposition of misfolded, protease-resistant PrP associated with CWD. Prion infection resulted in translocation of CD21/35 to lipid rafts in B cells, and FDC expression of CD21/35 mediated a strong germinal center response that may be conducive to prion amplification.

Complement component C3 is a central protein in the complement system whose activation is essential for the elimination of infectious pathogens. C3 is the most abundant complement protein, being found in the blood at physiological concentrations of 1 mg/ml. Among the complement proteins, C3 is perhaps the most adaptable and multifunctional protein identified to date, having evolved structural characteristics that allow it to associate with over 25 different proteins. Previous experiments suggest a vital role of C3 in scrapie prion pathogenesis. In the last chapter of my thesis we showed that lack of C3 expression by 5037 mice either transiently or genetically leads to delays in prion pathogenesis. C3 impacts disease progression in the early stages of disease by slowing the kinetic rate of accumulation and/or replication of PrP^{RES}. This slower kinetic increase in PrP^{RES} correlates with an increase in survival time in mice deficient in C3. This delay in disease is in sharp contrast to the complete rescue we saw in CWD infected Tg 5037;CD21$^{-/-}$ mice. This suggests a role for CD21/35 in peripheral prion pathogenesis independent of their endogenous ligands.

Taken together we show that the innate immune system dictates the course of CWD. We have discovered novel immune cells, trafficking pathways, and complement components important in CWD pathogenesis. These data not only highlight the key role of the innate immune system in CWD, but also provide a strong foundation for future immunological studies of prion diseases.

ACKNOWLEDGEMENTS

Many people contributed to the work described in this dissertation and I am very grateful to all of them. I gratefully acknowledge the assistance and support of Theodore Johnson and Adam Ferguson. Their dedication and technical support allowed for the successful progress in these projects. I would also like to acknowledge Christy Wyckoff, Crystal Meyerett-Reid, Bruce Pulford, Heather Bender, and Britta Wood for their helpful advice and discussion of the projects and data. I am grateful to everyone in the CSU Prion Research Center, but would like to recognize the Veternarian Diagnostic Laboratory for processing animal tissues for immunohistochemistry. I would like to thank Elisa French and the CSU Laboratory Animal Resources staff.

My PhD committee has been very supportive throughout my graduate career. Ed Hoover, Steve Dow, and Eric Ross have provided me with great ideas and valuable guidance throughout my studies. I would especially like to thank my advisor Mark Zabel. Mark has not only been a great PI, but also a great mentor. Mark has given me the proper scientific tools to excel in the scientific community. He is the epitome of a great scientist, and personifies class. I can only hope to be as good of a scientist and role model as him.

DEDICATION

I would like to dedicate this work to my fiancé Jaime Breed. She has provided loving support and great enthusiasm throughout these studies. I would also like to thank my parents Tom and Sally, who encouraged me to go to college and fulfill my dream of being a successful scientist. Without there love and support none of this would have been possible.

TABLE OF CONTENTS

CHAPTER 1:

INTRODUCTION

Prion disorders, also known as transmissible spongiform encephalopathies (TSEs), are a set of unique neurodegenerative disorders that affect a wide range of mammalian species [1]. According to the widely accepted "protein only" hypothesis, prions are composed mainly, if not solely, of PrP^{Sc}, an abnormal isoform of the host glycoprotein, PrP^{C} [2]. Transmission and propagation of PrP^{Sc} occur through a process of seeded polymerization, in which PrP^{C} is recruited into PrP^{Sc}, adopting its abnormal conformation [3,4]. While PrP^{C} and PrP^{Sc} both appear essential in disease replication and transmission, the roles each play in cellular function and neurodegeneration remain unclear.

Chronic wasting disease (CWD) is a prion disease that affects both captive and free ranging cervids [5-7]. CWD is unique among TSEs in that it seems to be the most contagious prion disease, transmitting in natural settings with high efficiency. Recently, increased surveillance across the United States revealed incidents of CWD in states where hunting big game is extremely popular [6]. This finding raises legitimate concerns about the transmissibility of CWD to humans, as typified by the zoonotic transmission of bovine spongiform encephalopathy (BSE) [8,9]. Although there is no direct evidence of CWD transmission to humans, the staggering rise in CWD cases in the United States underscores a need for a better understanding of this disease.

As with other TSEs, CWD exhibits a strong correlation between inflammatory responses and neurological abnormalities. Although these neurological inflammatory events are of grave importance, it may be that the initial events in a CWD infection dictate the outcome of disease progression. These inaugural events seem in most cases to involve the peripheral immune system [10,11]. Although numerous experiments provide great insight into the immunological events that precede neuroinvasion, many questions still remain on the nature of this response and the cells involved. Within this context, we sought to characterize the early immunological events involved in the development of CWD.

Gaining crucial insight into the immunological events in CWD may have far reaching implications in our understanding of other protein misfolding diseases. For example, it is well known that non-prion protein misfolding disorders, such as Alzeimer's disease and Parkinson's disease, mirror certain morphological and pathophysiological features seen in prion disorders [12]. With this in mind, it seems reasonable to think that prion diseases may represent a general model for amyloidogenic disorders in their ability to elicit an immune response, replicate, and transmit disease. Therefore, advances in our knowledge of prion diseases may not only provide critical insight into other protein misfolding disorders, but may also provide critical therapeutic interventions and preventative measures necessary for control of these devastating diseases.

PrP^C structure

As revealed by nuclear magnetic resonance (NMR) and gene sequencing, the amino acid sequence and atomic structure of mature PrP^C is highly conserved between mammalian species [13-15]. Mature PrP^C is a glycosyl phosphatidyl inositol (GPI)-linked glycoprotein composed of a highly flexible NH2-proximal tail proceeded by a well-defined globular COOH-proximal domain (Figure 1). Although the NH2-terminal region is disordered, it contains a highly conserved octapeptide-repeat region. This region has been shown to bind divalent cations Cu^{2+}, Zn^{2+}, Ni^{2+}, and Mn^{2+} [16-19]. The COOH-globular domain consists of three alpha helices corresponding to residues 144-154, 173-194, and 200-228. Interspersed within these alpha helices are two antiparallel β-strands, which make up residues 128-131 and 161-164. A disulfide bond, C179-C214, join helices 2 and 3, while the second β-strand and α-helix are linked by a large loop with intriguing structural properties [13-15,20]. Analysis by NMR shows this loop to be extremely flexible in most species, including humans, bovine, sheep, mouse, and hamsters, but it is almost completely inflexible in the prion protein of elk and deer [15,20-23]. The importance of this rigid β2–α2 loop of PrP may extend beyond structural–biological curiosity. Some hypothesize that this rigid loop my influence other properties of PrP such as PrP^{Sc} conversion and transmission [24]. Interestingly, Sigurdson *et al.* postulates that similarities in the local structure of β2–α2 loop might be an essential element of interspecies transmission efficiency [25].

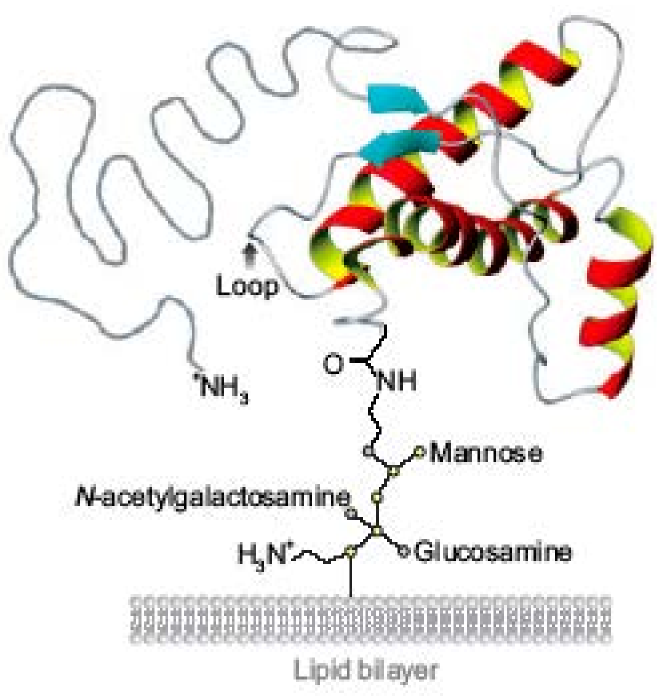

Figure 1.1 Aguzzi A, Sigurdson C, Heikenwaelder M. Molecular mechanisms of prion pathogenesis. *Annu. Rev. Pathol.* **3**, 11-40 (2008).

PrP physiological function

Although advances towards the characterization of PrP^C structure have been made, the physiological function of PrP^C remains controversial [26]. To date, there is no evidence that a naturally occurring *Prnp*-null allele exists in any mammalian species. This lack of *Prnp*-null allele, coupled with the broad and diverse expression of PrP^C in the CNS and many of the peripheral organs implies a highly conserved and broad physiological function [27]. Several functions have been ascribed to PrP^C, including functions in neuronal survival, cellular signaling, immune cell activation, and as a pattern recognition receptor (PRR) for misfolded proteins [28-36]. Insight into these physiological functions will have profound influence on the way scientists approach prion research.

Apoptosis

Neuroprotection against apoptosis may be the most attributed function of PrP^C. Cultured $Prnp^{-/-}$ neurons were suggested to be more prone to develop apoptosis during serum-deprivation than were cells expressing PrP^C [28]. Albeit an interesting observation, some researchers attributed this effect to dopple (Dpl) overexpression rather than PrP ablation [37]. Doppel, a protein encoded by the gene *Prnd*, shows similarities to PrP^C in amino acid sequence, primary structure, and subcellular localization [38]. Although dopple appears to show many biochemical similarities PrP^C, it's overexpression in the brain has been shown to be deleterious in certain PrP deficient mice[39-41]. Other studies suggest that PrP^C offers a cytoprotective function to cells against harmful agents. This hypothesis is supported by the finding that PrP^C diminishes the rate of apoptosis caused by certain apoptotic stimuli such as Bax overexpression or TNF-α [42,43].

It has been shown that artificially generating cytosolic PrP in neurons induces cell death [44]. However, several other studies argue against this neurotoxicity and showed a more cytoprotective role of cyPrP. Data from these studies suggested that cyPrP might function as an anti-apoptotic protein against Bax-mediated apoptosis by inhibiting the Bax proapoptotic conformational changes that takes place initially in Bax activation [45,46]. PrP^C also exerts its cytoprotective function against TNF-α in a human MCF-7 breast cancer cell line [43]. In this experiment it was demonstrated that PrP^C overexpression transformed TNF-sensitive MCF-7 cells into TNF-resistant cells. It was speculated that the mechanism of transformation involved alteration of cytochrome *c* release from mitochondria and nuclear condensation.

Role in cell signaling

Attachment to the plasma membrane by a GPI anchor and localization in lipid rafts has made PrP^C an ideal candidate for signal transduction. PrP^C has shown an ability to regulate many signaling components and pathways involved in neuronal survival; therefore, PrP^C has been suggested to function as a trophic receptor [30,47-49]. Signal transduction pathways triggered by PrP^C, through antibody crosslinking or PrP binding peptides, has been partially characterized and is mediated by tyrosine kinase p59fyn and cAMP/PKA-dependent pathways [30,49]. Some groups have suggested that interaction of PrP^C with membrane proteins can also transduce neuroprotective signals. Stress-induced protein I (STI1) co-immunoprecipitated with PrP^C, and interaction of PrP^C with this molecule induced neuroprotective signals through camp/protein kinase A and Erk signaling pathways [47]. This interplay between PrP and STI1 produced distinct signaling pathways, promoting neuroprotection and neuritogenesis by activation of PKA and MAPK pathways respectively [48].

Role in the immune system

Several studies have suggested that PrP^C may exert its physiological function in the early stages of immune cell development. PrP^C has been detected on $CD34^+$ hematopoietic stem cells

(HSCs) [50]. This PrP^C expression seems to be transient, as differentiation into $CD15^+$ granulocytes leads to PrP^C down regulation. Similarly, $CD43^+$Gr-1 granulocyte precursors transiently express PrP^C before differentiating into neutrophils [51]. Although the role of this transient expression of PrP^C remains unknown, it seems reasonable to suggest that it may play a role in development of certain myeloid lineages. Using affinity purification techniques and bone marrow transplantation experiments, PrP^C expression by HSCs has recently been shown to be important in self-renewal [52]. Although the molecular mechanism of this self-renewal is not known, the authors suggest that PrP^C might be a coreceptor for a hormone that affects HSC activity.

PrP^C's physiological role may extend beyond immune cell development. PrP^C can be detected on T and B lymphocytes, plateletes, monocytes, DCs, FDCs, and NK cells [32,35,50,53-58]. The role of PrP^C expression by these immune cells has not been fully elucidated; however, several studies suggest that PrP^C may function in immune cell activation. PrP^C expression by T lymphocytes was upregulated within hours following mitogenic activation with concanavalin A (ConA), phytohaemagglutinin (PHA), or anti-CD3 antibodies [32-35]. As mentioned above, PrP may function as a signaling molecule; therefore, this upregulation of PrP by these immune cells may lead to interactions with specific ligands that results in signal transduction. Indeed, antibody induced PrP cross-linking on T lymphocytes led to phosphorylation of signaling proteins ERK1/2 and Src family kinases [59-61]. Similar results could be seen in a monocyte/macrophage cell line treated with PrP^C fusion proteins [62]. Although these experiments identify a plausible role of PrP^C in immune cell activation and signaling, it has yet to be seen whether these events have any real affect on prion pathogenesis.

PrP^C's role in Alzheimer's disease

Recently several studies have implicated PrP^C as a receptor for other abnormally folded proteins [36]. In Alzheimer's disease (AD), accumulation of amyloid-β (Aβ) is thought to be responsible for dementia and neurodegeneration. Tiny, soluble aggregates of Aβ hinder memory by disturbing memory-related functions of synaptic junctions between neurons [63,64]. It has been suggested that PrP mediates these pathogenic effects by binding to Aβ. Indeed, treatment of normal hippocampal slices with Aβ inhibited long-term potentiation (LTP) compared to hippocampal slices lacking PrP^C, and this effect was mediated by Aβ binding to amino acids 95-110 on PrP^C [36]. Recently these same authors crossed familial AD transgenes into PrP deficient mice to address the need of PrP for AD-related pathogenesis in vivo [65]. AD transgenic mice lacking PrP^C, but containing Aβ plaques derived from AD transgenes, showed no noticeable impairment of spatial learning and memory. These data indicate the requirement for PrP^C in Aβ induced memory impairment.

Although binding of PrP^C to Aβ oligomers is thought to trigger Alzheimer's disease pathophysiology, the molecular mechanisms underlining this toxicity remains unknown. N-methyl-D-aspartate receptors (NMDAR) are a key ionotropic glutamate/glycine receptor in the CNS that plays a critical role in development, memory, and learning [66,67]. Alterations in this receptor have been shown to contribute to AD pathogenesis [64,68,69]. Some scientists hypothesize that Aβ-PrP^C complexes modify NMDARs through a phosphorylation event mediated by Fyn signaling. Indeed, Aβ binding to PrP^C activated a Fyn signaling pathway that led to NR2B phosphorylation, altered NMDAR localization, and loss of dendritic spines [70].

Other scientists provide evidence that Aβ neurotoxicity might depend on interactions between copper ions, PrP^C, and NMDARs [71]. Here it is suggested that under normal physiological conditions, PrP^C forms a complex with NMDAR in a copper-dependent manner to reduce glycine affinity for this receptor. This desensitization of NMDARs to glycine by PrP^C protects neurons from calcium overload and neuronal toxicity. However, under certain pathological states of excessive Aβ production, Aβ functions as copper chelator, precluding copper ions from binding to PrP^C. This lack of binding of copper ions to PrP^C in turn alters the ability of PrP^C to regulate NMDAR desensitization and/or causes separation of the two proteins. Ultimately Aβ sequestration of copper ions leads to an increase in glycine affinity, resulting in prolonged steady-state current and pathological calcium influx.

These findings have come with great excitement and skepticism. Although it is tempting to extrapolate these findings towards real AD, one should do so with extreme caution as several findings conflict with the results mentioned above. Indeed, Balducci *et al.* has shown that synthetic Aβ oligomers impedes long-term memory independently of cellular PrP^C [72]. Using a second, independent AD transgenic mouse model, Calella *et al.* showed that removal or overexpression of PrP^C has no effects on the impairment of hippocampal synaptic plasticity [73].

Ever since the identification of the *Prnp* gene in 1986 and the subsequent development of *Prnp* knockout mice in 1992, research into the physiological function of PrP^C has intensified [74,75]. Despite being a central player in the development of prion disease, PrP^C has failed to show any definitive molecular function. As mentioned above, several functions can be attributed to PrP^C; however, further understanding into these physiological functions is needed to establish a peripheral therapeutic strategy.

Development of the protein only hypothesis

Tikvah Alper and colleagues first described the agent that causes TSEs through experiments that elegantly showed that PrP^{Sc} infectivity is resistant to inactivation by UV and ionizing irradiation [76,77]. These findings led to a plethora of hypotheses on the chemical make up PrP^{Sc}, including the prophetic notion by John Griffith in 1967 that PrP^{Sc} may be composed of self-replicating protein [78]. Later it was shown that a reduction in infectivity could be achieved if purified fractions of scrapie, derived from hamster brain, were treated with procedures that alter or denature protein structure [79-82]. These findings, along with the inability to show a dependence on an infectious scrapie-specific nucleic acid led Stanley Prusiner to proclaim the infectious agent a prion, which is presently defined as a small protienacious infectious particle that resists treatments that modify nucleic acids [2].

While a wealth of scientific evidence gathered over the past decade provides substantial support for the prion hypothesis, observed *in vitro* refolding of synthetic or bacterially derived PrP into an infectious conformation would be the final proof of the protein only hypothesis. Developments in the use of transgenic mice, synthetic and recombinant PrP (recPrP), and protein misfolding cyclic amplification (PMCA) have provided significant advancement toward achieving this goal.

Initial attempts to create prions in the laboratory laid the foundation for recent advances in the validation of the protein only hypothesis. The use of Tg mice greatly facilitates this progress by showing a tight genetic linkage of inherited prion diseases to the *Prnp* gene. Nowhere is this genetic linkage more apparent than in Tg(GSSPrP)174 mice. These Tg mice express PrP with a Pro100Leu mutation, which corresponds to the mutation that causes Gerstmann-Straussler Scheinker syndrome (GSS) in humans. High-level expression of this transgene results in neurodegeneration, with disease onset times that correlate with the level of expression [83].

Similar to Tg(GSSPrP)174 mice, Tg196 mice also express the PrP(Pro101Leu) transgene. However, Tg196 mice express much lower levels of this transgene and were used as a model to help produce evidence that prions can be artificially generated in the absence of an infectious seed. Disease acceleration or initiation in these mice can be achieved through the inoculation of a chemically synthesized 55-mer peptide that was folded into a beta-rich conformation containing the Pro101Leu mutation [84]. Similar results are shown in Tg9949 mice, which overexpress N terminally truncated mouse PrP (PrP(89-231)). When amyloid fibrils consisting of recMoPrP(89-230) were inoculated into these mice, a progressive neurological dysfunction was observed [85]. These data show that a chemically synthesized peptide refolded into the right conformation can act as an infectious agent that causes TSEs.

Although the use of Tg mice, synthetic PrP, and recPrP represents a major step forward, some argue that essential issues emerge in the interpretation of these experiments [86]. First, prions created de novo in Tg(GSSPrP)174 mice only infect mice expressing the identical mutation at lower levels (some of which develop spontaneous disease later in life). Second, primary passage of infectivity to Tg9949 mice requires these mice to over express PrP^{C} by 16 fold. Another interpretation of these results is that these Tg mice are predisposed to develop spontaneous prion disease, and that onset of disease in these mice represents a disease acceleration process, due to the inoculation of further PrP [86]. Therefore, the term “transmissibility” may be unsuitable for this disease acceleration process [87].

This begs the question of whether these experiments actually produce prions. Some contend that these scientists simply created an agent that triggered prion production in a host that, due to the high levels of PrP^{C} expression, is on the verge of developing spontaneous disease [86]. Although a valid point, recent data demonstrates that brain homogenates derived from uninoculated aged Tg9949 mice show no evidence of prions by biochemical analysis, histological analysis, or by serial transmission of their brain homogenates. This indicates that prions were indeed generated in a cell free system and not just in the host [88].

Recently, a more ideal mouse model has been generated that gives the strongest case yet that PrP misfolding induced by mutations and associated with genetic prion diseases is sufficient to create prions in vivo. Jackson *et al*. created knock-in mice to express a PrP mutation, which correlates with a well-defined human prion disease, fatal familial insomnia (FFI) [89]. These mice spontaneously develop prion disease different from that of other mouse prion models and very similar to FFI in humans. Although similar results were found in Tg(GSSPrP)174 mice, the knock-in FFI mice offered several key advantages over Tg(GSSPrP)174 mice. First, with a knock-in model FFI mutations are introduced into the *Prnp* locus. This is crucial because it assures that the allelic modifications will continue to be governed by all of the regulatory elements that typically control the expression pattern of PrP. Second, an additional substitution was introduced in these mice to create a strong transmission barrier against prions that already exist. This additional mutation was important because it made these mice highly resistant to infection with pre-existing prions, which enabled the authors to conclude that infectivity in these mice did not arise from a contaminating agent [89].

In addition to describing infectivity, the protein only hypothesis also needs to explain the phenomenon of prion strains. Through altering pH, temperature, the length of recPrP constructs, and using varying concentrations of urea, Colby *et al.* made it possible to design and construct various prion strains [90]. When these recPrP amyloids were inoculated into mice that overexpress full-length PrP^C, the incubation periods and the resulting prion strains relied on the conformational stability of the recPrP amyloid from which they were derived from. This correlation between disease phenotype and amyloid conformational stability strongly indicates that synthetic prions originated from recombinant amyloid preparations, and not from host or contamination. These results led some to believe that if prions had arisen spontaneously in these mice, then the autonomous properties of these strains would be enough to distinguish them from the amyloid properties [91]. As powerful as these results may be, the inability to infect wild-type mice on primary passage left some to doubt whether these artificially generated peptides are indeed prions. Others argue that the inability to infect wild-type animals is not a question of whether these peptides are prions, but rather a consequence of low titers of infectivity or the lack of nonproteinaceous phospholipids and RNA [86,92].

The use of PMCA resolves the issues of low infectious titers and lack of cofactors. PMCA is able to create new infectious PrP^{Sc} molecules by combining PrP^{Sc} with PrP^{c} and short bursts of ultrasound [93,94]. Using this technique, Soto and co-workers demonstrated that it is possible, through serial dilutions, to create new PrP^{Sc} in the absence of the original PrP^{Sc} used to seed the experiment [95]. This experiment not only supports the protein only hypothesis, but also shows that prions can be propagated in vitro indefinitely. As powerful as these results are, it is the spontaneous generation of infectivity by Supattapone and co-workers that led many to believe that PMCA could be used as a tool to generate prions de novo [96]. However, no one experiment supports the protein only hypothesis more than the one performed by Wang *et al.* [97]. This study elegantly demonstrates that highly infectious prions capable of infecting wild type mice could be generated from recPrP using PMCA in the presence of lipids and RNA. This experiment also implies that cofactors likely aid in the production of prions with relatively high specific infectivity. Future research will need to address whether these cofactors are vital parts of an infectious protein complex, or just simply catalyze the formation of prions from PrP^{C}.

Prions and Their Role in Neurodegeneration

One question that has puzzled researchers over the past two decades is "how do prions cause neurodegeneration?" Despite substantial knowledge about the characteristics of prions, this question remains shrouded in mystery. Several models have been put forth that may explain the neurodegeneration seen at terminal disease. These models include direct toxic activity by PrP^{Sc}, alteration in PrP^{C} signaling, PrP^{C} mislocalization, and the creation of a PrP-derived oligomeric species. With the ability to transmit infection, arise sporadically, or be inherited as an autosomal dominant condition, prions may exert their neurotoxicity through a multitude of mechanisms depending on how one acquires the disease. Whatever the case, understanding the mechanism by which prions cause neurodegernation is vital in our understanding of prion diseases.

Direct Toxicity of PrP^{Sc}

The development of PrP^{C} deficient mice greatly facilitated our knowledge of prion-mediated toxicity. Early models proposed that it was a loss of function that facilitated the process of neurodegeneration; however, mice deficient in PrP^{C} remain relatively healthy and it was speculated that a related or different protein adopts the missing prion protein within the cell, or that the function is redundant [98]. This finding rules out neuronal toxicity due to PrP^{C} loss of function. A more accepted idea is that PrP^{Sc} is directly neurotoxic. This idea is logically supported by the observation that other more common neurodegenerative disorders, such as Alzheimer's disease and Parkinson's disease, also feature cerebral accumulation of misfolded protein aggregates [99-101]. Although several lines of in vitro data show PrP^{Sc} to be directly neurotoxic [102,103], observations in vivo show this model to be too simplistic. There seems to be an inconsistency between the amount of PrP^{Sc} amyloids and the magnitude of brain damage and disease [83,104-106]. Furthermore, PrP^{C} deficient mice inoculated with scrapie show no signs of disease [74]. This finding is of particular interest because it implies that induction of neurotoxicity by PrP^{Sc} may depend on a PrP^{C} process. Support of this hypothesis was shown by an experiment in which neural tissue graphs overexpressing PrP^{C} were implanted into the brains of mice deficient in PrP^{C} [107]. Inoculation of these mice with scrapie prions resulted in a lack of clinical signs, despite histopathological changes in the grafted tissue, which were similar to scrapie inoculated wildtype mice. Interestingly pathology never spread into the recipient brain, despite the appearance of PrP^{Sc} in both graft and host tissue. This experiment clearly demonstrates the need for PrP^{C} in neurotoxicity, as the presence of a continuous source of PrP^{Sc} is insufficient to cause neuropathological changes in PrP^{C} deficient mice [107]. Similarly, suppressing the expression of neuronal PrP^{C} during an established prion infection will avert neuronal loss and prevent signs that are associated with disease [108,109]. This prevention of prion disease occurs even though the extraneuronal PrP^{Sc} accumulates to levels seen in terminally infected animals [108]. These findings show that it is the expression of PrP^{C}, not the extracellular deposition of PrP^{Sc}, that dictates the development of disease.

Aberrant PrP^{C} Signaling

Some hypothesize that it is not only the expression of PrP^{C} that is important in neurotoxicity, but also the localization of PrP^{C} within the plasma membrane. Transgenic mice expressing PrP lacking the GPI membrane anchor do not develop clinical signs when inoculated with scrapie prions [110]. This study is of particular interest because it implies that the PrP^{C} GPI anchor plays a critical role in the pathogenesis of prion diseases. With GPI-anchored molecules playing an important role in signal transduction, it has been hypothesized that transgenic mice deficient in GPI anchored PrP molecules lack the ability to send apoptotic signals when binding to PrP^{Sc} [110].

Indeed, antibody induced cross-linking of PrP^C leads to neuronal cell death [111]. Although this antibody induced neurotoxicity represents a plausible model in which PrP^{Sc} binding to PrP^C causes neurodegeneration, another laboratory failed to show similar results [112]. However, due to the structure and location of PrP^C, it seems reasonable that apoptotic signaling by PrP^C plays a critical role in prion pathogenesis.

Altered PrP^C Trafficking and Abnormal Topology

Another suggested mechanism by which PrP can mediate neurotoxicity is through aberrant trafficking of PrP from the ER to the cytoplasm. Here it is the normal cellular process of protein synthesis and degradation that may contribute to prion induced neurotoxicity. Protein synthesis, under normal circumstances, can occur through a co-translational process by which proteins are translocated into the ER lumen during biosynthesis [113,114]. While in the lumen, chaperones assist in folding of the protein. However in the event of misfolding, proteins are transported out of the ER lumen by a retrograde process marking the beginning of ER-associated degradation (ERAD) [115]. This process culminates in the polyubiquitination and degradation of the misfolded protein by the proteosome. It is this quality control mechanism within the ER that ensures fidelity of protein synthesis. Although this process is essential in maintaining PrP^C homeostasis, it has been shown that ERAD mediated transport of PrP peptides into the cytoplasm and PrP accumulation through inhibition of the proteasome leads to PrP^{Sc} formation and neurotoxicity [44,116]. Thus, this mechanism of protein quality control by the ER may have a negative effect on the cell as it leads to the toxic accumulation and aggregation of PrP in the cytoplasm.

Although ERAD may play an important role in (cyPrP)-induced neurotoxicity, other cellular mechanisms may contribute to the generation of cyPrP during neurodegernation. Indeed, Rane *et al.* describes a possible mechanism by which nascent PrP peptides bypass translocation into the ER lumen leading to their toxic accumulation in the cytoplasm [117]. In this model it is ER stress, due to PrP^{Sc} accumulation, that activates a "preemptive" quality control system (pQC). This system aborts PrP translocation into the ER lumen, allowing its degradation in the cytoplasm by the proteasome. It is this rerouting into the cytoplasm through translocation attenuation that reduces PrP entry into and misfolding within the ER lumen. This pathway of PrP rerouting represents a defense mechanism to inhibit nascent peptide entry into the ER lumen during a time when the ER's normal function is in jeopardy. However, during a TSE infection, chronic ER stress may cause a constant rerouting of PrP into the cytoplasm. Consequently this influx of PrP may overwhelm the proteasome thereby causing neuronal cell death [118].

In addition to aberrant trafficking, different topological forms of PrP^C are suggested to be involved in the development of prion disease. Although the majority of PrP^C is found at the plasma membrane attached by its GPI anchor, a minor population of PrP can also be found within the ER membrane. This population located within the ER comprises two transmembrane topologies, ${}^{Ctm}PrP$ and ${}^{Ntm}PrP$, which have either their COOH or NH2 terminus in the ER lumen, respectively [119, 120]. It is suggested that inefficiencies of translocation during PrP biosynthesis is responsible for the generation of these topological forms [120-122]. Interestingly, by using transgenic mice that express PrP mutations that alter the relative ratios of these topological isoforms, it was shown that ${}^{Ctm}PrP$ produce neurodegenerative changes in mice with features similar to that of a prion disease [123,124]. This finding may extend beyond the laboratory, as it is known that a specific mutation found in GSS causes an increase formation of ${}^{Ctm}PrP$ [123]. Thus the ability to form CtmPrP and NtmPrP intermediates could lead to neurotoxicity and the formation of prion disease.

Although the above models explain various phenomena observed in prion diseases, some argue that aberrant signaling, altered trafficking, and abnormal topology of PrP^C is challenged by the observation of subclinical infections [86]. Subclincal infections occur when prions from one species are inoculated into a second species. These carrier states are characterized by slow prion propagation, which eventually leads to titers of PrP^{Sc} seen in end stage clinical disease. It is these carrier states that have led some to hypothesize that it is the creation of a toxic PrP-derived oligomeric species during replication that is responsible for neurodegeneration [86]. This idea of small toxic oligomers is gaining great attention, as a growing number of scientists believe that it is these small aggregates that are the cause of other protein misfolding disorders [125].

Linking Prion Propagation Kinetics to Neurotoxicity

Some researchers suggest that a model of prion toxicity through the generation of toxic PrP oligomers, can account for these subclinical infections. This model of prion neurodegeneration links prion propagation kinetics to neurotoxicity [86]. It is hypothesized that during prion replication an intermediate form of the prion (PrPL) is created.

This model developed by John Collinge can be written as:

$$PrP^{Sc}+PrP^{C}\rightarrow PrP^{Sc}{:}PrP^{C}\xrightarrow{K_1} PrP^{Sc}{:}PrP^{L}\xrightarrow{K_2} PrP^{Sc}{:}PrP^{Sc}\rightarrow PrP^{Sc}+PrP^{Sc}$$

Here, PrP^L represents the toxic species, and the relative concentrations of PrP^L and PrP^{Sc} are controlled by the ratio of the initial rate of conversion (K_1) to the rate of maturation (K_2) [86]. This formula for prion neurodegeneration adequately explains subclinical infections, where the initial rate of conversation (K_1) would be relatively slow compared to the rate of the rate of maturation (K_2). Consequently, this would result in low levels of PrP^L, but relatively high levels of PrP^{Sc} [84]. Indeed, WT mice inoculated with hamster prions develop very high levels of PrP^{Sc} in their brains, yet these mice live a relatively normal life [126]. This model also explains why prion infected *Prnp*$^{+/-}$ mice (50% of wild-type PrP^{C} expression) succumb later to disease than *Prnp*$^{+/+}$ mice. The decreased expression of PrP^{C} in *Prnp*$^{+/-}$ mice results in a slower rate of infectivity titer, which may result in a slower rate of accumulation of PrP^{L}. On the other hand, Tga20 mice, which express 10 fold more PrP^{C} than WT mice, have a short incubation time. This is due to the higher (K_1) compared to (K_2). Consequently, this leads to rapid build up of PrP^{L} and a short incubation period. In these mice it is the high level of PrP^{C} expression that allows for more PrP^{Sc}:PrP^{C} complexes. The increase in these encounters allow for a high level of PrP^{Sc}:PrP^{L} and therefore a short life span. Thus, the ability of prions to infect and cause disease in a host is determined by the delicate balance between (K_1) and (K_2) [86].

Another alternative, but related model, postulated by John Collinge is that PrP^{L} is not produced as an intermediate along the pathway to mature PrP^{Sc} [86]. In this scenario, mature PrP^{Sc} acts as a surface template for the convertion of PrP^{C} to PrP^{L}. So essentially in this model PrP^{L} is a toxic templated side product. The difference between this model and the one mentioned above is that PrP^{L} is not generated as an intermediate, but a side product generated by PrP^{Sc}. This model of generating PrP^{L} may explain why in vivo prion propagation and toxicity occur in two distinct phases [127]. In phase one nontoxic prions (PrP^{Sc}) replicate until they reach a similar plateau regardless of PrP^{C} expression levels. In phase two, where there is no increase in infectivity (PrP^{Sc}), the rate of formation of PrP^{L} is dependent on the expression of PrP^{C}.

Although the above model describes a situation where production of PrP^{L} is directly proportional to PrP^{C} concentration, many argue another interpretation of this model can be extrapolated [128]. It is hypothesized that there is no need to postulate PrP^{L} to account for the well-accepted fact that PrP^{C} expression determines the speed of prion disease. With PrP^{L} being undefined, it is thought that PrP^{L} may be identical to PrP^{Sc} and that PrP^{C} controls neurotoxic signals arising from PrP^{Sc}. This idea of toxic signaling is interesting because it postulates that lower PrP^{C} expression leads to a decrease in sensitivity of neurons to toxicity. This concept of toxic signaling threshold may explain why $Prnp^{+/-}$ mice (with 50% of the WT PrP^{C} expression) shows delays in incubation period when compared to WT mice. It is also thought that it may explain the findings by Mallucci *et al*., in which depletion of neuronal PrP during a established brain infection rescues mice from developing clinical disease [108, 128]. Although, this represents a valid model it still may not account for subclinical infections. It is logical to suggest that prions, with their ability to arise through many etiologies, may exploit many of these mechanisms.

Chronic Wasting Disease

CWD was originally recognized as a syndrome in captive mule deer in the late 1960s at a wildlife research facility in Fort Collins, Colorado. Initially, it was believed that the syndrome was the result of nutritional deficiencies, intoxication, or stress associated with captivity [129]. It was not until 1978 that E.S. Williams and S. Young observed clinical features and histopathological changes that were strikingly similar to other prion diseases. It was these similarities that led E.S. Williams and S. Young to correctly identified CWD as a spongiform encephalopathy [5]. Today CWD is recognized as a highly contagious prion disease of unknown origin affecting both wild and farmed raised deer, moose, and elk [5-7].

Although the majority of natural sources of prion diseases are well established, the origin of CWD remains unknown. It has been hypothesized that CWD is a spontaneous disease of cervids however, this notion is difficult to confirm. The ability of other prion diseases to cross species barriers has led to the belief that CWD emerged by transmission of prions from another species. Reports of sheep scrapie in the US, along with the ability of sheep, deer and elk to share pastures, has led to the idea that trans-species transmission occurs between these animals [24]. Support of this notion comes from studies showing transmission of scrapie prions to both elk and cervidized mice [130, 131]. Interestingly, polymorphisms at codon 132 of elk have been shown to dictate the susceptibility of cervids to scrapie [131].

Once thought of as a rare TSE disease located exclusively in the central US, CWD has since become the most contagious and least understood of the prion diseases. Recent surveillance shows that the geographical distribution of CWD has expanded beyond Colorado and Wyoming, effecting 17 states and two Canadian provinces (Alberta and Saskatchewan) [24,132]. Noncontiguous clusters characterize the geographical distribution of CWD with reported cases seen as far West as Utah and extending as far East to New York and West Virginia. Recently, imports of deer from Canada have expanded the distribution of CWD to include countries outside North America, such as South Korea [133]. With a seeming inability to control or contain CWD, it appears likely that this prion disease will continue to expand its geographical distribution throughout North America and possibly other countries.

With the prevalence rates of CWD in wild and captive herds reaching as high as 50% and >90% respectively, intensive research has been put forth to determine the mode of transmission [24, 134]. Infectious prions have been found in blood, saliva, feces, and urine from cervids affected with CWD [135-138]. These bodily fluids, along with decomposing carcasses, represent possible contaminants by which CWD could be transmitted in a natural environment. There is also considerable evidence that prions can exist in the environment for extended periods of time, and this persistence in the environment represents a possible reservoir for CWD transmission [139-141]. It is well established that prions are inherently stable, showing an ability to withstand UV, heat, and proteases [2,76,77]. This perceived stability has led many to hypothesize that prions are capable of withstanding natural stresses such as UV, freeze/thaw cycles, and extracellular enzymes from fungi and bacteria [24]. Prions have also been shown to adhere to metals within soil and remain infectious for many years [139,141-143]. This remarkable persistence of prions in the environment may result in efficient transmission to naïve cervids that forage or drink from the same water sources as CWD infected animals.

The clinical signs of CWD are similar between experimentally inoculated animals and wild cervids that are naturally exposed to the disease. Most descriptions of clinical signs come from experimentally inoculated animals and are characterized by a long incubation period followed by a rapid clinical course. Terminally sick animals present with progressive weight loss, polyuria, odontoprisis, and sialorrhea [134]. In captive animals sudden death is rare, and clinical disease can range from months to even a year in some cases [144]. In wild populations, behavioral changes including depression and isolation from the herd have been observed. Extreme environmental conditions, predation, and an inability to forage or find water may decrease this period of clinical disease in wild cervids [24].

CWD presents as a neurological disorder with clinical signs that include ataxia and head tremors [134]. The histopathological features observed in CWD in many ways mirror what are seen in other prion diseases [145,146]. Histolopathological analyses show lesions in the grey matter that are bilaterally symmetrical and anatomically uniform among cervids [24]. Severe vacuolization of neuronal perikarya and neuronal processes may be accompanied by deposition of PrP^{CWD} plaques, astrocytic hyperplasia and hypertrophy [147,148]. Post-mortem analysis may also show PrP^{CWD} deposition in extraneuronal sites such as secondary lymphoid organs (SLOs) [146,149].

Due to the dissemination, persistence, and migratory capacity of wild cervids, control of CWD is extremely difficult. Although no increase in cases of CJD have been reported in places where CWD is endemic, the possibility of transmission remains feasible [24]. Therefore, wildlife disease management and prion researchers must design diagnostic techniques and possible strategies to control and contain CWD. Emphasis in control and containment may be needed most, as CWD seems to be expanding its geographical distribution.

Peripheral Prion Immunology

In a laboratory setting the most effective way to induce a prion disease is by delivering prions directly to the brain by intracerebral inoculation. This route of infection may be of particular significance when studying neuroimmunological events in prion disease. However, this artificial route of infection does not correspond to what is normally seen in nature, and when studying the early events in prion disease, it is essential to explore other more natural routes of infection [119]. Typically, infection through various different peripheral routes is the standard when studying incunabular events in prion mediated immune cell responses. The majority of prions that cause human TSEs are acquired through oral challenge [150-153]. Prions can also infect the host through the blood, peritoneal cavity, skin, and eye [154-157]. Of these routes of infection, oral, intraperitoneal, intravenous, and skin scarification have all been shown to involve cells of the lymphoreticular system (LRS) [10, 164, 191,164].

Although TSEs are thought of as neurological diseases, it is the early immunological events that dictate the course of prion pathogenesis. Early transmission experiments showed that SLOs contain prions and led to the hypothesis that prions exploit lymphoid tissues for self-propagation before entry into the CNS [158-160]. Since these early findings, substantial evidence showed that B lymphocytes, follicular dendritic cells (FDCs), complement proteins and complement receptors are the main immune components involved in peripheral prion replication [161-163]. While the involvement of these components in prion replication remains crucial in pathogenesis, recent data suggests that cells of the innate immune system also play an important role in dictating the outcome of infection. Temporarily depleting certain antigen presenting cells (APCs) or disrupting their pattern recognition receptors (PRRs) significantly alters prion pathogenesis [164,165]. Today it is well recognized that the immune system plays an instrumental role in prion pathogenesis; therefore, the identification of the cells and molecules involved in prion pathogenesis might pinpoint potential targets for therapeutic interventions.

Prion uptake and trafficking: phagocytes take center stage

Oral exposure

Many TSEs, including Kuru, variant Creutzfeldt–Jakob disease (vCJD), BSE, scrapie, and CWD, are acquired through an oral route of infection [141,150,151,153,166]. After oral exposure prions accumulate in the distal ileum, and within several weeks can be found to accumulate and traffic in a defined temporal sequence throughout peripheral nerves.[119,167]. This process of neuroinvasion relies on prion replication by follicular dendritic cells (FDCs) located in gut-associated lymphoid tissue (GALT) [168-170]. Several immune cell interactions with prions precede this replication phase and are vital for establishing a disease. Recently, several groups have identified a variety immune cell types that are important in uptake and transport of these prions during an oral infection.

After ingestion of prion-contaminated food, it is critical for prions to cross the intestinal epithelium before replication on FDCs within Peyer's patches (PP). One way by which this is accomplished is through the follicle-associated epithelium (FAE), which is a unique cell layer comprised of enterocytes and specialized endocytic epithelial cells called Microfold cells (M cells) [171]. The FAE is located above the PP and establishes an interface between the GALT and the intestinal luminal. PPs are devoid of afferent lymphatics, so antigens must travel from the gut into PP through M cells. This cell type plays a crucial role in microbial survalance because is allows the host to sample the intestinal lumen and induce the proper immune response [172,173]. However, many pathogens have evolved to take advantage of this trans-epithelial transport to gain access into the mucosal tissues; therefore, it has been suggested that M cells play a crucial role in prion transcytosis after oral infection [174-176]. Studies show that orally administered prions incorporate into M Cells, and depleting these cells by RANKL neutralization at the time of oral exposure leads to ablation of disease [177-180].

Several other studies show that enterocytes transport prions independent of M-cells, and this trancytosis may depend on a receptor-mediated pathway [181,182]. Ferritin was found to form a complex with PrP^{Sc} upon transcytosis across Caco-2 epithelial cells. Ferritin is an intracellular protein that stores iron and is abundantly present in meat dishes [183]. It has been suggested that this PrP^{Sc}-ferritin complex facilitates prion transport through a receptor-mediated pathway across the intestinal epithelium [182].

After transcytosis by M cells and epithelial cells, antigen acquisition by dendritic cells and macrophages is thought to occur [184-186]. These cells are positioned in the sub-epithelial dome of PPs, where they sample antigens from the FAE. Several experiments indicate that DCs and macrophages take up prions after oral infection and transport them to sites of replication within germinal centers of lymphoid tissues [164,179,187,188]. In some cases, this prion uptake and transport was independent of PrP^{C} expression [179]. Although a model of prion capture and transport from the gut lumen to germinal centers of lymphoid tissues is well established, the mechanisms of how prions infect the peripheral enteric nervous system remains unknown.

Phagocyte-prion interaction through other peripheral sites of infection

In addition to oral exposure, other routes of peripheral infection have been explored.

Skin scarification has long been known to be highly efficient at causing prion disease [189,190]. It is conceivable that DCs in the skin play an important role in the early phase of disease. Indeed, skin-derived dendritic cells capture and degrade prions following in vitro exposure [191]. However, in vivo evidence of skin-derived DCs acquiring, degrading, or even trafficking prions remains unknown. The notion that these cells take up and traffic prions to resident draining lymph nodes and the CNS is supported by a number of experiments [164,188,192,193]. One particular experiment shows that prion infected splenic DCs can propagate infection from the periphery to the CNS in the absence of any additional lymphoid elements [193]. This result is intriguing, as peripheral prion replication seem to be dispensable in this process.

Prion diseases can also be initiated through the intraperitoneal route of infection [155]. Just as in oral infection and skin scarification, immune cells seem to dictate the early stages of disease. Temporarily depleting CD11c+ dendritic cells after intraperitoneal infection results in delays in lymphoinvasion [192]. It is worth noting, however, that transient depletion of CD11c+ cells in CD11c-DTR transgenic mice, initially thought to specifically deplete DCs, has also been shown to reduce macrophage subsets in the lymph node and spleen [194,195]. This involvement of DCs and macrophages, along with the observation that peritoneal macrophages associate with and degrade prions, indicates a critical role of these cells in the intraperitoneal route of infection [196]. While these experiments hint at a possible role of the LRS after i.p. infection, little is known about the initial confrontation between prions and these innate immune cells.

Prion mediated activation of phagocytes

Prion protein Fragment PrP 106-126

Examination of human prion diseases has shown the existence of amyloid fibril deposits made up of insoluble cleavage products from PrP^{Sc} [197]. These amyloid fragments, which can reach high concentrations in the brain of infected individuals, have been shown to consist of N-terminally truncated forms of PrP that contain amino acids 106-126 [198]. $PrP_{106\text{-}126}$, which has been shown to be toxic to cultured neuronal cells expressing PrP^{C}, demonstrates high tendencies to form amyloid like fibrils morphologically similar to PrP^{Sc}. It also contains high β-sheet content, is partially resistant to proteases, and is capable of activating glial cells [103,199-202]. Due to these biochemical properties, $PrP_{106\text{-}126}$ is a suitable tool to model the molecular immunological features of prion disease.

Prion mediated proinflammatory response

As with other pathogens, prions show an ability to elicit an inflammatory response. In prion infected mice, several inflammatory transcription factors and mRNA transcripts have been characterized [203-207]. Treatment in vitro with $PrP_{106\text{-}126}$ results in activation of microglial cells, monocyte-derived dendritic cells and macrophages [208-210]. This activation by $PrP_{106\text{-}126}$ and prions involves transcription factors p38 mitogen-activated protein kinase (MAPK) and nuclear factor-κB (NFκB), which resulted in secretion of pro-inflammatory cytokines IL-6, TNF-α, and IL-1β [209,211-213]. These data demonstrate that although there is no humoral response to prions, activation of the innate immune system, possibly through PRRs, may play a critical role in the early events of infection. Indeed, activation of toll-like receptor 4 (TLR-4) has shown to suppress prion disease after both ip and ic inoculations [165]. Interestingly, this suppression by TLR-4 was shown to be independent of MyD88, as infection of MyD88 deficient and wild-type mice exhibited similar incubation periods, infection kinetics, neuropathologies [214].

Although immune cell uptake, activation, and trafficking remain an important aspect of prion diseases, several scientific groups have tried to elucidate the molecular and cellular mechanisms involved in peripheral prion propagation. Interestingly, unlike many other pathogens, prion trafficking to lymphoid tissues leads to enhanced susceptibility to disease. Over the last 20 years great strides in our knowledge of peripheral prion replication has led to a better understanding of how these TSEs infect and cause disease in the host.

Lymphoid tissues; Sites of prion replication

Although prion diseases are classified as a neurodegenerative disorder, it is well known that infectious prions colonize secondary lymphoid organs in infected hosts. This colonization of lymphoid tissue results in lack of pathology despite replication of prionsto high titers [215]. This is in contrast to what is seen in the CNS, where prion replication leads to severe spongiosis, astrosytosis, and neuronal cell death [1].

It is generally well accepted that during a prion infection lymphoid tissues play a vital role in pathogenesis. Following intracerebral (ic), ip or oral exposure, prions can be detected in the spleen, lymph nodes, PP, and tonsils [10,74,158,170,216,217]. Prions can be identified in these lymphoid tissues in a matter of hours or days, whereas detection in the brain can only be observed after several months post inoculation [10]. Mice that have their spleen surgically removed prior to, or shortly after, peripheral inoculation of prions show delays in prion pathogenesis [158,215, 218]. Similar results are seen in asplenic mice. This is in stark contrast to what is observed in mice deficient in a thymus [219]. Inoculation of these mice with prions results in no alteration of disease. This indicates that T lymphocytes have little to no role in prion pathogenesis. Studies of splenectomy at various times after ip inoculation show that pathogenesis becomes independent of the spleen once prions have initiated replication in the spinal cord [220]. However, this requirement for the spleen in prion pathogenesis is not absolute, as inoculation of the Fukuoka-1 strain of Creutzfeldt-Jakob disease agent or scrapie (263K) into asplenic mice or hamsters, respectively, has no effect on disease progression [221,222]. Natural cases of BSE and atypical scrapie also show no PrP^{Sc} in their lymph nodes, further exemplifying that prion replication by the LRS may be strain dependent [223,224]. These data suggest that prion strains can be categorized as either lymphotropic or neurotrophic depending on the requirement of the LRS.

After it was suggested that lymphoid tissues contain infectious prions, cell isolation experiments were performed in an attempt to find the prion distribution among the LRS. Cells separated in density gradients of isotonic albumin showed that immune cells associated with relatively high infectivity had a density gradient characteristic of lymphoblasts, myeoblasts, and macrophages [225]. Although these initial studies implicated these cell populations in prion uptake, prion replication by these cells could not be demonstrated. In an effort to characterize the cell compartment important in prion replication (or accumulation), spleen fractions were isolated from mice infected with scrapie. It was shown that stromal compartments of the spleen contained 10 times greater infectivity than the pulp. There was a strong correlation between the total titers in the stroma and the weight of both whole spleen and stroma fractions [226]. This observation led to the hypothesis that replication takes place on the metabolically and structurally stable cells of the stroma. It was also suggested that these cells involved in prion replication were not mitotically active. Whole body irradiation, which selectively targets mitotically active cells, failed to alter the disease progression in mice infected with scrapie [227]. Taken together, these data show that replicate or accumulate of prions occurs largely on radioresistant, post-mitotic cells located in the stromal compartments of lymphoid tissues.

Peripheral Immune Cells involved in prion replication

The role of B lymphocytes in prion replication

With the discovery that lymphoid tissues transmit infectivity to naïve animals, it was becoming increasingly apparent that immune cells participate in peripheral prion pathogenesis. With the use of immunocompromised mice and bone marrow reconstitution experiments, cells of hematopoietic origin were soon shown to be involved in prion replication. Although their involvement was evident, it became clearer that only a subset of these immune cells contributed to prion replication in lymphoid tissues.

Characterizing immune cells important in prion replication using a panel of immune-deficient mice provided crucial information about prion pathogenesis. When mice deficient in CD4, CD8, β_2 microglobulin, poriforin, and therefore T lymphocytes, were exposed to prions, they developed disease and latency periods similar to WT control mice. However, ip inoculation of μMT and Rag-deficient mice, both of which are devoid of B lymphocytes, showed no disease or infectivity in the spleen [161]. These data indicated that defects in B lymphocytes, but not T lymphocytes, had a profound impact on prion disease progression. However, the question of whether these B lymphocytes directly participated in prion replication or played a more indirect role still was not known. It was not until scientists employed the use of adoptive transfer experiments and transgenic mice that information on the role of B lymphocytes in prion replication become clear.

To assess the requirement of PrP^C expression by B lymphocytes in prion replication and neuroinvasion, fetal liver cells (FLCs) derived form either PrP^C expressing or PrP^C deficient mice were used to repopulate SCID and Rag deficient mice [228]. FLCs from both PrP^C expressing and PrP^C deficient mice had the same ability in restoring peripheral replication and neuroinvasion after ip inoculation of prions. Furthermore, repopulating these immunocompromised mice with FLCs from T lymphocyte deficient mice, but not from B lymphocyte deficient mice, successfully restored disease. This indicated that while B lymphocytes are important in prion replication and neuroinvasion, the expression of PrP^C by these cells were not. Although PrP^C expression was dispensable in these processes, splenic B lymphocytes could be observed associating with prions [229]. This raised the question of whether B lymphocytes had the capacity to replicate prions or just acquire them from other cells. Using Tg mice, which express PrP exclusively on B lymphocytes, it was shown that these cells failed to replicate prions in the spleen after ip inoculation [230]. These data indicated that B lymphocytes themselves are unlikely involved in replication, and further supported the observation that cells of the stromal compartment are the main cell type involved in prion replication. In light of these findings it was soon hypothesized that B lymphocytes play a critical role in prion pathogenesis by supporting or maintaining cells important in prion replication.

The role of FDCs in prion replication

Follicular dendritic cells (FDCs) are the main cell type responsible for prion replication, and the capacity of FDCs to replicate prions is dependent on B lymphocytes [231-237]. These cells express high levels of PrP^C and are found in the follicles of lymphoid tissues. FDCs under normal physiological conditions are responsible for the maintenance of the lymphoid microarchitecture [238,239]. However, after exposure to pathogens these cells are involved in antigen trapping of immune complexes by Fcγ receptors. FDCs also bind opsonized antigens through complement receptors CD21/35 [240-242]. These specific characteristics of FDCs establish these cells as important contributors to prion replication and neuroinvasion.

Not only do FDCs accumulate PrP^{Sc} following inoculation of mice with prions, but many studies suggest that replication of prions in the spleen requires PrP^C-expressing FDCs [234,236]. FDC development and maintenance was shown to be dependent on tumor necrosis factor (TNF) and lymphotoxins (LTs) α and β, which are proinflammatory cytokines mainly produced by B lymphocytes [237]. Treatment of mice with soluble lymphotoxin-β receptor, which depletes LT, resulted in a lack of mature FDCs and significantly impaired peripheral prion pathogenesis [236]. This indicated that mice deficient in LT signaling show a significant resistance to peripheral prion exposure. These data not only highlight the role of B lymphocytes in peripheral prion pathogenesis, but give substantiating evidence for a direct role of FDCs in prion replication.

Although FDCs play a critical role in peripheral prion replication, it has been suggested that other cells may also participate in prion replication. $TNFR^{-/-}$ and $TNF\alpha^{-/-}$ mice inoculated ip with prions showed similar attack rates to WT mice [243]. Despite the absence of FDCs or germinal centers in these mice prion infectivity could be detected in the lymph nodes; however, no infectivity could be detected in the spleens. This illustrates that prion infectivity could be restricted to certain lymphoid tissues, and prion replication by FDCs are expendable in this process [243].

Recently, ectopic prion replication in granulomas was shown in mice inoculated with prions [244]. Reciprocal bone-marrow grafting experiments indicated that cells of stromal origin were the source of PrP^{C} and prion replication. Interestingly, granulomas from these prion-inoculated mice lacked FDCs, but expressed almost equal amounts of LTβR mRNA as $Prnp^{+/+}$ mouse spleens. Treatment of these mice with a LTβR-immunoglobulin fusion protein (LTBR-Fc) suppressed prion replication in these granulomas. However, LTβR-Fc treatment did not alter PrP^{C} expression, formation, maintenance, and morphology of these inflammatory stromal cells. These data showed that stromal cells distinct from FDCs could attain prion-replication capability in vivo in a LTβR-signaling-dependent manner [244].

The Complement system; its role in FDC mediated prion uptake and replication

The complement system, composed of nearly 30 soluble and cellular membrane proteins, is a group of heat-labile proteins found in normal plasma that provides an innate immune defense mechanism against invading pathogens [245,246]. All pathogens express a unique set of pathogen-associated molecular patterns (PAMPS) that are involved in the activation of the complement cascade [247,248].

Once activated, complement proteins can interact with one another to aid in the opsonization of pathogens, lyse infected cells, and promote a series of inflammatory responses. Not only does the complement system eliminate infectious microorganisms, but it also provides a bridge between the innate and adaptive immune systems [249,250]. One immune cell that facilitates this complement mediated bridge between the innate and adaptive immune system is the FDC.

The main function of FDCs during an immune response is to trap and retain antigens derived from pathogens. These antigens, in the form of antigen:antibody:complement complexes, are retained on the cell surface for extended amounts of time through Fc and complement receptors [241,251-253]. These immune complexes are presented to B lymphocytes initiating a humoral response, and hence, eliminating the pathogen [253]. Thus complement activation leads to bound immune complexes and initiation of an antibody response. However, many pathogens have countered this complement-mediated assault by developing unique strategies to disrupt complement regulatory components to prevent being eliminated. Other pathogens have persisted and replicated in the host by taking advantage of complement interactions, which facilitated their attachment to host cells. [163, 254-256].

The contribution of the complement system during a prion infection has been studied for several years. Mice lacking complement components C1q, factor B, C2, C4, and C3 have been used to show the role of the complement system in retention of PrP^{Sc} in lymphoid tissues after peripheral exposure to prions. These experiments demonstrate that depletion of these complement components leads to a decrease in PrP^{Sc} accumulation and an increase in survival time [11]. Interestingly, depletion of C1q has a greater impact on prion disease progression than an absence in the other downstream complement components. This implies that C1q might directly bind and mediate uptake of prions after peripheral exposure. Indeed, C1q has bound PrP^{C} in vitro in a conformation- and density-dependent manner, and these C1q-PrP complexes have been shown to activate the complement classical pathway [257-260]. These data indicate that complement activation and opsonization is the main mechanism by which FDCs accumulate and retain prions in lymphoid tissues.

With the knowledge that FDCs associate with complement opsonized antigens through the complement receptor CD21/35, many scientists speculate whether there is a role of this complement receptor in prion disease pathogenesis. Through reciprocal adoptive bone marrow transfer experiments between WT and CD21/35$^{-/-}$ mice, it was shown that FDCs deficient in CD21/35 exhibit an incomplete attack rate or a delay in incubation time when exposed peripherally to prions [163]. Interestingly, elimination of CD21/35 impacted prion trapping and disease more profoundly than ablating their ligand sources, C3 and C4. This implies a role for CD21/35 in peripheral prion pathogenesis independent of their endogenous ligands.

Ectopic prion replication

Although the contribution of immune cells and proinflammatory cytokines during prion replication are well established, several studies have suggested that prion replication may extend beyond lymphoid tissues, expanding the tissue tropism of prions [261,262]. CJD patients suffering from inclusion body myositis, an inflammatory disease of muscle, accumulate PrP^{Sc} [263]. This ectopic prion replication in nonlymphoid organs is suggested to involve similar immune cells and proinflammatory cytokines as lymphoid tissues. Indeed, inoculation of prions into mice suffering from nephritis, hepatitis, or pancreatitis showed PrP^{Sc} accumulation and a strong upregulation of LT and FDCs in these inflamed organs [262]. These data suggest that prion distribution throughout the host could be dictated by inflammation or exacerbated by concurrent infections.

Farmed raised animals are commonly exposed to inflammatory pathogens. This opportunistic interaction has led to the hypothesis that ectopic prion replication may be a common occurrence in livestock. Indeed, Sarda sheep with natural scrapie infections and coexisting mastitis accumulated PrP^{Sc} in their mammary glands [261]. Interestingly, some of these chronic inflammatory disorders affect organs that are important in secretion of bodily fluids. Milk from lentiviral-induced mastitis or urine from mice suffering from nephritis infected naïve suckling lambs and mice respectively [264,265]. Taken together these data implicate inflammatory processes in the tissue distribution and horizontal transmission of prion diseases.

Conclusion

Advances in the development of techniques and tools have enabled prion biologists to answer some long-standing questions in prion biology; however, several questions still remain. The exact physiological function of PrP^{C} remains to be clarified. Answering this vital question could potentially help prion biologist understand the exact molecular mechanism of prion-induced toxicity. Although significant progress has been made in prion immunology, several long standing-questions remain unanswered. The initial immunological events that occur upon infection remain to be characterized.

Although several experiments implicate immune cells in prion trafficking, no real direct evidence has been put forth to show this to be the case. In addition, several studies have shown immune cells to play a vital role in prion replication; however, the role of complement proteins and their receptors in CWD remains shrouded in mystery. Elucidation of these immunological events could better help researchers understand the process of peripheral prion pathogenesis. Furthermore, the characterization of immune cells involved in prion capture, trafficking, and replication would have dramatic implications in prion immunotherapeutics.

Introduction to work in this Dissertation Research

The main objective of the current research is to gain a greater understanding of the immunological events involved in a CWD prion infection. **The overall hypothesis for the thesis is that early immunological events in CWD prion infection dictate the course of disease.** Utilizing fluorescently labeled prion rods and transgenic mice deficient in certain complement components we addressed the following questions:

Question 1: What are the immune cells that associate with prions in the earliest stages of a CWD prion infection?

While prions most likely interact with the innate immune system shortly following infection, little is known about this initial encounter. Here we investigated incunabular events in lymphotropic and intranodal prion trafficking by following highly enriched, fluorescent prions from infection sites to draining lymph nodes. As we have shown in an earlier study, prions can be detected in the draining lymph nodes within hours of intraperitoneal inoculation. However, through adoptive transfer experiments we demonstrate here that prions arrive in draining lymph nodes cell autonomously within two hours of intraperitoneal infection. We show that DCs and monocytes require C1q and/or C3 for optimal prion capture, whereas macrophages predominantly and efficiently captured prions independent of these complement components. We show an incredible proportion of prion bearing B cells in MedLNs at early time points, and suggest that these cells are most likely receiving prions from other immune cells, most likely

SCS macrophages and resident DCs within the lymph nodes. Based on these data, we introduce an updated, more detailed model of lymphotropic and intranodal prion trafficking by immune cells.

Question 2: What is the role of complement receptor CD21/35 in a CWD prion infection?

The Complement System has been shown to play an integral part in peripheral prion pathogenesis. Mice lacking Complement receptors CD21/35 showed delays in prion pathogenesis when exposed peripherally to mouse-adapted scrapie prions. Chronic wasting diseae (CWD) is a highly contagious prion disease of captive and free-ranging cervid populations, and similar to scrapie has been suggested to involve the peripheral immune system. Here we show that mice overexpressing the cervid prion protein and susceptible to CWD (Tg(cerPrP)5037 mice) but lack CD21/35 expression completely resist clinical CWD upon peripheral infection. This resistance to CWD by Tg 5037;CD21$^{-/-}$ strongly correlates with little or no pathology in the brain. Semi-quantitative analysis of these mice suggests an impairment of splenic prion accumulation and replication throughout disease. We show that CD21/35 translocates to lipid rafts during a prion infection and is accompanied by a strong germinal center response. We postulate that this germinal center response provides an ideal environment for prion accumulation and replication. Lastly, we propose that CD21/35 may exhibit a conformational bias towards certain prion quasi-species present in prion strains. This may lead to selection of certain prion quasi-species that exhibit differential zoonotic potential compared to the parental strains.

Question 3: What is the role of complement component C3 in CWD prion infection?

Commonly described as linear in nature, the complement system actually functions as a hub-like network with C3 being one of the main components [245]. C3 is the most abundant complement protein, being found in the blood at physiological concentrations of 1 mg/ml. Previous experiments suggest a vital role of C3 in scrapie prion pathogenesis. Here we show that lack of C3 expression by 5037 mice either transiently or genetically leads to delays in prion pathogenesis. Using semiquantitative PMCA we show that C3 impacts disease progression in the early stages of disease by slowing the kinetic rate of accumulation and/or replication of PrP^{RES}. This slower kinetic increase in PrP^{RES} correlates with an increase in survival time in mice deficient in C3. This delay in disease is in sharp contrast to the complete rescue we saw in CWD infected Tg 5037;$CD21^{-/-}$ mice. This suggests a role for CD21/35 in peripheral prion pathogenesis independent of their endogenous ligands.

REFERENCES

1. Collinge, J. Prion diseases of humans and animals: their causes and molecular basis. *Annu. Rev. Neurosci.* **24**, 519–550 (2001).
2. Prusiner, S. B. Novel proteinaceous infectious particles cause scrapie. *Science* **216**, 136–144 (1982).
3. Carleton Gajdusek, D. Transmissible and non-transmissible amyloidoses: autocatalytic post-translational conversion of host precursor proteins to β-pleated sheet configurations. *J. Neuroimmunol.* **20**, 95–110 (1988).
4. Jarrett, J. T. & Lansbury, P. T., Jr. Seeding 'one-dimensional crystallization' of amyloid: A pathogenic mechanism in Alzheimer's disease and scrapie? *Cell* **73**, 1055–1058 (1993).
5. Williams, E. S. & Young, S. Chronic wasting disease of captive mule deer: a spongiform encephalopathy. *J. Wildl. Dis.* **16**, 89–98 (1980).
6. Baeten, L. A., Powers, B. E., Jewell, J. E., Spraker, T. R. & Miller, M. W. A natural case of chronic wasting disease in a free-ranging moose (Alces alces shirasi). *J. Wildl. Dis.* **43**, 309–314 (2007).
7. Williams, E. S. & Young, S. Spongiform encephalopathy of Rocky Mountain elk. *J. Wildl. Dis.* **18**, 465–471 (1982).
8. Hill, A. F. *et al.* The same prion strain causes vCJD and BSE. *Nature* **389**, 448–450 (1997).
9. Scott, M. R. *et al.* Compelling transgenetic evidence for transmission of bovine spongiform encephalopathy prions to humans. *Proc. Natl. Acad. Sci. U.S.A.* **96**, 15137–15142 (1999).
10. Michel, B. *et al.* Incunabular immunological events in prion trafficking. *Sci. Rep.* **2**, 440 (2012).
11. Klein, M. A. *et al.* Complement facilitates early prion pathogenesis. *Nat. Med.* **7**, 488–492 (2001).
12. Soto, C. Unfolding the role of protein misfolding in neurodegenerative diseases. *Nat. Rev. Neurosci.* **4**, 49–60 (2003).
13. Riek, R., Hornemann, S., Wider, G., Glockshuber, R. & Wuthrich, K. NMR characterization of the full-length recombinant murine prion protein, mPrP(23–231). *FEBS Lett.* **413**, 282–288 (1997).
14. Riek, R. *et al.* NMR structure of the mouse prion protein domain PrP(121-231). *Nature* **382**, 180–182 (1996).
15. Zahn, R. *et al.* NMR solution structure of the human prion protein. *Proc. Natl. Acad. Sci. U.S.A.* **97**, 145–150 (2000).
16. Hornshaw, M. P., McDermott, J. R., Candy, J. M. & Lakey, J. H. Copper Binding to the N-Terminal Tandem Repeat Region of Mammalian and Avian Prion Protein: Structural Studies Using Synthetic Peptides. *Biochem. Biophys. Res. Commun.* **214**, 993–999 (1995).
17. Garnett, A. P. & Viles, J. H. Copper binding to the octarepeats of the prion protein. Affinity, specificity, folding, and cooperativity: insights from circular dichroism. *J. Biol. Chem.* **278**, 6795–6802 (2003).

18. Hornshaw, M. P., McDermott, J. R. & Candy, J. M. Copper Binding to the N-Terminal Tandem Repeat Regions of Mammalian and Avian Prion Protein. *Biochem. Biophys. Res. Commun.***207**, 621–629 (1995).
19. Jackson, G. S. *et al.* Location and properties of metal-binding sites on the human prion protein. *Proc. Natl. Acad. Sci. U.S.A.* **98**, 8531–8535 (2001).
20. Gossert, A. D., Bonjour, S., Lysek, D. A., Fiorito, F. & Wuthrich, K. Prion protein NMR structures of elk and of mouse/elk hybrids. *Proc. Natl. Acad. Sci. U.S.A.* **102**, 646–650 (2005).
21. López García, F., Zahn, R., Riek, R. & Wuthrich, K. NMR structure of the bovine prion protein. *Proc. Natl. Acad. Sci. U.S.A.* **97**, 8334–8339 (2000).
22. Lysek, D. A. *et al.* Prion protein NMR structures of cats, dogs, pigs, and sheep. *Proc. Natl. Acad. Sci. U.S.A.* **102**, 640–645 (2005).
23. Liu, H. *et al.* Solution structure of Syrian hamster prion protein rPrP(90-231). *Biochemistry* **38**, 5362–5377 (1999).
24. Gilch, S. *et al. Top. Curr. Chem.* **305**, 51–77 (Springer Berlin Heidelberg: Berlin, Heidelberg, 2011).
25. Christina J Sigurdson *et al.* molecular switch controls interspecies prion disease transmission in mice. *J. Clin Invest.* **120**, 2590 (2010).
26. Nicolas, O., Gavin, R. & del Rio, J. A. New insights into cellular prion protein (PrPc) functions: The 'ying and yang' of a relevant protein. *Brain Res. Rev.* **61**, 170–184 (2009).
27. Aguzzi, A. & Polymenidou, M. Mammalian prion biology: one century of evolving concepts. *Cell* **116**, 313–327 (2004).
28. Kuwahara, C. *et al.* Prions prevent neuronal cell-line death. *Nature* **400**, 225–226 (1999).
29. Chiarini, L. B. Cellular prion protein transduces neuroprotective signals. *EMBO J.* **21**, 3317–3326 (2002).
30. Mouillet-Richard, S. Signal Transduction Through Prion Protein. *Science* **289**, 1925–1928 (2000).
31. Graner, E. *et al.* Cellular prion protein binds laminin and mediates neuritogenesis. *Mol. Brain Res.* **76**, 85–92 (2000).
32. Li, R. L. *et al.* The expression and potential function of cellular prion protein in human lymphocytes. *Cell Immunol.* **207**, 49–58 (2001).
33. Mabbott, N. A., Brown, K. L., Manson, J. & Bruce, M. E. T-lymphocyte activation and the cellular form of the prion protein. *Immunology* **92**, 161–165 (1997).
34. Kubosaki, A. *et al.* Expression of normal cellular prion protein (PrPc) on T lymphocytes and the effect of copper ion: analysis by wild-type and prion protein gene-deficient mice. *Biochem. Biophys. Res. Commun.* **307**, 810–813 (2003).
35. Cashman, N. R. *et al.* Cellular isoform of the scrapie agent protein participates in lymphocyte activation. *Cell* **61**, 185–192 (1990).
36. Laurén, J., Gimbel, D. A., Nygaard, H. B., Gilbert, J. W. & Strittmatter, S. M. Cellular prion protein mediates impairment of synaptic plasticity by amyloid-β oligomers. *Nature* **457**, 1128–1132 (2009).
37. Aguzzi, A., Baumann, F. & Bremer, J. The prion's elusive reason for being. *Annu. Rev. Neurosci.* **31**, 439–477 (2008).

38. Behrens, A. & Aguzzi, A. Small is not beautiful: antagonizing functions for the prion protein PrPC and its homologue Dpl. *Trends Neurosci.* **25**, 150–154 (2002).
39. Weissmann, C. & Aguzzi, A. Perspectives: neurobiology. PrP's double causes trouble. *Science* **286**, 914–915 (1999).
40. Moore, R. C. *et al.* Ataxia in prion protein (PrP)-deficient mice is associated with upregulation of the novel PrP-like protein doppel. *J. Mol. Biol.* **292**, 797–817 (1999).
41. Sakaguchi, S. *et al.* Loss of cerebellar Purkinje cells in aged mice homozygous for a disrupted PrP gene. *Nature* **380**, 528–531 (1996).
42. Bounhar, Y. Prion Protein Protects Human Neurons against Bax-mediated Apoptosis. *J. Biol. Chem.* **276**, 39145–39149 (2001).
43. Diarra-Mehrpour, M. Prion Protein Prevents Human Breast Carcinoma Cell Line from Tumor Necrosis Factor-Induced Cell Death. *Cancer Res.* **64**, 719–727 (2004).
44. Ma, J. & Lindquist, S. Conversion of PrP to a self-perpetuating PrPSc-like conformation in the cytosol. *Science* **298**, 1785–1788 (2002).
45. Roucou, X., Guo, Q., Zhang, Y., Goodyer, C. G. & LeBlanc, A. C. Cytosolic prion protein is not toxic and protects against Bax-mediated cell death in human primary neurons. *J. Biol. Chem.* **278**, 40877–40881 (2003).
46. Roucou, X. *et al.* Cellular prion protein inhibits proapoptotic Bax conformational change in human neurons and in breast carcinoma MCF-7 cells. *Cell Death Differ.* **12**, 783–795 (2005).
47. Zanata, S. M. *et al.* Stress-inducible protein 1 is a cell surface ligand for cellular prion that triggers neuroprotection. *EMBO J.* **21**, 3307–3316 (2002).
48. Lopes, M. H. *et al.* Interaction of cellular prion and stress-inducible protein 1 promotes neuritogenesis and neuroprotection by distinct signaling pathways. *J. Neurosci.* **25**, 11330–11339 (2005).
49. Chen, S., Mangé, A., Dong, L., Lehmann, S. & Schachner, M. Prion protein as trans-interacting partner for neurons is involved in neurite outgrowth and neuronal survival. *Mol. Cell. Neurosci.* **22**, 227–233 (2003).
50. Dodelet, V. C. & Cashman, N. R. Prion protein expression in human leukocyte differentiation. *Blood* **91**, 1556–1561 (1998).
51. Lin, T. *et al.* Normal cellular prior protein is preferentially expressed on subpopulations of murine hemopoietic cells. *J. Immunol.* **166**, 3733–3742 (2001).
52. Zhang, C. C., Steele, A. D., Lindquist, S. & Lodish, H. F. Prion protein is expressed on long-term repopulating hematopoietic stem cells and is important for their self-renewal. *Proc. Natl. Acad. Sci. U.S.A.* **103**, 2184–2189 (2006).
53. Burthem, J., Urban, B., Pain, A. & Roberts, D. J. The normal cellular prion protein is strongly expressed by myeloid dendritic cells. *Blood* **98**, 3733–3738 (2001).
54. Politopoulou, G., Seebach, J. D., Schmugge, M., Schwarz, H. P. & Aguzzi, A. Age-related expression of the cellular prion protein in human peripheral blood leukocytes. *Haematologica* **85**, 580–587 (2000).
55. Barclay, G. R., Hope, J., Birkett, C. R. & Turner, M. L. Distribution of cell-associated prion protein in normal adult blood determined by flow cytometry. *Br. J. Haematol.* **107**, 804–814 (1999).
56. Antoine, N. *et al.* Differential expression of cellular prion protein on human blood and tonsil lymphocytes. *Haematologica* **85**, 475–480 (2000).

57. Holada, K. & Vostal, J. G. Different levels of prion protein (PrPc) expression on hamster, mouse and human blood cells. *Br. J. Haematol.* **110**, 472–480 (2000).
58. Thielen, C. *et al.* Human FDC express PrPc in vivo and in vitro. *Dev. Immunol.* **8**, 259–266 (2001).
59. Hugel, B. *et al.* Modulation of signal transduction through the cellular prion protein is linked to its incorporation in lipid rafts. *Cell. Mol. Life Sci.* **61**, 2998–3007 (2004).
60. Stuermer, C. A. O. *et al.* PrPc capping in T cells promotes its association with the lipid raft proteins reggie-1 and reggie-2 and leads to signal transduction. *The FASEB J.* **18**, 1731–1733 (2004).
61. Schneider, B. *et al.* NADPH oxidase and extracellular regulated kinases 1/2 are targets of prion protein signaling in neuronal and nonneuronal cells. *Proc. Natl. Acad. Sci. U.S.A.* **100**, 13326–13331 (2003).
62. Krebs, B. *et al.* Prion protein induced signaling cascades in monocytes. *Biochem. Biophys. Res. Commun.* **340**, 13–22 (2006).
63. Lesné, S. *et al.* A specific amyloid-beta protein assembly in the brain impairs memory. *Nature* **440**, 352–357 (2006).
64. Shankar, G. M. *et al.* Natural oligomers of the Alzheimer amyloid-beta protein induce reversible synapse loss by modulating an NMDA-type glutamate receptor-dependent signaling pathway. *J. Neurosci.* **27**, 2866–2875 (2007).
65. Gimbel, D. A. *et al.* Memory Impairment in Transgenic Alzheimer Mice Requires Cellular Prion Protein. *Journal of Neuroscience* **30**, 6367–6374 (2010).
66. MacDonald, J. F., Jackson, M. F. & Beazely, M. A. Hippocampal Long-Term Synaptic Plasticity and Signal Amplification of NMDA Receptors. *Crit. Rev. Neurobiol.* **18**, 71–84 (2006).
67. Yashiro, K. & Philpot, B. D. Regulation of NMDA receptor subunit expression and its implications for LTD, LTP, and metaplasticity. *Neuropharmacology* **55**, 1081–1094 (2008).
68. Lacor, P. N. *et al.* Abeta oligomer-induced aberrations in synapse composition, shape, and density provide a molecular basis for loss of connectivity in Alzheimer's disease. *J. Neurosci.* **27**, 796–807 (2007).
69. Snyder, E. M. *et al.* Regulation of NMDA receptor trafficking by amyloid-β. *Nat. Neurosci.* **8**, 1051–1058 (2005).
70. Um, J. W. *et al.* Alzheimer amyloid-β oligomer bound to postsynaptic prion protein activates Fyn to impair neurons. *Nat. Neurosci.* **15**, 1227–1235 (2012).
71. You, H. *et al.* Aβ neurotoxicity depends on interactions between copper ions, prion protein, and N-methyl-D-aspartate receptors. *Proc. Natl. Acad. Sci. U.S.A.* **109**, 1737–1742 (2012).
72. Balducci, C. *et al.* Synthetic amyloid-beta oligomers impair long-term memory independently of cellular prion protein. *Proc. Natl. Acad. Sci. U.S.A.* **107**, 2295–2300 (2010).
73. Calella, A. M. *et al.* Prion protein and Aβ-related synaptic toxicity impairment. *EMBO Mol. Med.* **2**, 306–314 (2010).
74. Büeler, H. *et al.* Mice devoid of PrP are resistant to scrapie. *Cell* **73**, 1339–1347 (1993).
75. Basler, K. *et al.* Scrapie and cellular PrP isoforms are encoded by the same chromosomal gene. *Cell* **46**, 417–428 (1986).

76. Alper, T., Cramp, W. A., Haig, D. A. & Clarke, M. C. Does the Agent of Scrapie Replicate without Nucleic Acid ? *Nature* **214**, 764–766 (1967).
77. Alper, T., Haig, D. A. & Clarke, M. C. The exceptionally small size of the scrapie agent. *Biochem. Biophys. Res. Commun.* **22**, 278–284 (1966).
78. Griffith, J. S. Nature of the Scrapie Agent: Self-replication and Scrapie. *Nature* **215**, 1043–1044 (1967).
79. Prusiner, S. B., Cochran, S. P. & Downey, D. E. Determination of scrapie agent titer from incubation period measurements in hamsters. *Adv. Exp. Med. Biol.* **134,** 1043-1044 (1981).
80. Prusiner, S. B. *et al.* Measurement of the scrapie agent using an incubation time interval assay. *Ann Neurol.* **11**, 353–358 (1982).
81. Prusiner, S. B., Groth, D. F., Cochran, S. P. & Masiarz, F. R. Molecular properties, partial purification, and assay by incubation period measurements of the hamster scrapie agent. *Biochemistry* **19,** 4883-4891 (1980).
82. Prusiner, S. B. *et al.* Further purification and characterization of scrapie prions. *Biochemistry* **21**, 6942–6950 (1982).
83. Hsiao, K. *et al.* Spontaneous neurodegeneration in transgenic mice with mutant prion protein. *Science* **250**, 1587–1590 (1990).
84. Kaneko, K. *et al.* A synthetic peptide initiates Gerstmann-Sträussler-Scheinker (GSS) disease in transgenic mice. *J. Mol. Biol.* **295**, 997–1007 (2000).
85. Legname, G. *et al.* Synthetic mammalian prions. *Science* **305**, 673–676 (2004).
86. Collinge, J. & Clarke, A. R. A General Model of Prion Strains and Their Pathogenicity. *Science* **318**, 930–936 (2007).
87. Nazor, K. E. *et al.* Immunodetection of disease-associated mutant PrP, which accelerates disease in GSS transgenic mice. *EMBO J* **24**, 2472–2480 (2005).
88. Colby, D. W. *et al.* Protease-Sensitive Synthetic Prions. *PLoS Pathog.* **6**, e1000736 (2010).
89. Jackson, W. S. *et al.* Spontaneous Generation of Prion Infectivity in Fatal Familial Insomnia Knockin Mice. *Neuron* **63**, 438–450 (2009).
90. Colby, D. W. *et al.* Design and construction of diverse mammalian prion strains. *Proc. Natl. Acad. Sci. U.S.A.* **106**, 20417–20422 (2009).
91. Colby, D. W. & Prusiner, S. B. De novo generation of prion strains. *Nat. Rev. Micro.* **9**, 771–777 (2011).
92. Supattapone, S. Biochemistry. What makes a prion infectious? *Science* **327**, 1091–1092 (2010).
93. Saá, P., Castilla, J. & Soto, C. Ultra-efficient replication of infectious prions by automated protein misfolding cyclic amplification. *J. Biol. Chem.* **281**, 35245–35252 (2006).
94. Saborio, G. P., Permanne, B. & Soto, C. Sensitive detection of pathological prion protein by cyclic amplification of protein misfolding. *Nature* **411**, 810–813 (2001).
95. Castilla, J., Saá, P., Hetz, C. & Soto, C. In Vitro Generation of Infectious Scrapie Prions. *Cell* **121**, 195–206 (2005).

96. Deleault, N. R., Harris, B. T., Rees, J. R. & Supattapone, S. From the Cover: Formation of native prions from minimal components in vitro. *Proc. Natl. Acad. Sci. U.S.A.* **104**, 9741–9746 (2007).
97. Wang, F., Wang, X., Yuan, C. G. & Ma, J. Generating a Prion with Bacterially Expressed Recombinant Prion Protein. *Science* **327**, 1132–1135 (2010).
98. Büeler, H. *et al.* Normal development and behaviour of mice lacking the neuronal cell-surface PrP protein. *Nature* **356**, 577–582 (1992).
99. Tiraboschi, P., Hansen, L. A., Thal, L. J. & Corey-Bloom, J. The importance of neuritic plaques and tangles to the development and evolution of AD. *Neurology* **62**, 1984–1989 (2004).
100. Spillantini, M. G. *et al.* Alpha-synuclein in Lewy bodies. *Nature* **388**, 839–840 (1997).
101. Goedert, M. Alpha-synuclein and neurodegenerative diseases. *Nat. Rev. Neurosci.* **2**, 492–501 (2001).
102. Hetz, C., Russelakis-Carneiro, M., Maundrell, K., Castilla, J. & Soto, C. Caspase-12 and endoplasmic reticulum stress mediate neurotoxicity of pathological prion protein. *EMBO J.* **22**, 5435–5445 (2003).
103. Forloni, G. *et al.* Neurotoxicity of a prion protein fragment. *Nature* **362**, 543–546 (1993).
104. Collinge, J. *et al.* Transmission of fatal familial insomnia to laboratory animals. *Lancet* **346**, 569–570 (1995).
105. Medori, R. *et al.* Fatal familial insomnia: a second kindred with mutation of prion protein gene at codon 178. *Neurology* **42**, 669–670 (1992).
106. Lasmézas, C. I. *et al.* Transmission of the BSE agent to mice in the absence of detectable abnormal prion protein. *Science* **275**, 402–405 (1997).
107. Brandner, S. *et al.* Normal host prion protein necessary for scrapie-induced neurotoxicity. *Nature* **379**, 339–343 (1996).
108. Mallucci, G. Depleting Neuronal PrP in Prion Infection Prevents Disease and Reverses Spongiosis. *Science* **302**, 871–874 (2003).
109. Mallucci, G. R. *et al.* Targeting Cellular Prion Protein Reverses Early Cognitive Deficits and Neurophysiological Dysfunction in Prion-Infected Mice. *Neuron* **53**, 325–335 (2007).
110. Chesebro, B. *et al.* Anchorless prion protein results in infectious amyloid disease without clinical scrapie. *Science* **308**, 1435–1439 (2005).
111. Solforosi, L. *et al.* Cross-linking cellular prion protein triggers neuronal apoptosis in vivo. *Science* **303**, 1514–1516 (2004).
112. Klöhn, P. C. *et al.* PrP antibodies do not trigger mouse hippocampal neuron apoptosis. *Science* **335**, 52 (2012).
113. Rapoport, T. A., Jungnickel, B. & Kutay, U. Protein transport across the eukaryotic endoplasmic reticulum and bacterial inner membranes. *Annu. Rev. Biochem.* **65**, 271–303 (1996).
114. Andrews, D. W. & Johnson, A. E. The translocon: more than a hole in the ER membrane? *Trends Biochem. Sci.* **21**, 365–369 (1996).
115. Hampton, R. Y. ER-associated degradation in protein quality control and cellular regulation. *Curr. Opin. Cell Biol.* **14**, 476–482 (2002).

116. Ma, J. & Lindquist, S. Wild-type PrP and a mutant associated with prion disease are subject to retrograde transport and proteasome degradation. *Proc. Natl. Acad. Sci. U.S.A.* **98**, 14955–14960 (2001).
117. Rane, N. S., Kang, S. W., Chakrabarti, O., Feigenbaum, L. & Hegde, R. S. Reduced translocation of nascent prion protein during ER stress contributes to neurodegeneration. *Dev. Cell.* **15**, 359–370 (2008).
118. Kristiansen, M. *et al.* Disease-Associated Prion Protein Oligomers Inhibit the 26S Proteasome. *Mol. Cell* **26**, 175–188 (2007).
119. Aguzzi, A. & Calella, A. M. Prions: protein aggregation and infectious diseases. *Physiol. Rev.* **89**, 1105–1152 (2009).
120. Kim, S. J. & Hegde, R. S. Cotranslational partitioning of nascent prion protein into multiple populations at the translocation channel. *Mol. Biol. Cell* **13**, 3775–3786 (2002).
121. Kim, S. J., Mitra, D., Salerno, J. R. & Hegde, R. S. Signal sequences control gating of the protein translocation channel in a substrate-specific manner. *Dev. Cell.* **2**, 207–217 (2002).
122. Kim, S. J., Rahbar, R. & Hegde, R. S. Combinatorial control of prion protein biogenesis by the signal sequence and transmembrane domain. *J. Biol. Chem.* **276**, 26132–26140 (2001).
123. Hegde, R. S. *et al.* A transmembrane form of the prion protein in neurodegenerative disease. *Science* **279**, 827–834 (1998).
124. Hegde, R. S. *et al.* Transmissible and genetic prion diseases share a common pathway of neurodegeneration. *Nature* **402**, 822–826 (1999).
125. Silveira, J. R. *et al.* The most infectious prion protein particles. *Nat. Cell Biol.* **437**, 257–261 (2005).
126. Hill, A. F. *et al.* Species-barrier-independent prion replication in apparently resistant species. *Proc. Natl. Acad. Sci. U.S.A.* **97**, 10248–10253 (2000).
127. Sandberg, M. K., Al-Doujaily, H., Sharps, B., Clarke, A. R. & Collinge, J. Prion propagation and toxicity in vivo occur in two distinct mechanistic phases. *Nature* **470**, 540–542 (2011).
128. Aguzzi, A. & Falsig, J. Prion propagation, toxicity and degradation. *Nat Neurosci* **15**, 936–939 (2012).
129. Salman, M. D. Chronic wasting disease in deer and elk: scientific facts and findings. *J. Vet. Med. Sci.* **65**, 761–768 (2003).
130. Hamir, A. N. *et al.* Transmission of sheep scrapie to elk (Cervus elaphus nelsoni) by intracerebral inoculation: final outcome of the experiment. *J. Vet. Diagn. Invest.* **16**, 316–321 (2004).
131. Green, K. M. *et al.* The elk PRNP codon 132 polymorphism controls cervid and scrapie prion propagation. *J. Gen. Virol.* **89**, 598–608 (2008).
132. Argue, C. K., Ribble, C., Lees, V. W., McLane, J. & Balachandran, A. Epidemiology of an outbreak of chronic wasting disease on elk farms in Saskatchewan. *Can. Vet. J.* **48**, 1241–1248 (2007).
133. Kim, T. Y. *et al.* Additional cases of Chronic Wasting Disease in imported deer in Korea. *J. Vet. Med. Sci.* **67**, 753–759 (2005).
134. Williams, E. S. Chronic wasting disease. *Vet. Pathol.* **42**, 530–549 (2005).
135. Mathiason, C. K. *et al.* Infectious Prions in the Saliva and Blood of Deer with Chronic Wasting Disease. *Science* **314**, 133–136 (2006).

136. Safar, J. G. J. *et al.* Transmission and detection of prions in feces. *J. Infect. Dis.* **198**, 81–89 (2008).
137. Tamgüney, G. *et al.* Asymptomatic deer excrete infectious prions in faeces. *Nature* **461**, 529–532 (2009).
138. Haley, N. J., Seelig, D. M., Zabel, M. D., Telling, G. C. & Hoover, E. A. Detection of CWD prions in urine and saliva of deer by transgenic mouse bioassay. *PLoS ONE* **4**, e4848 (2009).
139. Johnson, C. J. *et al.* Prions Adhere to Soil Minerals and Remain Infectious. *PLoS Pathog.* **2**, e32 (2006).
140. Miller, M. W., Williams, E. S., Hobbs, N. T. & Wolfe, L. L. Environmental sources of prion transmission in mule deer. *Emerg. Infect. Dis.* **10**, 1003–1006 (2004).
141. Seidel, B. *et al.* Scrapie Agent (Strain 263K) Can Transmit Disease via the Oral Route after Persistence in Soil over Years. *PLoS ONE* **2**, e435 (2007).
142. Genovesi, S. *et al.* Direct detection of soil-bound prions. *PLoS ONE* **2**, e1069 (2007).
143. Rigou, P., Rezaei, H., Grosclaude, J., Staunton, S. & Quiquampoix, H. Fate of Prions in Soil: Adsorption and Extraction by Electroelution of Recombinant Ovine Prion Protein from Montmorillonite and Natural Soils. *Environ. Sci. Technol.* **40**, 1497–1503 (2006).
144. Williams, E. S. & Miller, M. W. Chronic wasting disease in deer and elk in North America. *Rev. Sci. Tech.* **21,** 305-316 (2002).
145. Spraker, T. R. *et al.* Comparison of histological lesions and immunohistochemical staining of proteinase-resistant prion protein in a naturally occurring spongiform encephalopathy of free-ranging mule deer (Odocoileus hemionus) with those of chronic wasting disease of captive mule deer. *Vet. Pathol.* **39**, 110–119 (2002).
146. Williams, E. S. Scrapie and chronic wasting disease. *Clin. Lab. Med.* **23**, 139–159 (2003).
147. Williams, E. S. & Young, S. Neuropathology of chronic wasting disease of mule deer (Odocoileus hemionus) and elk (Cervus elaphus nelsoni). *Vet. Pathol.* **30**, 36–45 (1993).
148. Liberski, P. P., Guiroy, D. C., Williams, E. S., Walis, A. & Budka, H. Deposition patterns of disease-associated prion protein in captive mule deer brains with chronic wasting disease. *Acta. Neuropathol.* **102**, 496–500 (2001).
149. Spraker, T. R. T. *et al.* Validation of monoclonal antibody F99/97.6.1 for immunohistochemical staining of brain and tonsil in mule deer (Odocoileus hemionus) with chronic wasting disease. *J. Vet. Diagn. Invest.* **14**, 3–7 (2002).
150. Anderson, R. M. *et al.* Transmission dynamics and epidemiology of BSE in British cattle. *Nature* **382**, 779–788 (1996).
151. Collinge, J. *et al.* Kuru in the 21st century - an acquired human prion disease with very long incubation periods. *Lancet* **367**, 2068–2074 (2006).
152. Marsh, R. F. & Hadlow, W. J. Transmissible mink encephalopathy. *Rev. sci. tech.* **11,** 539-550 (1992).
153. Hilton, D. A. Pathogenesis and prevalence of variant Creutzfeldt-Jakob disease. *J. Pathol.* **208**, 134–141 (2006).
154. Llewelyn, C. A. *et al.* Possible transmission of variant Creutzfeldt-Jakob disease by blood transfusion. *Lancet* **363**, 417–421 (2004).
155. Kimberlin, R. H. & Walker, C. A. Pathogenesis of mouse scrapie: effect of route of inoculation on infectivity titres and dose-response curves. *J. Comp. Path.* **88**, 39–47 (1978).

156. Scott, J. R., Foster, J. D. & Fraser, H. Conjunctival instillation of scrapie in mice can produce disease. *Vet. Microbiol.* **34**, 305–309 (1993).
157. Mabbott, N. A. & MacPherson, G. G. Prions and their lethal journey to the brain. *Nat. Rev. Micro.* **4**, 201–211 (2006).
158. Fraser, H. H. & Dickinson, A. G. A. Pathogenesis of scrapie in the mouse: the role of the spleen. *Nature* **226**, 462–463 (1970).
159. Pattison, I. H. & Millson, G. C. Further observations on the experimental production of scrapie in goats and sheep. *J. Comp. Pathol.* **70**, 182–193 (1960).
160. Pattison, I. H. & Millson, G. C. Distribution of the scrapie agent in the tissues of experimentally inoculated goats. *J. Comp. Pathol.* **72,** 233-244 (1962).
161. Klein, M. A. *et al.* A crucial role for B cells in neuroinvasive scrapie. *Nature* **390**, 687–690 (1997).
162. Brown, K. L. *et al.* Scrapie replication in lymphoid tissues depends on prion protein-expressing follicular dendritic cells. *Nat. Med.* **5**, 1308–1312 (1999).
163. Zabel, M. D. *et al.* Stromal complement receptor CD21/35 facilitates lymphoid prion colonization and pathogenesis. *J. Immunol.* **179**, 6144–6152 (2007).
164. Raymond, C. R., Aucouturier, P. & Mabbott, N. A. In vivo depletion of CD11c+ cells impairs scrapie agent neuroinvasion from the intestine. *J. Immunol.* **179**, 7758–7766 (2007).
165. Spinner, D. S. *et al.* Accelerated Prion Disease Pathogenesis in Toll-Like Receptor 4 Signaling-Mutant Mice. *J. Virol.* **82**, 10701–10708 (2008).
166. Sigurdson, C. J. *et al.* Oral transmission and early lymphoid tropism of chronic wasting disease PrPres in mule deer fawns (Odocoileus hemionus). *J. Gen. Virol.* **80**, 2757–2764 (1999).
167. McBride, P. A. *et al.* Early spread of scrapie from the gastrointestinal tract to the central nervous system involves autonomic fibers of the splanchnic and vagus nerves. *J. Virol.* **75**, 9320–9327 (2001).
168. Beekes, M. & McBride, P. A. Early accumulation of pathological PrP in the enteric nervous system and gut-associated lymphoid tissue of hamsters orally infected with scrapie. *Neurosci. Lett.* **278**, 181–184 (2000).
169. Glaysher, B. R. & Mabbott, N. A. Role of the GALT in scrapie agent neuroinvasion from the intestine. *J. Immunol.* **178**, 3757–3766 (2007).
170. Prinz, M. *et al.* Oral prion infection requires normal numbers of Peyer's patches but not of enteric lymphocytes. *Am. J. Pathol.* **162**, 1103–1111 (2003).
171. Murphy, K., Travers, P. & Walport, M. Janeway's Immunology. *Garland science* (2008).
172. Corr, S. C., Gahan, C. C. G. M. & Hill, C. M-cells: origin, morphology and role in mucosal immunity and microbial pathogenesis. *FEMS Immunol. Med. Microbiol.* **52**, 2–12 (2008).
173. Neutra, M. R., Pringault, E. & Kraehenbuhl, J. P. Antigen Sampling Across Epithelial Barriers and Induction of Mucosal Immune Responses. *Annu. Rev. Immunol.* **14,** 275-300 (1996).
174. Phalipon, A. & Sansonetti, P. J. Microbial-host interactions at mucosal sites. host response to pathogenic bacteria at mucosal sites. *Curr. Top. Microbiol. Immunol.* **236**, 163–189 (1999).

175. Sansonetti, P. J. & Phalipon, A. M cells as ports of entry for enteroinvasive pathogens: mechanisms of interaction, consequences for the disease process. *Semin. Immunol.* **11**, 193–203 (1999).
176. Siebers, A. & Finlay, B. B. M cells and the pathogenesis of mucosal and systemic infections. *Trends Microbiol.* **4**, 22–29 (1996).
177. Heppner, F. L. *et al.* Transepithelial prion transport by M cells. *Nat. Med.* **7**, 976–977 (2001).
178. Kujala, P. *et al.* Prion uptake in the gut: identification of the first uptake and replication sites. *PLoS Pathog.* **7**, e1002449 (2011).
179. Takakura, I. *et al.* Orally administered prion protein is incorporated by m cells and spreads into lymphoid tissues with macrophages in prion protein knockout mice. *Am. J. Pathol.* **179**, 1301–1309 (2011).
180. Donaldson, D. S. *et al.* M cell-depletion blocks oral prion disease pathogenesis. *Mucosal Immunology* **5**, 216–225 (2012).
181. Jeffrey, M. *et al.* Transportation of prion protein across the intestinal mucosa of scrapie-susceptible and scrapie-resistant sheep. *J. Pathol.* **209**, 4–14 (2006).
182. Mishra, R. S. *et al.* Protease-resistant human prion protein and ferritin are cotransported across Caco-2 epithelial cells: implications for species barrier in prion uptake from the intestine. *J. Neurosci.* **24**, 11280–11290 (2004).
183. Theil, E. C. Ferritin: Structure, Gene Regulation, and Cellular Function in Animals, Plants, and Microorganisms. *Annu. Rev. Biochem.* **56**, 289–315 (1987).
184. Mowat, A. M. Anatomical basis of tolerance and immunity to intestinal antigens. *Nat. Rev. Immunol.* **3**, 331–341 (2003).
185. Kiyono, H. & Fukuyama, S. Nalt- versus peyer's-patch-mediated mucosal immunity. *Nat. Rev. Immunol.* **4**, 699–710 (2004).
186. Neutra, M., Frey, A. & Kraehenbuhl, J. Epithelial M Cells: Gateways for Mucosal Infection and Immunization. *Cell* **86**, 345–348 (1996).
187. Maignien, T. *et al.* Role of gut macrophages in mice orally contaminated with scrapie or BSE. *Int. J. Pharm.* **298**, 293–304 (2005).
188. Huang, F. P., Farquhar, C. F., Mabbott, N. A., Bruce, M. E. & MacPherson, G. G. Migrating intestinal dendritic cells transport PrPSc from the gut. *J. Gen. Virol.* **83**, 267–271 (2002).
189. Carp, R. I. Transmission of scrapie by oral route: effect of gingival scarification. *Lancet* **1**, 170–171 (1982).
190. Taylor, D. M., McConnell, I. & Fraser, H. Scrapie infection can be established readily through skin scarification in immunocompetent but not immunodeficient mice. *J. Gen. Virol.* **77**, 1595–1599 (1996).
191. Mohan, J., Hopkins, J. & Mabbott, N. A. Skin‐derived dendritic cells acquire and degrade the scrapie agent following in vitro exposure. *Immunology* (2005).
192. Cordier-Dirikoc, S. & Chabry, J. Temporary Depletion of CD11c+ Dendritic Cells Delays Lymphoinvasion after Intraperitonal Scrapie Infection. *J. Virol.* **82**, 8933–8936 (2008).
193. Aucouturier, P. Infected splenic dendritic cells are sufficient for prion transmission to the CNS in mouse scrapie. *J. Clin. Invest.* **108**, 703–708 (2001).

194. Bradford, B. M., Sester, D. P., Hume, D. A. & Mabbott, N. A. Defining the anatomical localisation of subsets of the murine mononuclear phagocyte system using integrin alpha X (Itgax, CD11c) and colony stimulating factor 1 receptor (Csf1r, CD115) expression fails to discriminate dendritic cells from macrophages. *Immunobiology* **216**, 1228–1237 (2011).
195. Probst, H. C. *et al.* Histological analysis of CD11c-DTR/GFP mice after in vivo depletion of dendritic cells. *Clin. Exp. Immunol.* **141**, 398–404 (2005).
196. Carp, R. I. & Callahan, S. M. In vitro interaction of scrapie agent and mouse peritoneal macrophages. *Intervirology* **16**, 8–13 (1981).
197. Tagliavini, F *et al.* Amyloid protein of Gerstmann-Sträussler-Scheinker disease (Indiana kindred) is an 11 kd fragment of prion protein with an N-terminal glycine at codon 58. *EMBO J.* **10**, 513–519 (1991).
198. Chen, S. G. *et al.* Truncated forms of the human prion protein in normal brain and in prion diseases. *J. Biol. Chem.* **270**, 19173–19180 (1995).
199. De Gioia, L. *et al.* Conformational polymorphism of the amyloidogenic and neurotoxic peptide homologous to residues 106-126 of the prion protein. *J. Biol. Chem.* **269**, 7859–7862 (1994).
200. Forloni, G. *et al.* A neurotoxic prion protein fragment induces rat astroglial proliferation and hypertrophy. *Eur. J. Neurosci.* **6**, 1415–1422 (1994).
201. Selvaggini, C. *et al.* Molecular characteristics of a protease-resistant, amyloidogenic and neurotoxic peptide homologous to residues 106-126 of the prion protein. *Biochem. Biophys. Res. Commun.* **194**, 1380–1386 (1993).
202. Tagliavini, F. *et al.* Synthetic peptides homologous to prion protein residues 106-147 form amyloid-like fibrils in vitro. *Proc. Natl. Acad. Sci. U.S.A.* **90**, 9678–9682 (1993).
203. Brown, A. R. *et al.* Inducible cytokine gene expression in the brain in the ME7/CV mouse model of scrapie is highly restricted, is at a strikingly low level relative to the degree of gliosis and occurs only late in disease. *J. Gen. Virol.* **84**, 2605–2611 (2003).
204. Campbell, I. L. I., Eddleston, M. M., Kemper, P. P., Oldstone, M. B. M. & Hobbs, M. V. M. Activation of cerebral cytokine gene expression and its correlation with onset of reactive astrocyte and acute-phase response gene expression in scrapie. *J. Virol.* **68**, 2383–2387 (1994).
205. Walsh, D. T. D., Betmouni, S. S. & Perry, V. H. V. Absence of detectable IL-1beta production in murine prion disease: a model of chronic neurodegeneration. *J. Neuropathol. Exp. Neurol.* **60**, 173–182 (2001).
206. Williams, A., Van Dam, A. M., Ritchie, D., Eikelenboom, P. & Fraser, H. Immunocytochemical appearance of cytokines, prostaglandin E2 and lipocortin-1 in the CNS during the incubation period of murine scrapie correlates with progressive PrP accumulations. *Brain Res.* **754**, 171–180 (1997).
207. Williams, A. E., Lawson, L. J., Perry, V. H. & Fraser, H. Characterization of the microglial response in murine scrapie. *Neuropathol. Appl. Neurobiol.* **20**, 47–55 (1994).
208. Peyrin, J. M. *et al.* Microglial cells respond to amyloidogenic PrP peptide by the production of inflammatory cytokines. *Neuroreport* **10**, 723–729 (1999).
209. Bacot, S. M. Activation by prion peptide PrP106-126 induces a NF- B-driven proinflammatory response in human monocyte-derived dendritic cells. *J. Leukoc. Biol.* **74**, 118–125 (2003).

210. Zhou, X. M., Xu, G. X. & Zhao, D. M. In vitro effect of prion peptide PrP 106-126 on mouse macrophages: Possible role of macrophages in transport and proliferation for prion protein. *Microb. pathog.* **44,** 129-134 (2008).
211. Kim, J. I. *et al.* Expression of cytokine genes and increased nuclear factor-kappa B activity in the brains of scrapie-infected mice. *Brain Res. Mol. Brain Res.* **73**, 17–27 (1999).
212. Kordek, R. *et al.* Heightened expression of tumor necrosis factor alpha, interleukin 1 alpha, and glial fibrillary acidic protein in experimental Creutzfeldt-Jakob disease in mice. *Proc. Natl. Acad. Sci. U.S.A.* **93**, 9754–9758 (1996).
213. Fabrizi, C., Silei, V., Menegazzi, M. & Salmona, M. The stimulation of inducible nitric-oxide synthase by the prion protein fragment 106-126 in human microglia is tumor necrosis factor-alpha-dependent and involves p38 mitogen-activated protein kinase. *J. Biol. Chem.* **276,** 25692-25696 (2001).
214. Prinz, M. *et al.* Prion pathogenesis in the absence of Toll-like receptor signalling. *EMBO Rep.* **4**, 195–199 (2003).
215. Clarke, M. C. & Haig, D. A. Multiplication of Scrapie Agent in Mouse Spleen. *Res. Vet. Sci.* **12**, 195–& (1971).
216. Hill, A. F. *et al.* Investigation of variant Creutzfeldt-Jakob disease and other human prion diseases with tonsil biopsy samples. *Lancet* **353**, 183–189 (1999).
217. Eklund, C. M., Kennedy, R. C. & Hadlow, W. J. Pathogenesis of scrapie virus infection in the mouse. *J. Infect. Dis.* **117**, 15–22 (1967).
218. Dickinson, A. G. A. & Fraser, H. H. Scrapie: effect of Dh gene on incubation period of extraneurally injected agent. *Heredity (Edinb)* **29**, 91–93 (1972).
219. Fraser, H. & Dickinson, A. G. Studies of the lymphoreticular system in the pathogenesis of scrapie: the role of spleen and thymus. *J. Comp. Pathol.* **88**, 563–573 (1978).
220. Kimberlin, R. H. & Walker, C. A. The role of the spleen in the neuroinvasion of scrapie in mice. *Virus Res.* **12**, 201–211 (1989).
221. Mohri, S., Handa, S. & Tateishi, J. Lack of effect of thymus and spleen on the incubation period of Creutzfeldt-Jakob disease in mice. *J. Gen. Virol.* **68**, 1187–1189 (1987).
222. Kimberlin, R. H. & Walker, C. A. Pathogenesis of Scrapie (Strain 263K) in Hamsters Infected Intracerebrally, Intraperitoneally or Intraocularly. *J. Gen. Virol.* **67**, 255–263 (1986).
223. Bradley, R. BSE transmission studies with particular reference to blood. *Dev. Biol. Stand.* **99**, 35–40 (1999).
224. Benestad, S. L. *et al.* Cases of scrapie with unusual features in Norway and designation of a new type, Nor98. *Vet. Rec.* **153**, 202–208 (2003).
225. Lavelle, G. C. G., Sturman, L. L. & Hadlow, W. J. W. Isolation from mouse spleen of cell populations with high specific infectivity for scrapie virus. *Infect. Immune.* **5**, 319–323 (1972).
226. Clarke, M. C. & Kimberlin, R. H. Pathogenesis of mouse scrapie: Distribution of agent in the pulp and stroma of infected spleens. *Vet. Microbiol.* **9**, 215–225 (1984).
227. Fraser, H. & Farquhar, C. F. Ionising radiation has no influence on scrapie incubation period in mice. *Vet. Microbiol.* **13**, 211–223 (1987).
228. Klein, M. A. M. *et al.* PrP expression in B lymphocytes is not required for prion neuroinvasion. *Nat. Med.* **4**, 1429–1433 (1998).

229. Raeber, A. J. *et al.* PrP-dependent association of prions with splenic but not circulating lymphocytes of scrapie-infected mice. *EMBO J.* **18**, 2702–2706 (1999).
230. Montrasio, F. *et al.* B lymphocyte-restricted expression of prion protein does not enable prion replication in prion protein knockout mice. *Proc. Natl. Acad. Sci. U.S.A.* **98**, 4034–4037 (2001).
231. Kitamoto, T., Muramoto, T., Mohri, S., Doh-ura, K. & Tateishi, J. Abnormal isoform of prion protein accumulates in follicular dendritic cells in mice with Creutzfeldt-Jakob disease. *J. Virol.* **65**, 6292–6295 (1991).
232. Mabbott, N. A., Young, J., McConnell, I. & Bruce, M. E. Follicular dendritic cell dedifferentiation by treatment with an inhibitor of the lymphotoxin pathway dramatically reduces scrapie susceptibility. *J. Virol.* **77**, 6845–6854 (2003).
233. Mohan, J., Bruce, M. E. & Mabbott, N. A. Follicular dendritic cell dedifferentiation reduces scrapie susceptibility following inoculation via the skin. *Immunology* **114**, 225–234 (2005).
234. McCulloch, L. *et al.* Follicular Dendritic Cell-Specific Prion Protein (PrPc) Expression Alone Is Sufficient to Sustain Prion Infection in the Spleen. *PLoS Pathog.* **7**, e1002402 (2011).
235. Manuelidis, L. *et al.* Follicular dendritic cells and dissemination of Creutzfeldt-Jakob disease. *J. Virol.* **74**, 8614–8622 (2000).
236. Montrasio, F. *et al.* Impaired prion replication in spleens of mice lacking functional follicular dendritic cells. *Science* **288**, 1257–1259 (2000).
237. Browning, J. L. Inhibition of the lymphotoxin pathway as a therapy for autoimmune disease. *Immunol. Rev.* **223**, 202–220 (2008).
238. Pasparakis, M. M., Alexopoulou, L. L., Episkopou, V. V. & Kollias, G. G. Immune and inflammatory responses in TNF alpha-deficient mice: a critical requirement for TNF alpha in the formation of primary B cell follicles, follicular dendritic cell networks and germinal centers, and in the maturation of the humoral immune response. *J. Exp. Med.* **184**, 1397–1411 (1996).
239. Aguzzi, A. & Heikenwalder, M. Pathogenesis of prion diseases: current status and future outlook. *Nat. Rev. Micro.* **4**, 765–775 (2006).
240. Tew, J. G. *et al.* Follicular dendritic cells and presentation of antigen and costimulatory signals to B cells. *Immunol. Rev.* **156**, 39–52 (1997).
241. Heinen, E. E. *et al.* Retention of immune complexes by murine lymph node or spleen follicular dendritic cells. Role of antibody isotype. *Scand. J. Immunol.* **24**, 327–334 (1986).
242. Mandels, T. E., Phippsi, R. P., Abbot, A. & Tew, J. G. The Follicular Dendritic Cell: Long Term Antigen Retention During Immunity. *Immunol. Rev.* **53**, 29–59 (1980).
243. Prinz, M. *et al.* Lymph nodal prion replication and neuroinvasion in mice devoid of follicular dendritic cells. *Proc. Natl. Acad. Sci. U.S.A.* **99**, 919–924 (2002).
244. Heikenwalder, M. *et al.* Lymphotoxin-Dependent Prion Replication in Inflammatory Stromal Cells of Granulomas. *Immunity* **29**, 998–1008 (2008).
245. Ricklin, D., Hajishengallis, G., Yang, K. & Lambris, J. D. Complement: a key system for immune surveillance and homeostasis. *Nat. Immunol.* **11**, 785–797 (2010).
246. Sarma, J. V. & Ward, P. A. The complement system. *Cell Tissue Res.* **343**, 227–235 (2010).

247. Janeway, C. A. J. & Medzhitov, R. Innate Immune Recognition. *Annu. Rev Immunol.* **20**, 197-216 (2002).
248. Carroll, M. C. The complement system in regulation of adaptive immunity. *Nat. Immunol.* **5**, 981–986 (2004).
249. Dunkelberger, J. R. & Song, W. C. Complement and its role in innate and adaptive immune responses. *Cell Res.* **20**, 34–50 (2009).
250. Molina, H. *et al.* Markedly impaired humoral immune response in mice deficient in complement receptors 1 and 2. *Proc. Natl. Acad. Sci. U.S.A.* **93**, 3357–3361 (1996).
251. Reynes, M. *et al.* Human follicular dendritic cells express CR1, CR2, and CR3 complement receptor antigens. *J. Immunol.* **135**, 2687–2694 (1985).
252. Humphrey, J. H., Grennan, D. & Sundaram, V. The origin of follicular dendritic cells in the mouse and the mechanism of trapping of immune complexes on them. *Eur. J. Immunol.* **14**, 859–864 (1984).
253. Park, C. S. & Choi, Y. S. How do follicular dendritic cells interact intimately with B cells in the germinal centre? *Immunology* **114**, 2–10 (2005).
254. Lambris, J. D., Ricklin, D. & Geisbrecht, B. V. Complement evasion by human pathogens. *Nat. Rev. Micro.* **6**, 132–142 (2008).
255. Oliva, C., Turnbough, C. L. & Kearney, J. F. CD14-Mac-1 interactions in Bacillus anthracis spore internalization by macrophages. *Proc. Natl. Acad. Sci. U.S.A.* **106**, 13957–13962 (2009).
256. Wang, M. *et al.* Fimbrial proteins of porphyromonas gingivalis mediate in vivo virulence and exploit TLR2 and complement receptor 3 to persist in macrophages. *J. Immunol.* **179**, 2349–2358 (2007).
257. Dumestre-Perard, C. *et al.* Activation of classical pathway of complement cascade by soluble oligomers of prion. *Cell Microbiol.* **9**, 2870–2879 (2007).
258. Sim, R. B., Kishore, U., Villiers, C. L., Marche, P. N. & Mitchell, D. A. C1q binding and complement activation by prions and amyloids. *Immunobiology* **212**, 355–362 (2007).
259. Erlich, P. *et al.* Complement Protein C1q Forms a Complex with Cytotoxic Prion Protein Oligomers. *J. Biol. Chem.* **285**, 19267–19276 (2010).
260. Blanquet-Grossard, F., Thielens, N. M., Vendrely, C., Jamin, M. & Arlaud, G. J. Complement protein C1q recognizes a conformationally modified form of the prion protein. *Biochemistry* **44**, 4349–4356 (2005).
261. Ligios, C. *et al.* PrPSc in mammary glands of sheep affected by scrapie and mastitis. *Nat. Med.* **11**, 1137–1138 (2005).
262. Heikenwalder, M. *et al.* Chronic lymphocytic inflammation specifies the organ tropism of prions. *Science* **307**, 1107–1110 (2005).
263. Kovacs, G. G. *et al.* Creutzfeldt-Jakob disease and inclusion body myositis: Abundant disease-associated prion protein in muscle. *Ann. Neurol.* **55**, 121–125 (2003).
264. Seeger, H. *et al.* Coincident scrapie infection and nephritis lead to urinary prion excretion. *Science* **310**, 324–326 (2005).
265. Lacroux, C. *et al.* Prions in milk from ewes incubating natural scrapie. *PLoS Pathog.* **4**, e1000238 (2008).

CHAPTER 2:

INCUNABULAR IMMUNOLOGICAL EVENTS IN PRION TRAFFICKING[1]

Summary

While prions probably interact with the innate immune system immediately following infection, little is known about this initial confrontation. Here we investigated incunabular events in lymphotropic and intranodal prion trafficking by following highly enriched, fluorescent prions from infection sites to draining lymph nodes. We detected biphasic lymphotropic transport of prions from the initial entry site upon peripheral prion inoculation. Prions arrived in draining lymph nodes cell autonomously within two hours of intraperitoneal administration. Monocytes and dendritic cells (DCs) required Complement for optimal prion delivery to lymph nodes hours later in a second wave of prion trafficking. B cells constituted the majority of prion-bearing cells in the mediastinal lymph node by six hours, indicating intranodal prion reception from resident DCs or subcapsulary sinus macrophages or directly from follicular conduits. These data reveal novel, cell autonomous prion lymphotropism, and a prominent role for B cells in intranodal prion movement.

Introduction

Prion diseases, also known as transmissible spongiform encephalopathies (TSEs), are fatal neurodegenerative diseases that affect humans, cervids, bovids, and ovids. According to the protein only hypothesis, the causative agent of prion diseases is a misfolded, abnormal isoform

---

[1] Previously published: Michel, B. *et al.* Incunabular immunological events in prion trafficking. *Sci. Rep.* **2**, 440 (2012). http://www.nature.com/srep/2012/120606/srep00440/pdf/srep00440.pdf

of a normal, host-encoded protein[1]. Termed PrP^{C}, this 30-35 kDa glycoprotein is expressed most abundantly in the central nervous (CNS) and lymphoreticular systems, with lower expression in other tissues. The absolute requirement of PrP^{C} expression to generate prion diseases[2] and the lack of instructional nucleic acid make prions unique among infectious agents. The pathologic, protease-resistant isoform (PrP^{Sc}) typically accumulates in the CNS and secondary lymphoid tissues of infected animals. Upon neuroinvasion, prion diseases typically progress from transformation of PrP^{C} to PrP^{Sc} to neuropathology including amyloid plaque formation, astrogliosis, and neuronal cell loss to inevitable death.

Before prions accumulate on follicular dendritic cells (FDCs) in secondary lymphoid organs (SLOs)[3,4], they most likely interact with the innate immune system at the initial site of infection. Complement proteins like C3 and C1q are important innate immune molecules shown to bind foreign bodies and altered-self-particles[5], including protein amyloids[6] and high density prion protein[7]. C1q, C3 and the Complement receptor CD21/35 have been shown to expedite peripherally-induced prion pathogenesis[8-10]. These data suggest that initial events in prion infection include Complement opsonization and inflammatory immune cell uptake and transport of prions from initial infection sites to draining lymph nodes, where peripheral prion replication occurs. Complement may bind prions and enhance uptake by antigen presenting cells, as well as retention and replication of prions on FDCs in germinal centers.

Soluble complement proteins opsonize pathogens and facilitate their uptake by immune cells such as dendritic cells (DCs), macrophages (MΦs), and monocytes surveying nonlymphoid tissues. These innate immune responses represent the first line of defense against invading pathogens. Because these immune cells act as sentinels for microbial infections, investigators have implicated them as likely candidates for the uptake and spread of prions throughout the body. Indeed, DCs, MΦs, and monocytes have been reported to both positively and negatively impact prion disease pathogenesis [8,9].

Although substantial evidence links immune cells to prion disease, little data directly support a role for these cells in uptake and transport of prions hours after initial exposure. Because incunabular interactions between pathogens and immune cells often dictate the outcome of infection, insight into interactions of prions with the mononuclear phagocyte system at initial infection sites and within lymph nodes is vital to understanding incunabular events in prion infection. In this study we analyzed the inflammatory response to prions that occurs within hours of infection, including lymphotropic and intranodal prion trafficking.

Materials and Methods

Mice

PrP$^{-/-}$ (C57BL/6 X129sv), Tg(cerPrP)5037 and *C1q*$^{-/-}$ mice were generated as previously described[33-35]. FVB, and *C3*$^{-/-}$ (*C3*tm1Crr/J) mice were purchased from The Jackson Laboratory (Bar Harbor, ME). All mice were bred and maintained at Lab Animal Resources, accredited by the Association for Assessment and Accreditation of Lab Animal Care International, in accordance with protocols approved by the Institutional Animal Care and Use Committee at Colorado State University.

Fluorescent Prions

Enrichment and fluorochrome labeling of prions were performed as previously described[36-38] with slight modifications. 10% Elk brain homogenate prepared in 0.32M sucrose, 150 uM NaCl, 4 uM EDTA diluted in PBS (PMCA buffer) were centrifuged at 3,000g for 10 minutes at 4°. The resulting supernatant were removed and saved and the pellet treated in PMCA buffer then centrifuged again at 3,000g for 10 minutes at 4°C. Supernatants were then pooled and centrifuged at 100,000g for 1 hr at 4°C and the resulting pellet treated with triton X-100 at 0°C at a final detergent concentration of 2% wt/vol, bringing the protein concentration to 5mg/ml in TBS measured by the Bradford assay. The sample was then chilled on ice for 30 minutes and centrifuged at 100,000g for 30 minutes at 0°C. The pellet was then washed twice at 0°C in 10mM Tris HCL, 0.1 NaCl, 1mM EDTA, 5mM PMSF at a pH of 7.4 with and without 2% Triton X-100. The supernatant was discarded and the pellet resuspended in PBS containing 1% (wt/vol) sarcosyl and protease inhibitors and stirred for 2 hours at 37°C before centrifuging through 0.32M sucrose in PBS at 100,000g for 60 minutes at 10°C.   The pellet was resuspended in a 2.3M NACl, 5% sarcosyl solution and sonicated 5 times at 40 second bursts. The fractions were centrifuged at 13,000g for 15 minutes at 4°C, washed twice with TBS and stored at -70°C or conjugated to Dylight 649 using the Dylight Antibody Labeling Kit according to manufacturere's protocol (Thermo Scientific Pierce).

PK digestion and western blotting

Samples were digested with 50 µg/ml PK (Roche) for 30 min at 37°C. The reaction was stopped by adding lithium dodecyl sulfate sample loading buffer (Invitrogen) and incubating at 95 °C for 5 min. Proteins were electrophoretically separated through 12% sodium dodecyl sulfate-polyacrylamide gels (Invitrogen), and transferred to polyvinylidene difluoride membranes (Millipore). Non-specific membrane binding was blocked by incubation in 5% milk blocking solution (Bio-Rad) for 1 h. Membranes were then incubated for 1 h at room temperature with horseradish peroxidase-conjugated Bar224 anti-PrP monoclonal antibody (SPI bio) diluted 1:20,000 in Superblock (Pierce), washed 6 X10 min in PBS with 0.2% Tween 20, and incubated for 5 min with enhanced chemiluminescent substrate (Millipore). Membranes were digitally photographed using the FujiDoc gel documentation system equipped with a cooled charge-coupled diode camera (Fuji).

Prion Inoculations

Prion Inoculations were performed as previously described[37,38]. Briefly, ice were inoculated IP with 100µl of PBS, or various concentrations of red fluorescent microspheres (Flourophex) or a suspension of prion aggregates described above.

Live animal imaging

Mice were inoculated SC and PO with indicated amounts of fluorescent beads or prions, and visualized while anesthetized with 3 L/min Isofluorane in an IVIS 100 live animal imager (Caliper Life Sciences,Hopkinton, MA) at the indicated time points. We analyzed images using Living Image 4.0 software (Caliper).

Intraperitoneal wash

Immediately after euthanization of mice by $C0_2$ asphyxiation 10ml of PBS was injected into the peritoneal cavity of each mouse using a 12 ml syringe and 25 gauge x 1/2 in polypropylene hub hypodermic needle. The Mice were set on a rocker or gently rocked manually for 2 minutes. As much PBS as possible was recovered using the same 12ml syringe and a 16 gauge X 1½ in polypropylene hub hypodermic needle.

The peritoneal wash fluid was collected in a 15 ml conical tube (falcon) and centrifuged at 250 x g for five minutes. The supernatant was discarded and the pellet re-suspended in 1 ml fluorescence activated cell sorting (FACS) buffer and transferred to a 1.5 ml eppendorf tube for staining.

Isolation of cells from tissues

Following intraperitoneal wash the mediastinal lymph nodes (and where appropriate inguinal, spleen and mesenteric lymph nodes) were removed from the mice. Lymph nodes were stored in 1 ml RMPI medium on ice for no longer than 30 min prior to separation of cells. The lymph nodes were transferred to a 40 µm nylon cell strainer (Falcon ref 352340) with 1-3 ml PBS. Lymph nodes were pressed through the screen with the plunger of a sterile 1 ml syringe. Lose cells were rinsed through the screen with an additional 1-2 ml PBS and the filtrate was transferred to a 15 ml conical tube. The plate was washed with 4-6 ml of PBS and transferred to the same 15 ml conical. The 15 ml conical containing the single cell suspension from the lymph node was spun at 1000 rpm for 5 min. The supernatant was discarded and the pellet re-suspended in 1 ml FACS buffer and transferred to a 1.5 ml eppendorf tube for staining.

Antibody staining of cells

10^6 cells were aliquoted from single cell suspensions were pelleted at 250 x g for 5 minutes on a bench top centrifuge. Samples were washed twice in FACS buffer (0.1% BSA, 10mM EDTA in 1XPBS) by resuspending the cell pellet in 1 ml FACS followed by centrifugation at 1000 rpm for 5 minutes. Fc receptors were blocked using 2ng/ml solution of Purified rat anti-mouse CD16/CD32 (BD Pharmingen) and incubated on ice for 20 min. Fc block was removed by washing once with FACS buffer before staining solution was added to cell pellets. Cell pellets were stained using 50ul of a 1ng/mL solution of the antibodies listed in Table S1. Cells were washed twice following staining to remove unbound antibody and red blood cells were lysed by adding 1 ml of ACK buffer (150 mM NH_4Cl, 10 mM $KHCO_3$, 0.1 mM EDTA) to the cell pellet and immediately centrifuging a250 x g for 5 minutes. The supernatant was removed and cell pellets were resuspended in 1X FACS for analysis.

Confocal Microscopy

Antibody-stained peritoneal cells were cytospun onto glass slides and mounted with ProLong Gold medium (Life Technologies, Grand Island, NY) and dried overnight at 4°C. We acquired images with a LSM 510 Meta confocal microscope and software (Zeiss).

Flow cytometric and statistical analyses

Flow cytometry data was acquired using a DakoCytomation CyAnADP flow cytometer and analyzed using FlowJo version 8 (Tree Star, Ashland, OR). Nonparametric statistical analyses were performed using GraphPad Prism 5 (La Jolla, CA).

.

Table 2.1

REAGENT	FLUOROCHROME	CLONE	VENDOR
Prion rods	DyLight 649	E1/E2	proprietary
1 µm beads	AlexaFluor 660	N/A	Phosphorex
Antibodies			
CD11b	Phycoerythrin-Cy7	M1/70	BD Bioscience
	eFluor 605NC	ICRF44	eBiosciences
CD11c	eFluor 450	N418	eBiosciences
	Alexa 488	N418	Biolegend
Ly6C	Fluoroisothiocynate	ER-MP20	ABD Serotec
	Alexa 488	ER-MP20	ABD Serotec
	Alexa 700	HK1.4	ABD Serotec
Ly6G	PerCP-Cy5.5	1A8	BD Bioscience
	Alexa 488	RB6-8C5	ABD Serotec
CD21	eFluor 450	4.00E+03	eBiosciences
	DyLight 488	7G6	BD Bioscience
B220	Allophycocyanin-Cy7	6B2	BD Bioscience
CD3	Alexa 488	KD3	ABD Serotec
CD5	Fluoroisothiocynate	YTS 121.5.2	ABD Serotec
CD8	R-Phycoerythrin	53-6.7	BD Bioscience
CD23	R-Phycoerythrin	B3B4	ABD Serotec
CD169	Alexa 488	7D2	ABD Serotec
Rat IgG1	Alexa 488	RTK2071	Biolegend
Hamster IgG1	Alexa 488	HTK888	Biolegend

Results

Enrichment and fluorochrome conjugation of aggregated prion rods

In order to monitor prion trafficking from inoculation sites to draining lymph nodes, we first enriched prion rods from a brain of an elk terminally sick with CWD from one liter of 10% crude brain homogenate, concentrating prion aggregate volume 10^4-fold to a final volume of 100 μl using detergent solubilization and ultracentrifugation through a sucrose cushion (figure 2.1A). We enriched aggregated prion rods approximately 10^3-fold (compare lanes 1 and 2 to 3 and 4). Like the crude brain homogenate, purified prion rods showed partial PK resistance (lanes 2 and 4). Normal brain homogenate contained no PK-resistant PrP^C bands (lane 6). Intracranial injection of 1 μg of enriched, sonicated prion aggregates resulted in terminal disease in susceptible mice 122 ± 5 (n=5) days post inoculation (DPI) compared to 157 ± 16 DPI for mice inoculated with 30 μg of 1% crude brain homogenate (n=8, p=.0003). We then conjugated enriched prions to Dylight 649 fluorochrome (figure 2.1B). To evaluate the stability of the fluorochrome, we treated conjugated prions with PK (figure 2.1B, lanes 2 and 3) at physiological (lane 2) or supraphysiological temperatures (lane 3). DyLight 649 still fluoresced even after SDS and PK treatment followed by incubation at 95^OC. In addition to demonstrating partial SDS and PK resistance (lanes 2 and 3), fluorescent prions could also aggregate into high molecular weight oligomers (lane 1).

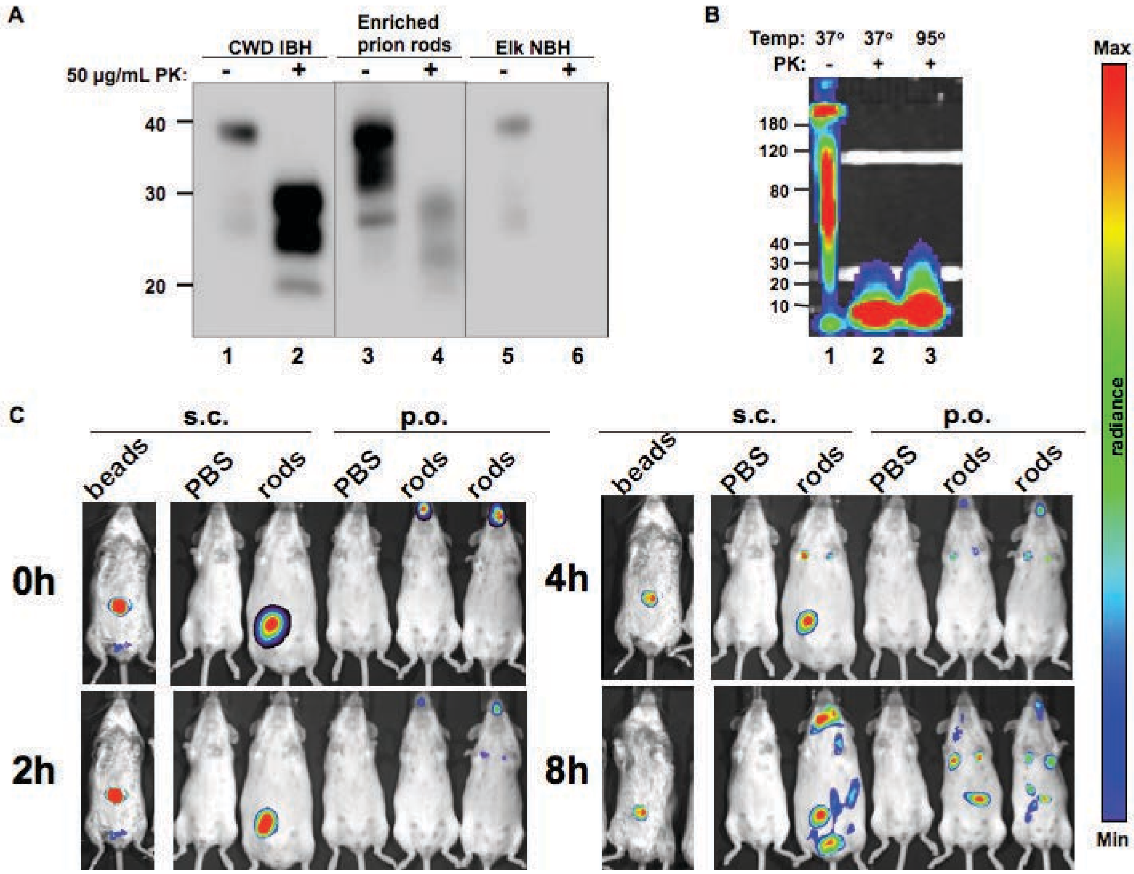

Figure 2.1 Purification and conjugation of prion rods from infected brain homogenate and real-time whole-mouse *in vivo* imaging. A. Western blot analysis depicting CWD infected elk brain homogenate used as starting material (5 µg in lane 1 and 100 µg in lane 2) from which we enriched prion rod aggregates (100 ng in lanes 3 and 4). Lanes 5 and 6 show 100 µg of control elk normal brain homogenate. **B.** SDS page gel depicting fluorochrome tagged prion rods. Prions treated at 37°C without Proteinase K (PK, lane 1) or with PK (lane 2), and at 95°C with PK (lane 3). Molecular weight markers are shown in kilodaltons to the left of the blots. **C.** *In vivo* detection of prion rods by epifluorescent whole-body optical imaging. Representative images of tg5037 mice injected orally or subcutaneously with PBS or fluorescent prion rods or 1 µm polystyrene microspheres (beads). Images were acquired at indicated time points after injection.

Prion trafficking in live animals

Resistance of fluorochrome conjugated prion rods to proteolytic and thermal degradation enabled us to visualize and track these fluorescent prions *in vivo* using whole mouse live imaging (Figure 2.1C). Inoculation of 2 and 5 μg of sonicated, fluorescent prions via subcutaneous (SC) and *per os* (PO) routes, respectively, resulted in prion trafficking to areas consistent with the location of axillary lymph nodes within 2 hours post inoculation (HPI) PO and 4 HPI SC. Within 8 HPI SC, prions disseminate to areas consistent with the location of submandibular lymph nodes, spleen, and bladder. Prion trafficking from the oral cavity after PO inoculation was restricted primarily to areas consistent with the location of Peyer's patches and axillary and mesenteric lymph nodes. We observed little or no dissemination of 10 μg of 1 μm fluorescent polystyrene microspheres (beads) from their SC injection site, indicating specific trafficking of prion rods.

Immune cells capture prions from the peritoneal cavity 2 HPI

Particulate antigen can be transported to SLOs via cell dependent and independent mechanisms [10,11]. The presence of prions, but not beads, in various locations consistent with lymph nodes that drain the injection site suggested active uptake and trafficking by migratory immune cells. To investigate this possibility, we first assessed whether immune cells associated with fluorescent prions hours after injection. Isolation of adequate cell numbers from subcutaneous tissue and the oral cavity proved difficult for characterizing innate immune cells at these injection sites. We therefore chose the peritoneal cavity (PC) as an alternative inoculation route because it provides an optimal site for collecting immune cells. We inoculated mice intraperitoneally (IP) with 5 μg of fluorescent prions, collected cells by peritoneal lavage 2 HPI and analyzed them by flow cytometry (Figures 2.2 and 2.3).

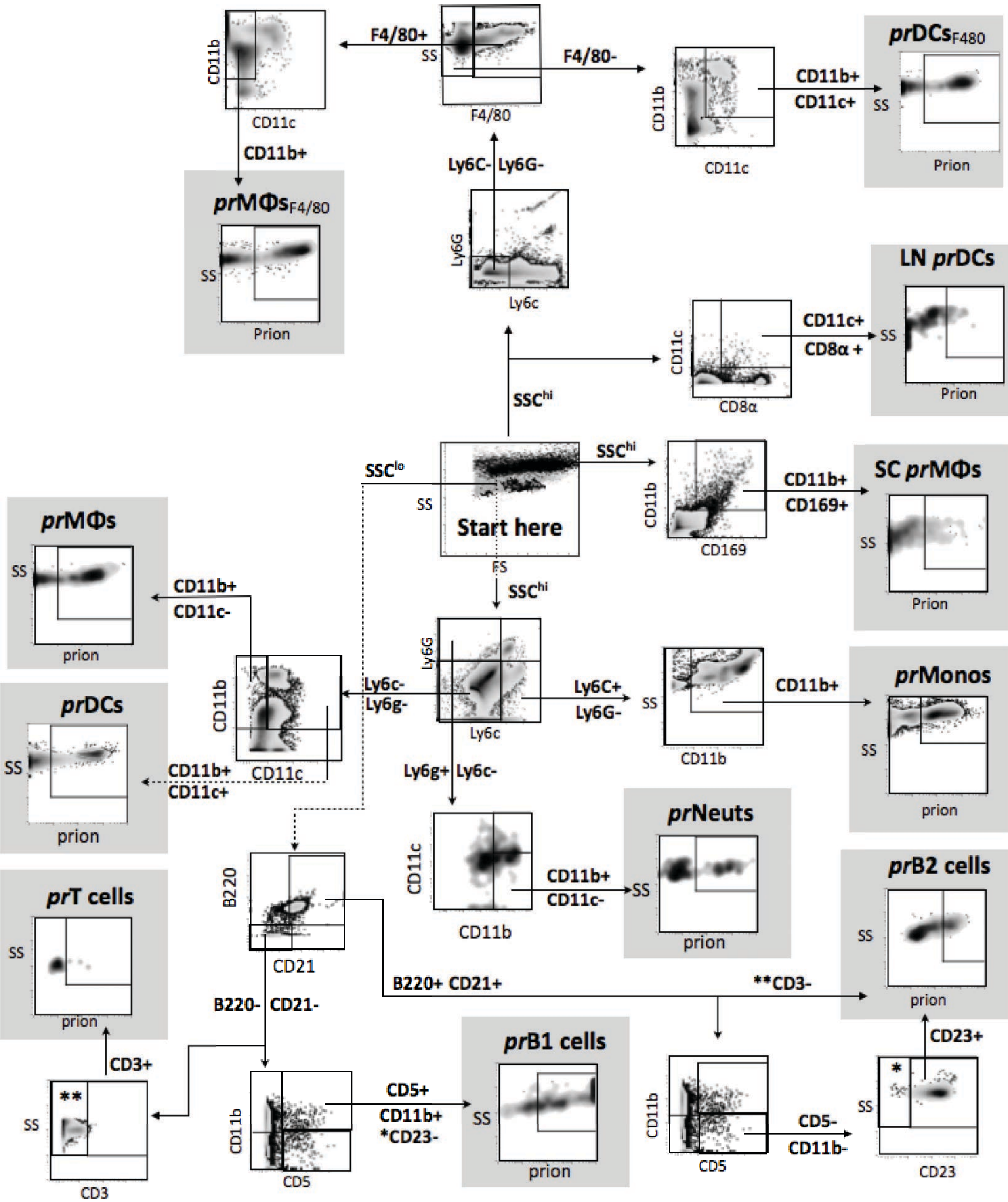

Figure 2.2. Gating strategy for flow cytometry. Side scatter parameter (SS or SSC) and all other axes are log scale except forward scatter (FS). *CD23 gate not shown, but was set identically to the indicated gate. **CD3 gate not shown, but was set identically to the indicated gate. MΦs$_{F4/80}$ and DCs$_{F4/80}$ cells were identified using F4/80 gating. *pr*, prionophilic; MΦs, macrophages; DCs, dendritic cells; LN, lymph node; SC, Subcapsulary.

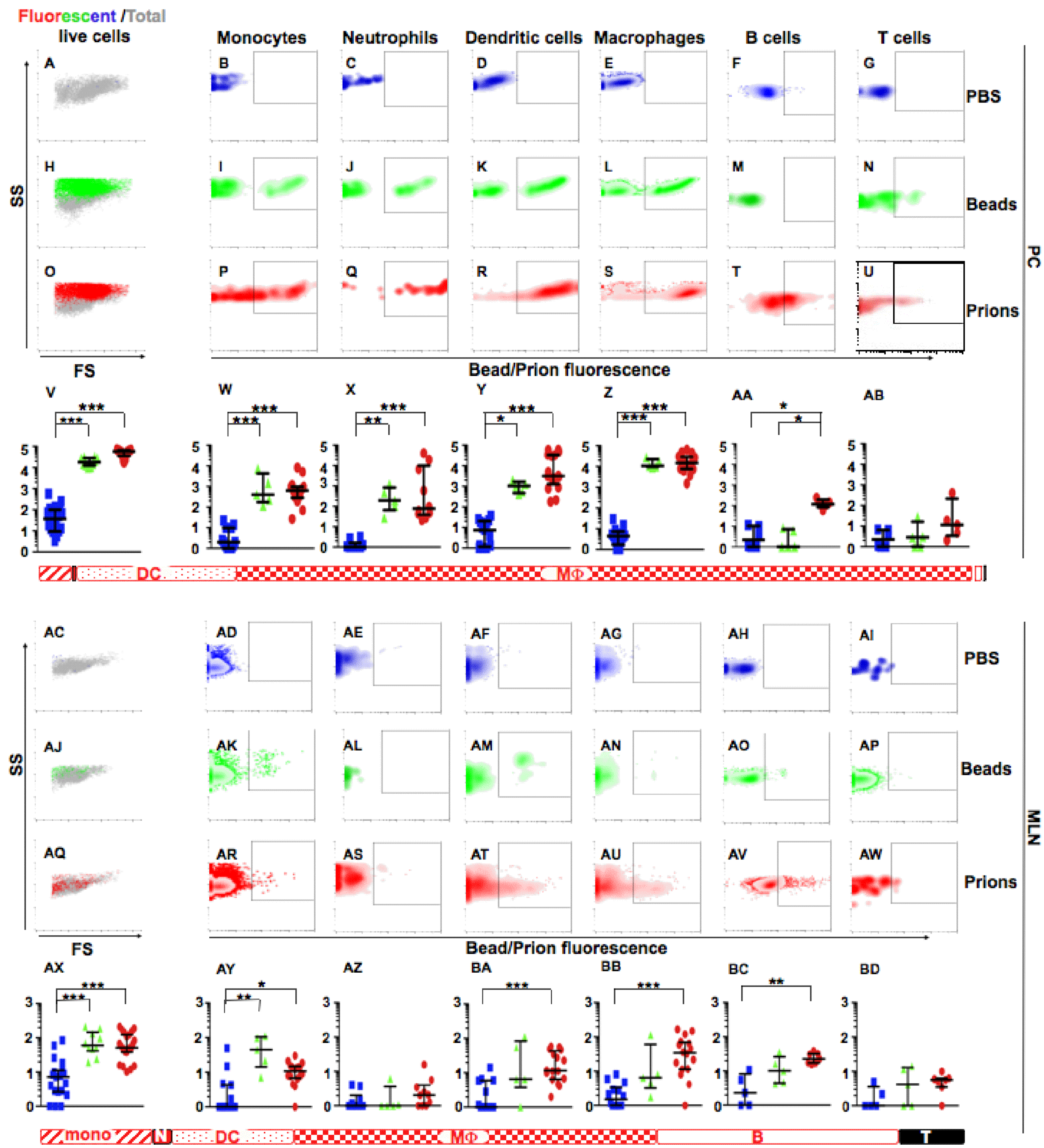

Figure 2.3. Flow cytometric analysis of immune cells trafficking prions from the PC to MedLN 2 HPI. PBS (rows a-g, v-ab, ac-ai, and ax-bd), fluorescent beads (h-n, v-ab, aj-ap, and ax-bd) or prion rods (o-u, v-ab, aq-aw, ax-bd) were injected into the PC of mice and cells harvested from peritoneal lavage fluid (a-ab) or mediastinal lymph nodes (ac-bd) two hours later. Graphs in the first column show cells from mice treated with PBS (panels a, v ac, and ax), fluorescent beads (h, v, aj, and ax) and prion rods (panels o, v, aq, and ax). Fluorescent cells (red or green dots) and total cells (grey dots) are plotted to show relative size (forward scatter, linear scale), granularity (side scatter, log scale) and proportion of total live cells that fluoresce. Cells were also stained

with antibodies against immune cell surface markers and gated for SSC^{hi}Ly6G- Ly6C+CD11b+ monocytes (panels b, i, p, w, ad, ak, ar, and ay), SSC^{hi}Ly6G+ Ly6C-CD11c- CD11b+ neutrophils (c, j, q, x, ae, al, as, and az), SSC^{hi}Ly6G- Ly6C-CD11b+CD11c+ DCs (d, k, r, y, af, am, at, ba), SSC^{hi}Ly6G-Ly6C-CD11c-CD11b+ MΦs, (e, l, s, z, ag, an, au, and b), SSC^{lo}B220+CD21+CD3- B cells (f, m, t, aa, ah, ao, av, and bc) and SSC^{lo}CD21-B220- CD3+ T cells (g, n, u, ab, ai, ap, aw, and bd). Cell counts in graphs are shown as $\log_{10}$ per 10^5 total cells. Horizontal bars below the PC and MedLN panels represent relative proportions of prion-bearing monocytes (red stripe), neutrophils (solid red), DCs (dotted), MΦs (checkered), B cells (white) and T cells (black).

DCs and MΦs comprise the majority of prion-bearing immune cells (prionophils) in the PC

We observed significant acquisition of prions and 10 μg of 1 μm fluorescent beads by immune cells present in the PC 2 HPI compared to PBS (Figures 2.3a, h and o). Of the major antigen presenting cells analyzed from the PC, $SSC^{hi}Ly6G^{-}Ly6C^{-}CD11b^{+}CD11c^{+}$ DCs (Figure 2.2 and 2.3r) and $SSC^{hi}Ly6G^{-}Ly6C^{-}CD11c^{-}CD11b^{+}$ MΦs (Figure 2.2 and 2.3s) were the predominant cell types capturing prions. Upregulation of CD11c on inflammatory MΦs can complicate their discrimination from DCs. Although we observed no increase in CD11c+ cells in the PC, we performed an alternative gating strategy that gated for SSC^{hi}Ly6C-Ly6G-F4/80+CD11b+ MΦs and SSC^{hi}Ly6C-Ly6G-F4/80-CD11b+CD11c+ DCs (Figure 2.2) to more clearly define these two cell populations. Both strategies yielded very similar results, and are reported here as combined data. We detected significant numbers of prionophilic DCs (*pr*DCs, Figure 2.3y, median=3177; IQR=1280 to 33,968 per 100,000 cells, n=16 mice) and MΦs (*pr*MΦs, Figure 2.3z, median=14,730, IQR=7598 to 29037, n=16) compared to DCs and MΦs from mice inoculated with PBS alone (*pbs*DCs, Figures 2.3d and y, e and z, median=8, IQR=1 to 20 and *pbs*MΦs, median=4, IQR=1 to 7, respectively, n=13, $p<0.001$). *pr*MΦs and *pr*DCs accounted for 78.6% and 16.9%, respectively, of total prionophils.

DCs and B cells preferentially capture prions

Comparing two particulate antigens, we detected three-fold more prDCs (median=3177) than bead-bound DCs (bDCs, median=1037, IQR=479 to 1654, n=5, p= 0.0262, Figure 2.3K and Y). In a subset of mice whose cells acquired prions, we observed 40-fold more prDCs (6/16, median=41,905. IQR= 31,234 to 59,043, p=0.0022) than bDCs.

We observed a small proportion (0.6% of total), yet significant number, of prionophilic SSC^{lo}B220+CD21+CD3- B cells (prB cells, Figures 2.2 and 2.3t and aa, median =117, IQR=84 to 192 $p<0.05$) in the PC compared to PBS (Figures 2.3f, and aa, median=2; IQR=0 to 10) but little to no bead-bearing B cells (Figures 2.3m and AA, median=0, IQR=0 to 7, n=5). We detected no significant difference in numbers of peritoneal prMΦs or bead-bearing MΦs (Figure 2.3z, median=10,700; IQR=9658 to 22,144, n=5).

Relatively few Monocytes and Neutrophils capture prion rods from the PC

$SSC^{hi}Ly6G^{-}Ly6C^{+}CD11b+$ monocytes and $SSC^{hi}Ly6C^{-}Ly6G^{+}CD11c^{-}CD11b^{+}$ neutrophils (Figure 2.2) also show a propensity to retain prions from the PC 2 HPI. We collected significant numbers of prionophilic monocytes (prMonos, Figure 2.3p and w, median=638, IQR=276 to 967, n=16) and neutrophils (prNeuts, Figure 2.3q and x, median=77, IQR=38 to 9874, n=10) compared to PBS inoculated controls (pbsMonos, Figures 2.3b and w, c and x, median=2; IQR 0 to 10, n=13 and pbsNeuts, median=0, IQR 0 to 2, n=10; $p<0.001$). Additionally, neutrophils exhibited the highest propensity for prion rod uptake, with up to 98% of neutrophils in PC capturing prions. Still, prMonos and prNeuts comprised only 3.4% and 0.4%, respectively, of total prionophils. We also collected significant numbers of bead-associated monocytes (bMonos, Figure 2.3i and w, j and x, median=401, IQR=171 to 4388; $p<0.01$) and neutrophils (bNeuts, IQR=66 to 839; n=5, $p<0.01$) compared to PBS, but observed no difference in numbers of prMonos/Neuts versus bMonos/Neuts. Finally, We detected no significant numbers of prionophilic or bead-associated SSC^{lo}B220-CD21-CD3+ T cells (Figure 2.2, prT and bT cells, respectively) in the PC at 2 HPI (Figures 2.3g,n, u and ab). We observed similar prionophil quantities and proportions from identical experiments using PrP^{C} deficient mice (data not shown).

Prionophils are present in the MedLN 2 HPI

We then searched for prionophils in LNs to which these cells migrate. We failed to identify significant numbers of prionophils in spleens or mesenteric lymph nodes in this assay, as expected for antigens injected IP. However, we observed significant acquisition of fluorescent prions and beads by immune cells present in the mediastinal lymph nodes (MedLN) 2 HPI compared to PBS (Figures 2.3ac, aj and aq). We also observed trafficking to inguinal lymph nodes, but at lower frequencies and cell counts compared to MedLNs (data not shown). Confocal microscopy revealed large prion aggregates in areas of MedLNs consistent with lymphoid follicles and capsules (Figure 2.4). Interestingly, we observed drastic changes in prionophil proportions in the MedLN compared to the PC.

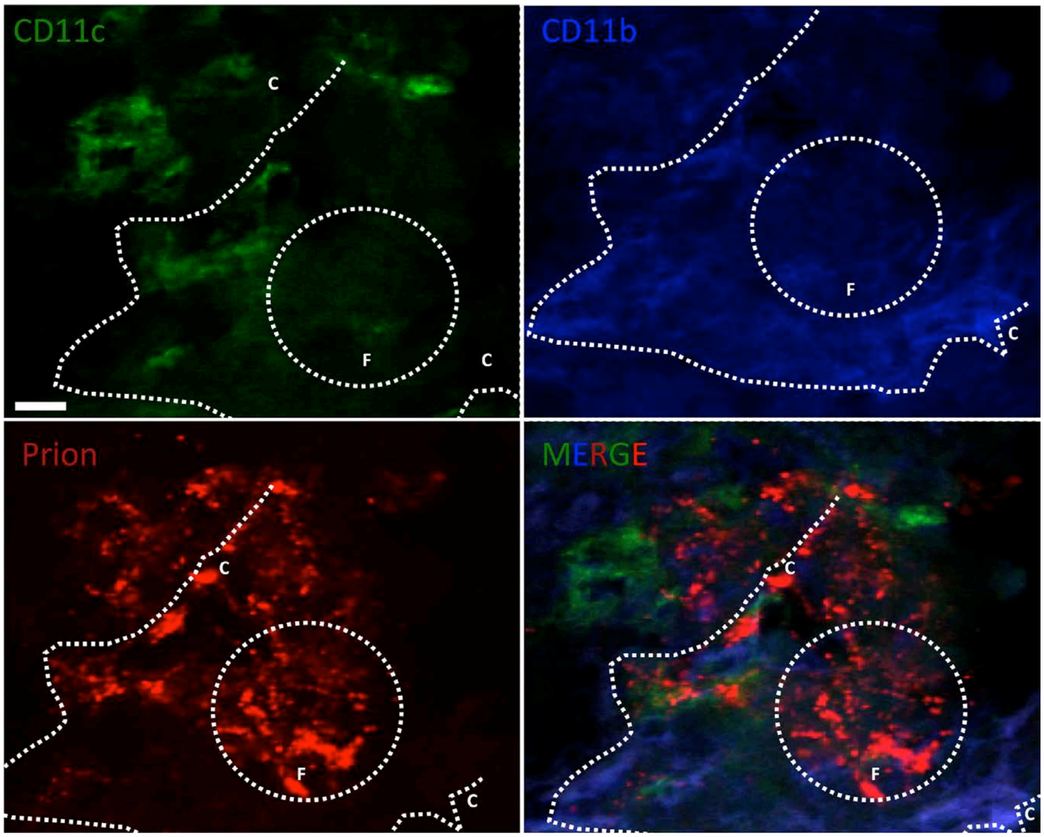

Figure 2.4. Confocal analysis of the mediastinal lymph node 2 hours post infection. Prion rods (labeled red) were injected into the PC of mice and mediastinal lymph nodes harvested 2 hours post infection. Mediastianal lymph nodes were cut into 20 µm sections, labeled with antibodies against CD11c (green) and CD11b (blue), and analyzed by confocal microscopy. Areas marked in the merge are consistent with the capsule (C) and follicle (F). Scale bar, 20 µm.

MΦs and B cells comprise the majority prionophils in the MedLN

We observed more *pr*MΦs than any other immune cell type analyzed (Figure 2.3au and bb, median=34, IQR=11 to 70 n=16, compared to *pbs*MΦs (Figures 2.3ag and bb, median=0, IQR=0 to 6 and n=13, $p<0.001$)), consistent with their predominance in the PC. Surprisingly, though, *pr*B cells represented the second highest number of prionophils in the MedLN (Figures 2.3av and bc, median=23, IQR=17 to 32 $p<0.01$ compared to PBS inoculated controls). This represents a 44-fold increase in the proportion of *pr*B cells in the MedLN (26.4%) compared to the PC (0.6%). The proportion of *pr*MΦs decreased 2.1-fold from the MedLN (39.1%)

compared to the PC (78.6%). We detected statistically insignificant numbers of *b*MΦs (Figure 2.3an and bb, median=6; IQR=3 to 61, n=5) and *bB* cells (Figure 2.3AO and BC, median=10, IQR=4 to 26) in the MedLN.

Increased proportion of monocytes in the MedLN

We collected half as many *pr*Monos (Figure 2.3ar and ay median=11; IQR 7 to 15; p<0.05) and *pr*DCs (Figure 2.3at and ba, median=11; IQR=6 to 44 per 10^5 cells, n=16 mice) from the MedLN compared to *pr*B cells. The proportion of *pr*Monos increased 3.7-fold in the MedLN (12.6%) compared to the PC (3.4%), while *pr*DC proportions decreased slightly. Interestingly, we detected four-fold more *b*Monos (Figure 2.3ak and ay median=45; IQR=14 to 105; p<0.01) than *pr*Monos. We observed no significant difference in the number of *pr*DCs and *b*DCs (Figure 2.3 am and ba, median=7, IQR=3 to 83, n=5), and found no significant numbers of *pr*Neuts (Figure 2.3as and az), *b*Neuts (al and az), *pr*T (aw and bd) or *b*T (ap and bd) cells in the MedLN.

Peritoneal prionophils both internalize and retain prion rods on their cell surfaces.

We assessed subcellular location of captured prions by visulaizing peritoneal prionophils by confocal microscopy. While *pr*Monos (Figure 2.5) and *pr*MΦs (Figure 2.6) showed a tendency to internalize prion rods, these cells, as well as *pr*DCs (Figure 2.7), and *pr*Neuts (Figure 2.8) demonstrated the ability to retain prion rods on both the cell surface and intracellular compartments. Internalized fluorescent prions generally appeared more diffuse, while cell surface prions appeared as bright, punctate fluorescent aggregates ranging in size from 1 -3 μm^3 on cell surfaces.

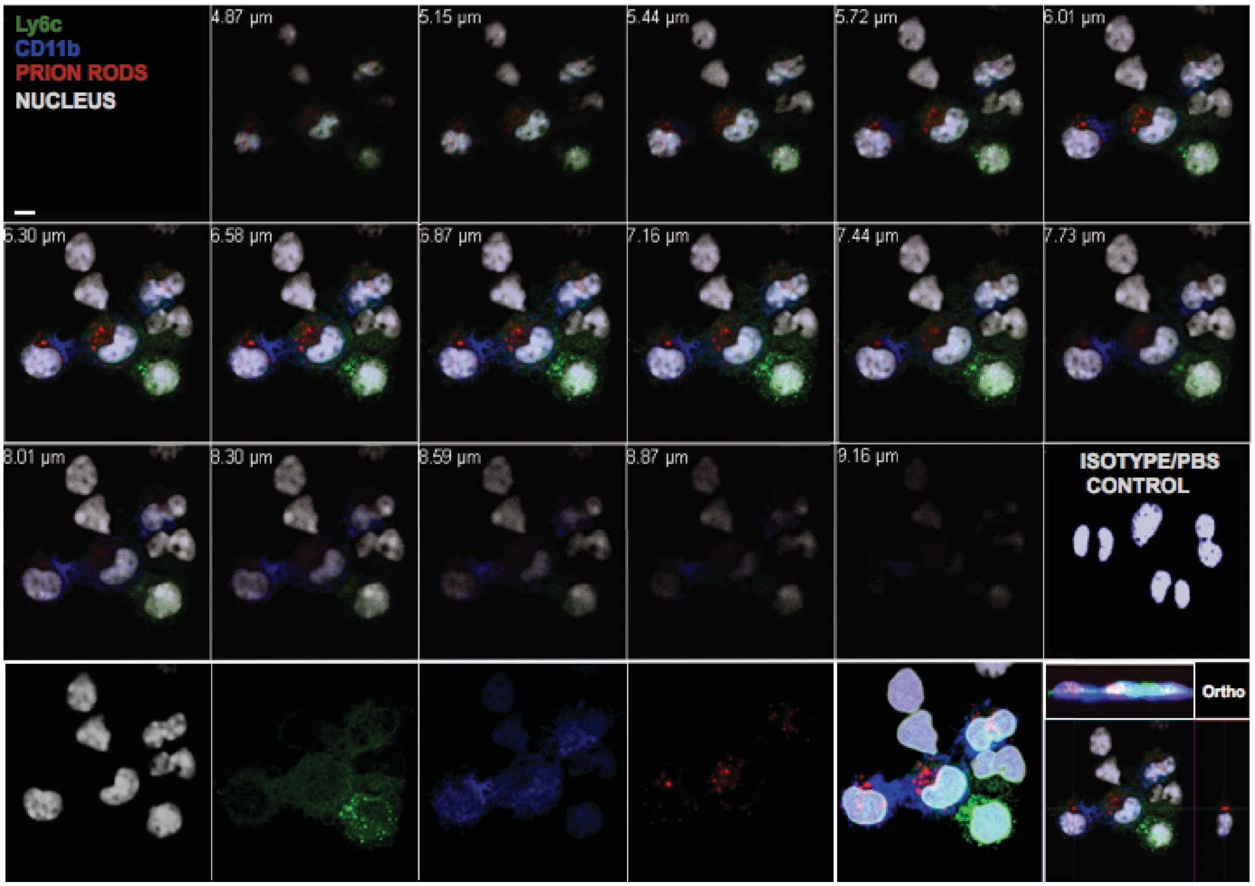

Figure 2.5. Analysis of monocytes capturing prion rods in the PC by confocal microscopy. PBS and prion rods (labeled red) were injected into the PC of mice and CD11b+Ly6C+ (labeled blue and green, respectively) monocytes were analyzed for prion retention. Z stack images were collected at 0.28 µm intervals and range from 0.64 to 7.31 µm. Image shown in row three, column six indicates isotype and PBS controls. Bottom row starting from the left show single stains of the nucleus (white), Ly6C, CD11b, and prion rods. The Last 2 panels in the bottom row represent a merged z stack image and an orthogonal image.

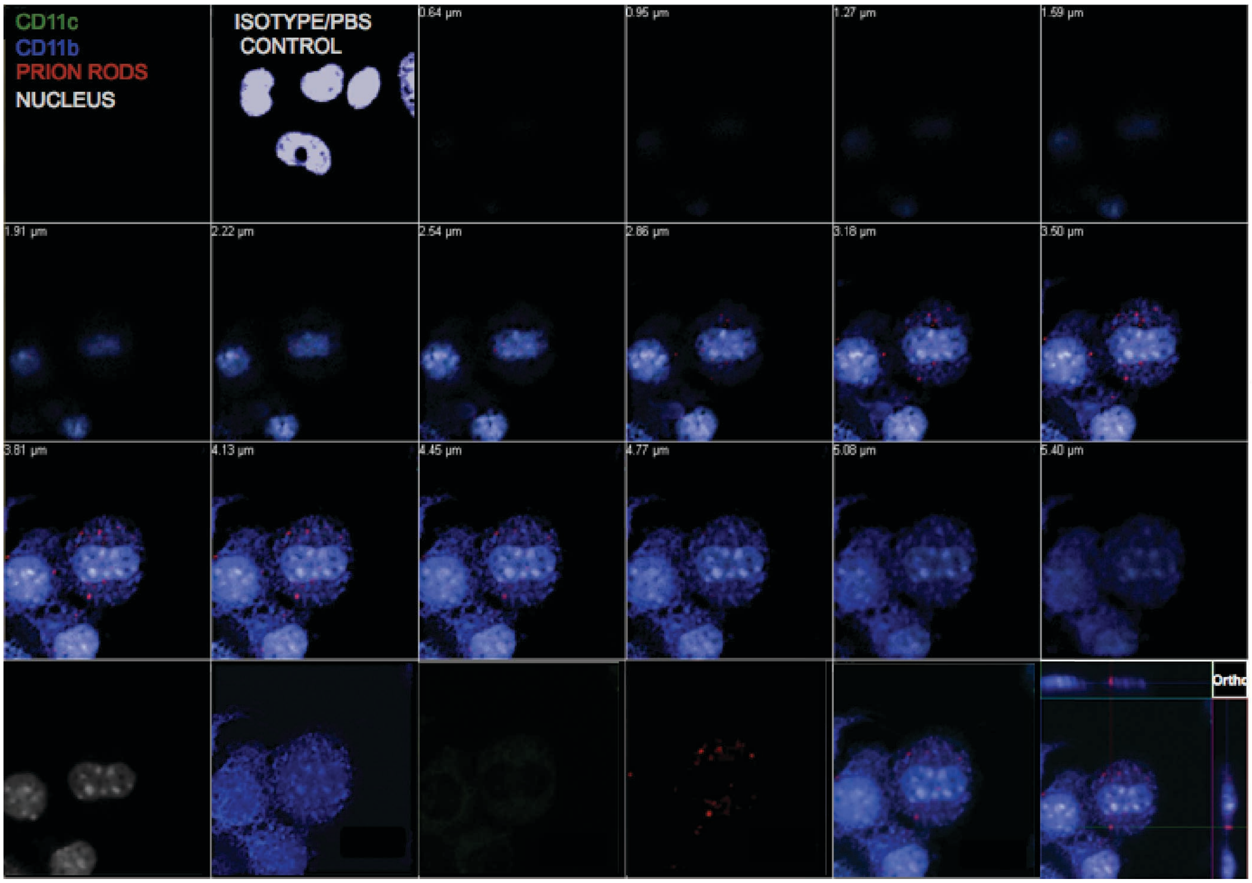

Figure 2.6. Analysis of MΦs capturing prion rods in the PC by confocal microscopy. PBS and prion rods (labeled red) were injected into the PC of mice and cells harvested from peritoneal lavage fluid and labeled with antibodies against cell surface markers, CD11b (blue) and CD11c (green). Cells were cytospun onto glass slides and Z-stack images were collected at 0.32 µm intervals and range from 0.64 to 5.40µm. Image shown in row one, column two indicates isotype and PBS controls. Bottom row starting from the left shows single stains of nuclei (white), CD11b, CD11c, and prion rods. Last two panels in bottom row represent a merged z stack and orthogonal image.

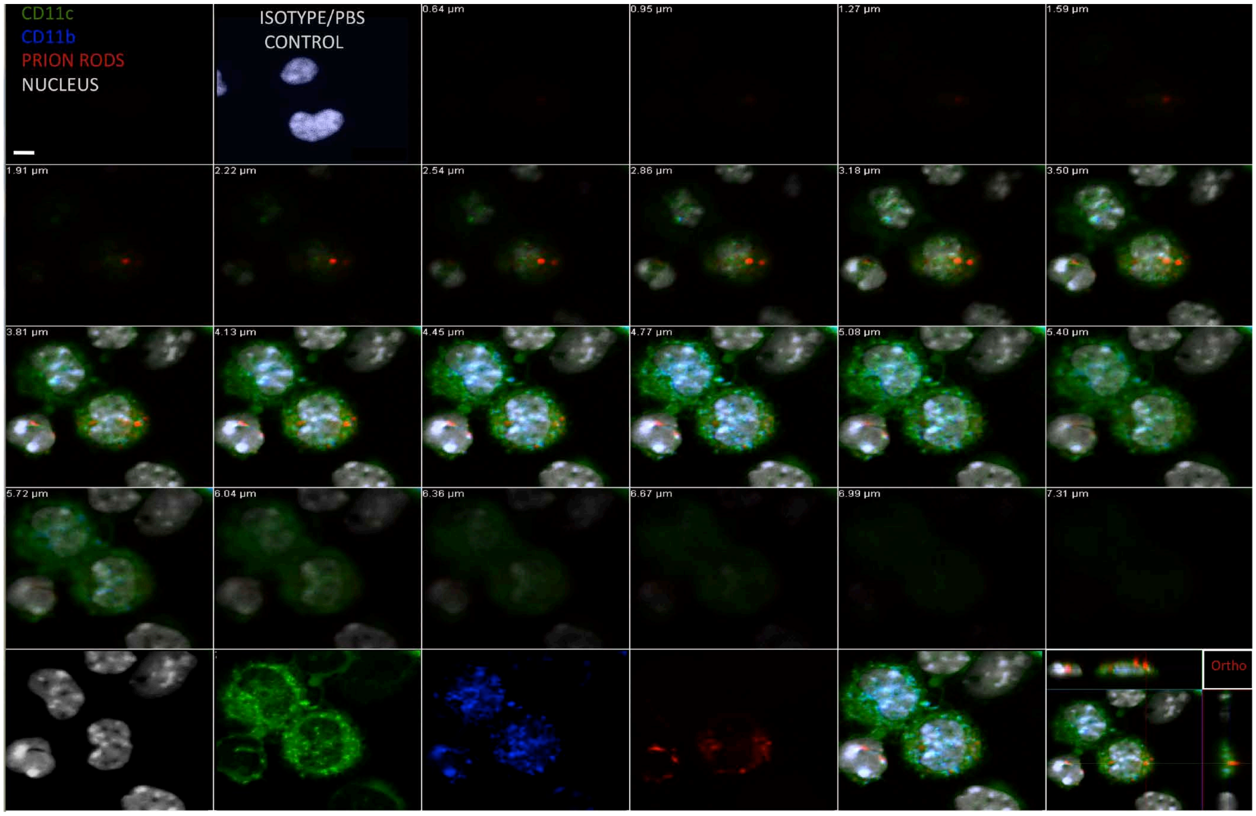

Figure 2.7. Analysis of DCs capturing prion rods in the PC by confocal microscopy. PBS and prion rods (labeled red) were injected into the PC of mice and cells harvested from peritoneal lavage fluid and labeled with antibodies against cell surface markers, CD11b (blue) and CD11c (green). Cells were cytospun onto glass slides and Z-stack images were collected at 0.32 µm intervals and range from 0.64 to 7.31µm. Image shown in row one, column two indicates isotype and PBS controls. Bottom row starting from the left shows single stains of nuclei (white), CD11c, CD11b, and prion rods. Last two panels in bottom row represent a merged z stack and orthogonal image.

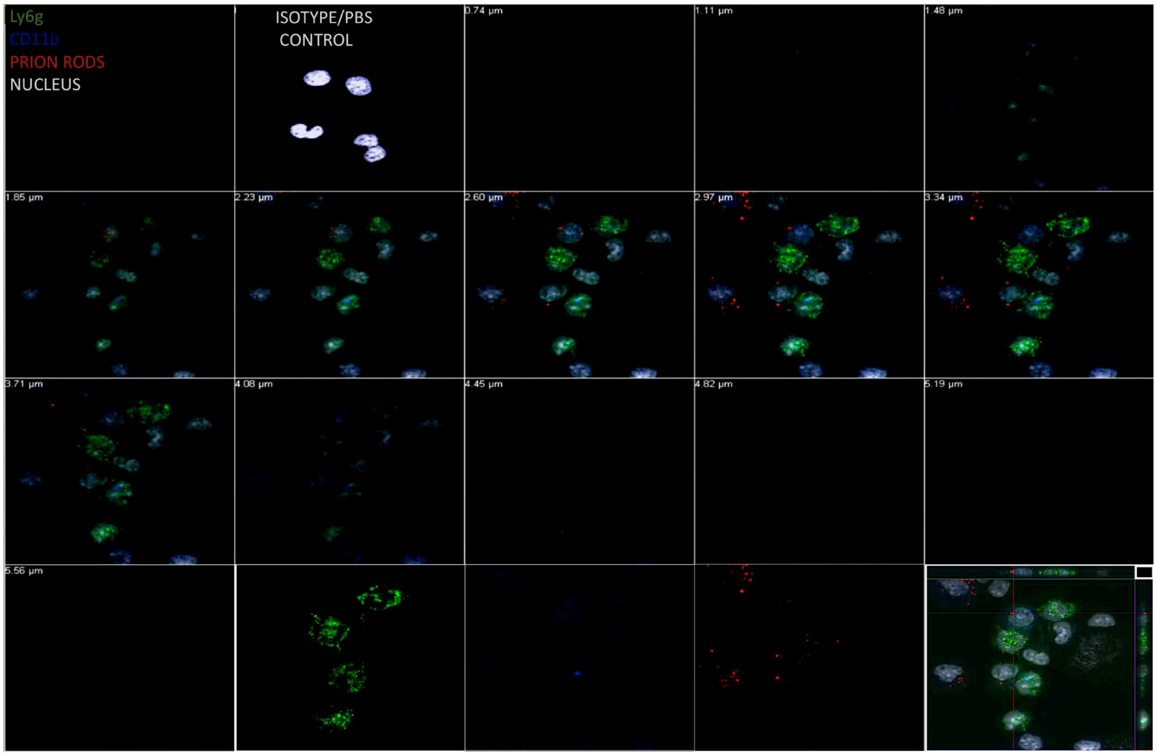

Figure 2.8. Analysis of neutrophils capturing prion rods in the PC by confocal microscopy. PBS and prion rods (labeled red) were injected into the PC of mice and cells harvested from peritoneal lavage fluid and labeled with antibodies against cell surface markers, CD11b (blue) and CD11c (green). Cells were cytospun onto glass slides and Z-stack images were collected at 0.32 µm intervals and range from 0.64 to 5.40µm. Image shown in row one, column two indicates isotype and PBS controls. Bottom row starting from the left shows single stains of nuclei (white), CD11b, CD11c, and prion rods. Last two panels in bottom row represent a merged z stack and orthogonal image.

Dynamics of prion trafficking kinetics over time

Most prionophil proportions in the PC remained relatively constant from 2 to 36 hours (Figure 2.9), except for a 26-fold increase in *pr*Neuts from 2 (0.4%) to 6 HPI (10.3%). Consistent with data collected 2 HPI, at 6 HPI *pr*B cells increased their proportion 201-fold from the PC (Figures 2.9 and 2.10, 0.3%) to the MedLN (60.3%), becoming the predominant prionophil, while the *pr*MΦ proportion decrease 6.4-fold from the PC (70.9%) to the MedLN (11.1%). By 16 HPI, we observed a relatively even distribution of all prionophils analyzed, save *pr*Neuts (Figures 2.9 and 2.11). The share of *pr*DCs increased 4.4-fold from the PC to MedLN at 16 HPI, then plateaued to 36 HPI (Figures 2.9, 2.11 and 2.12). Proportions of *pr*Monos from PC to MedLN increased steadily over every time point, reaching its maximum share of total prionophils in the MedLN at 36 HPI (41.8%). The distribution of the other prionophils analyzed remained relatively constant from 16 to 36 HPI, except for *pr*Monos, whose percentage increased two-fold over that time. We failed to detect any fluorescent prions or beads one week after inoculation (data not shown).

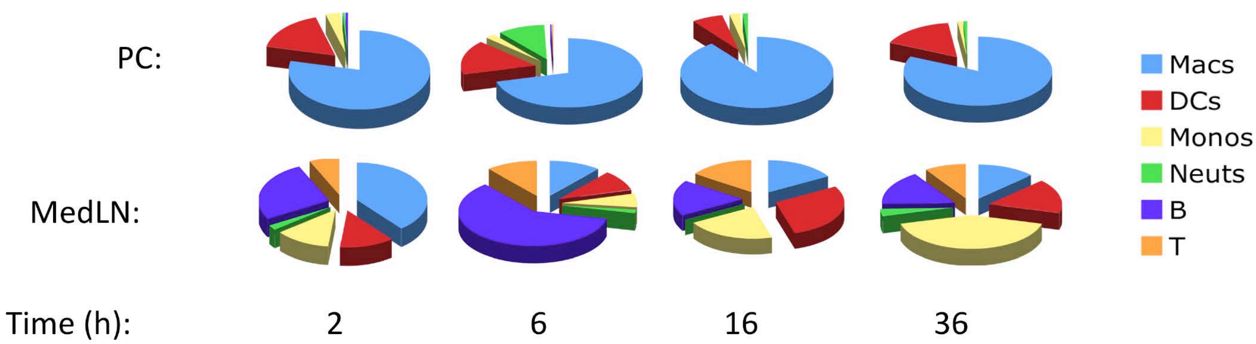

Figure 2.9. Dynamics of prion trafficking kinetics over time.

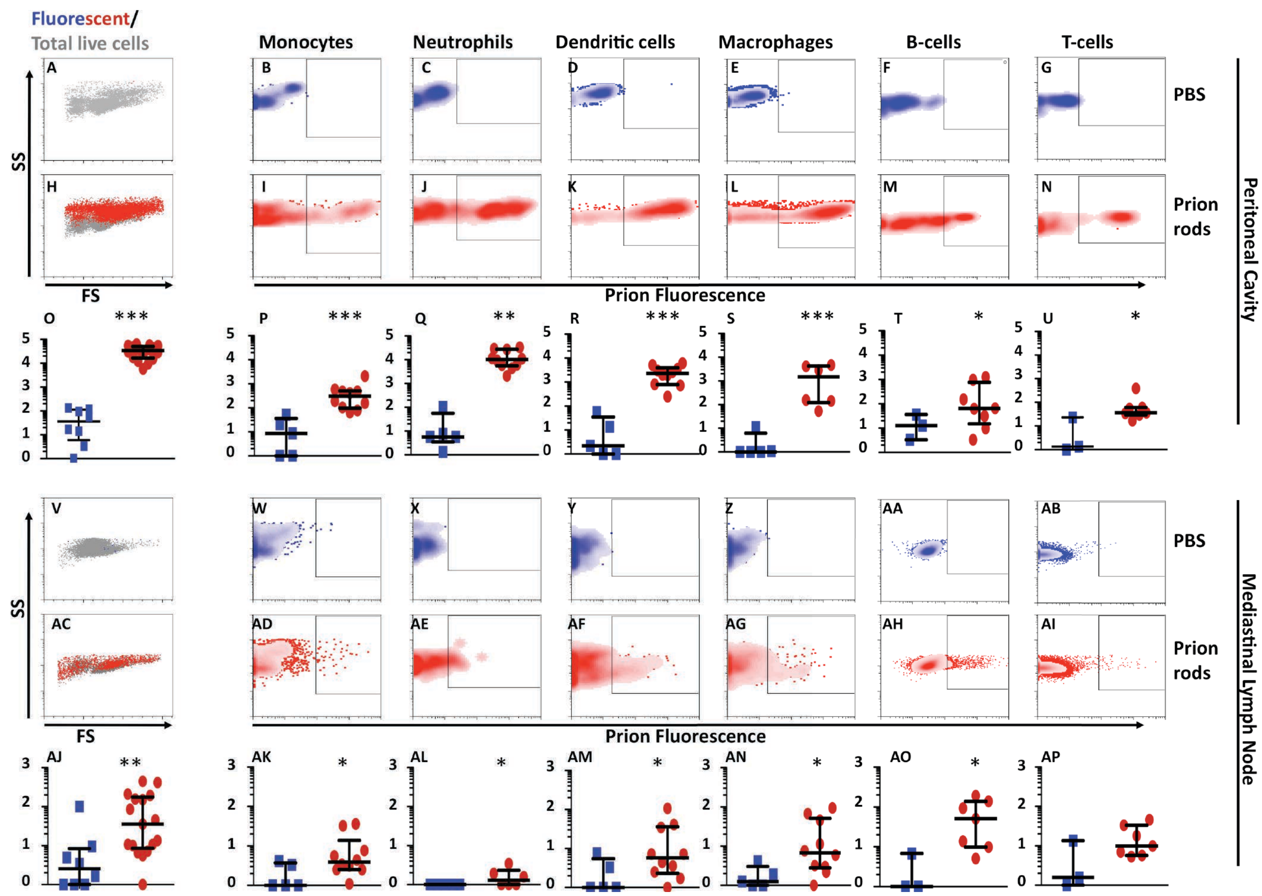

Figure 2.10. Flow cytometric analysis of immune cells trafficking prions from the PC to mediastinal lymph nodes 6 HPI. PBS (rows A-G, O-U, V-AB, and AJ-AP), or Prion rods (H-N, O-U, AC-AI, and AJ-AP) were injected into the PC of mice and cells harvested from peritoneal lavage fluid (A-U) or mediastinal lymph nodes (V-AP) six hours later. Graphs in the first column show cells from mice treated with PBS (panels A, O, V, and AJ), and prion rods (panels H, O, AC, and AJ). Total cells (grey dots) are plotted to show relative size (forward scatter), granularity (side scatter) and proportion of total live cells that fluoresce. Cells were also stained with antibodies against immune cell surface markers and gated as outlined in Figure 2.2 for monocytes (panels B, I, P, W, AD, and AK), neutrophils (C, J, Q, X, AE, and AL), DCs (D, K, R, Y, AF, and AM), MΦs, (E, L, S, Z, AG, and AN), B cells (F, M, T, AA, AH, and AO) and T cells (G, N, V, AB, AI, and AP). Graphs depict total number of monocytes in the PC and mediastinal lymph node (panels W and AY), neutrophils (X and AZ), DCs (Y and BA), MΦs (Z and BB), B cells (AA and BC), and T cells (AB and BD).

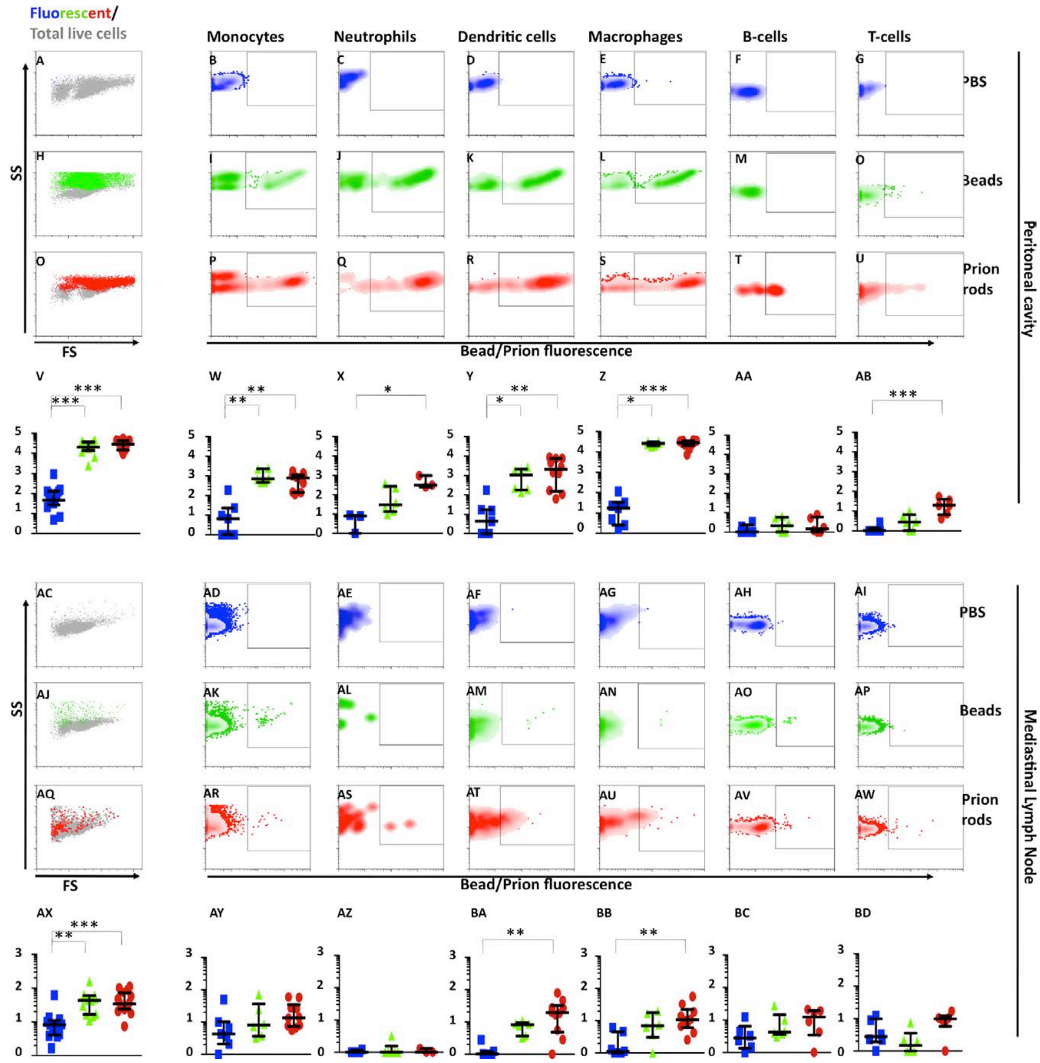

Figure 2.11. Flow cytometric analysis of immune cells trafficking prions from the PC to mediastinal lymph nodes 16 HPI. Figure panels are arranged identically as in figure 2. Graphs depict total number of monocytes in the PC and MedLN (panels W and AY), neutrophils (X and AZ), DCs (Y and BA), MΦs (Z and BB), B cells (AA and BC), and T cells (AB and BD).

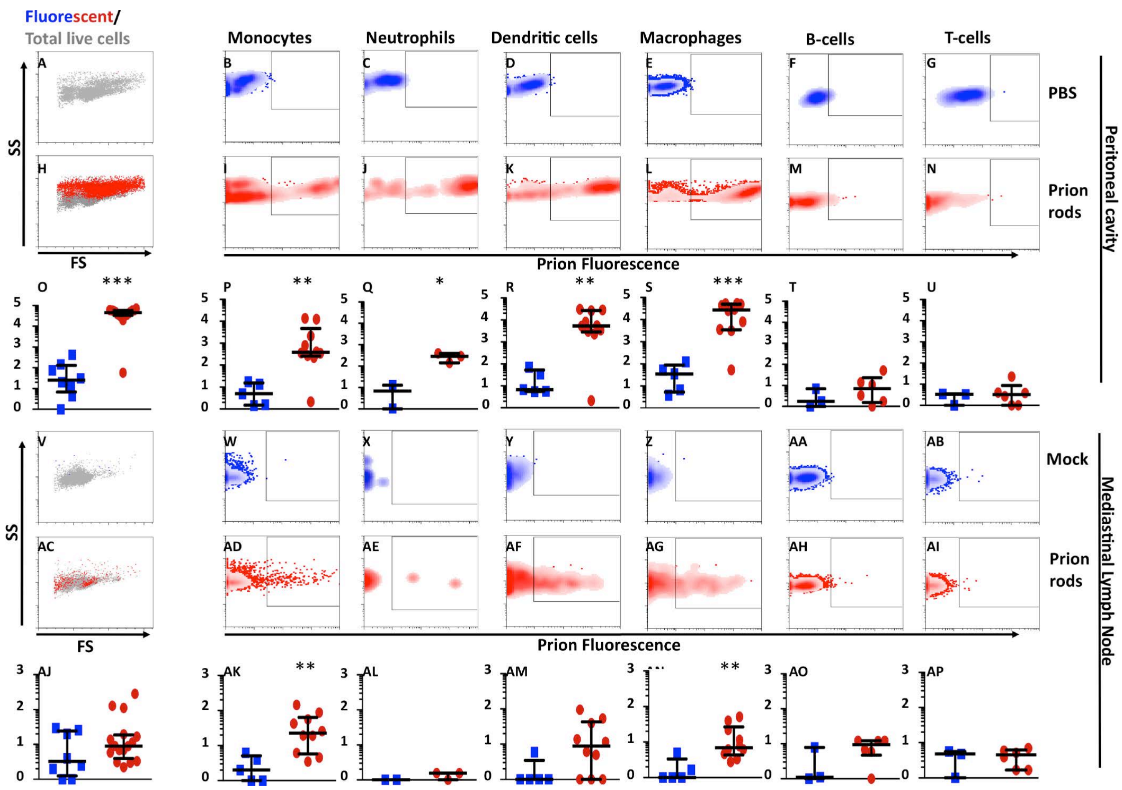

Figure 2.12. Flow cytometric analysis of immune cells trafficking prions from the PC to mediastinal lymph nodes 36 hours after inoculation. Figure panels are arranged identically as in figure 3. Graphs depict total number of monocytes in the PC and mediastinal lymph node (panels W and AY), neutrophils (X and AZ), DCs (Y and BA), MΦs (Z and BB), B cells (AA and BC), and T cells (AB and BD).

Passive and active transport of prions to MedLNs

Previous studies indicate that DC trafficking antigen to draining lymph nodes occurs 12 - 16 HPI [10-12]. Given the early detection of prionophils in the MedLN in as little as 2 HPI, we postulated passive prion delivery might occur at early time points whereas active transport by prionophils may occur later in infection. To test this hypothesis we injected prions IP into the PC of donor mice and harvested cells from the PC and MedLN two hours later. Peritoneal cells from donor mice were washed to remove unbound prions and 10^6 cells transferred into the PC of each recipient mouse. MedLN from donor and recipient mice were analyzed for resident and migratory prionophils, respectively.

SSC^{hi}CD11b+CD169+ subcapsulary sinus MΦs (SCS MΦs, Figure 2.13A) isolated from donor mice show a high propensity for prion uptake 2 HPI (Figure 2.13B (red cloud) and 13D (red dots), median=94; IQR=27 to 148 per 100,000 cells, n=17 mice, $p<0.01$) compared to mice inoculated with PBS (Figure 2.13B (blue cloud) and 13D (blue squares, median=6; IQR 2 to 7, n=3 mice). SSC^{hi}CD11c+CD8α+ resident DCs also show a significant ability to take up prions (Figure 2.13C and 2.13E (red cloud and dots) median=8; IQR 4 to 11, n=17, $p<0.05$) compared to PBS controls (blue cloud and dots, median=2; IQR 1 to 5, n=3).

We assessed active prion transport by isolating cells from the MedLN of recipient mice inoculated with prion-loaded donor cells. We detected a small number of *pr*Monos in MedLNs at two HPI (Figure 2.13F, H, and J, median=6 IQR=4 to 24) and 16 HPI (Figure 2.13G, I, and K, median=4 IQR=1 to 9). While these median numbers are low, we did detect 13 and 181 *pr*Monos in two mice, and 15 *pr*MΦs in one mouse at 16 HPI.

We also performed adoptive transfer experiments at 6 HPI to analyze MedLN cells for *pr*B cells to assess the drastic increase in their proportions at this time point. In donor MedLNs we detected significant numbers of prionophilic SSC^{lo}CD5-CD11b-B220+CD23+CD21+ follicular B2 cells (*pr*B2, Figure 1.14B and D, median=24; IQR=3 to 40, n=5, p=0.008). Surprisingly, we also detected significant numbers of prionophilic SSC^{lo}B220-CD21-CD23-CD11b+CD5+ B1 cells (*pr*B1, Figure 1.14C and E, median=7; IQR 4 to 21, n=7, p=0.005) there. MedLNs from recipient mice contained *pr*B2 (Figure 1.14G and H, red peak and dots, median=108 per 10^4 B cells, IQR=41 to 179, p=0.045), but not *pr*B1 (green, median=1, IQR=1 to 29) cells 6 HPI.

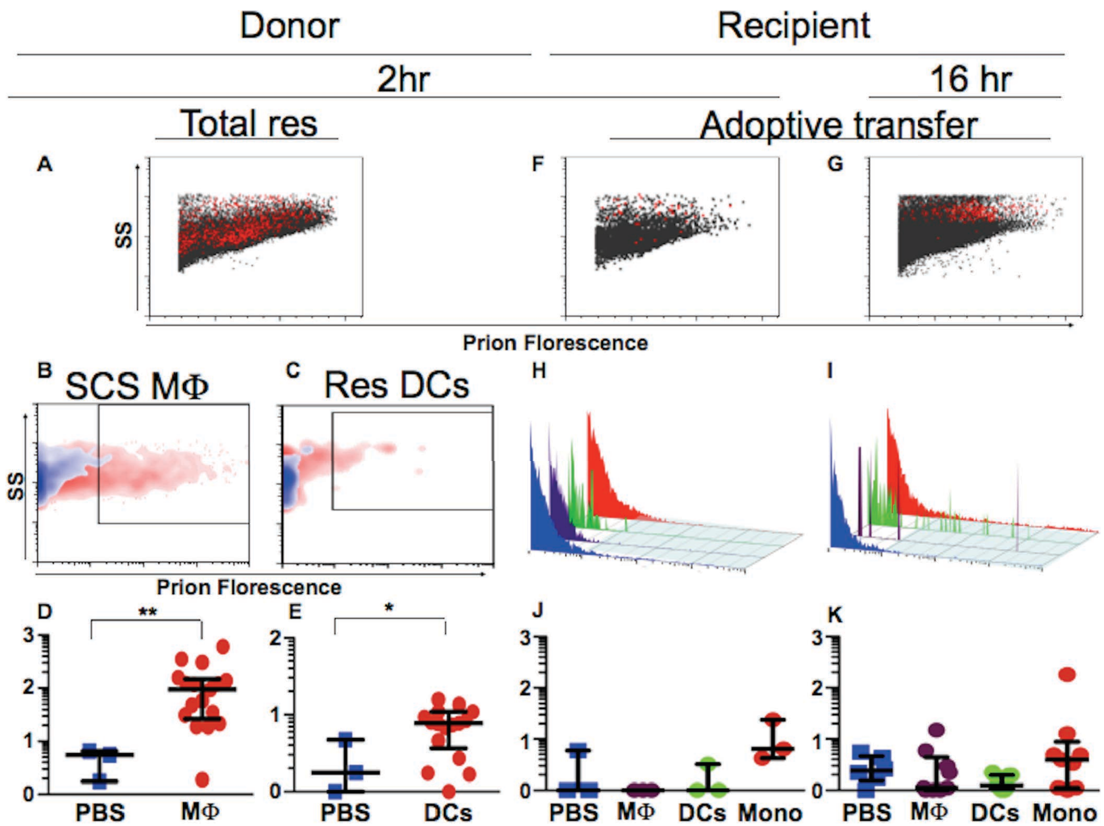

Figure 2.13. Flow cytometric analysis of passive and active transport of prion rods. Prion rods were injected IP into donor mice and two hours later immune cells harvested from the PC and mediastinal lymph nodes. Peritoneal cells were washed to remove unbould prion rods and transferred into the PC of recipient mice. MedLN from donor mice 2 HPI (panels a-e), and recipient mice 2 and 16 HPI (panels f-k), were analyzed for prion-bearing resident and migratory immune cells, respectively. Total cells from the MedLN (grey dots in panels a, f and g) are plotted to show relative size (forward scatter, linear scale), granularity (side scatter, log scale) and proportion of total live cells that bear prions (red dots). Resident MedLN cells were analyzed for SSC^{hi}CD11b+CD169+ SCS MΦs (b and d) and SSC^{hi}CD11c+CD8α+ DCs (c and e) bearing prion rods. Prion-loaded cells from donor mice were injected into the PC of recipient mice and lymph nodes harvested 2 and 16 hours later. Migratory immune cells were also analyzed for monocytes (depicted as red peaks (h and i) and dots (Jjand k)), DCs (green) and MΦs (purple) using the same phenotypic markers used in Figure 3. These cell subsets were compared to cells in MedLN from PBS inoculated control mice (blue). Cell counts in graphs d, e, j and k are shown as $\log_{10}$ per 10^5 total cells.

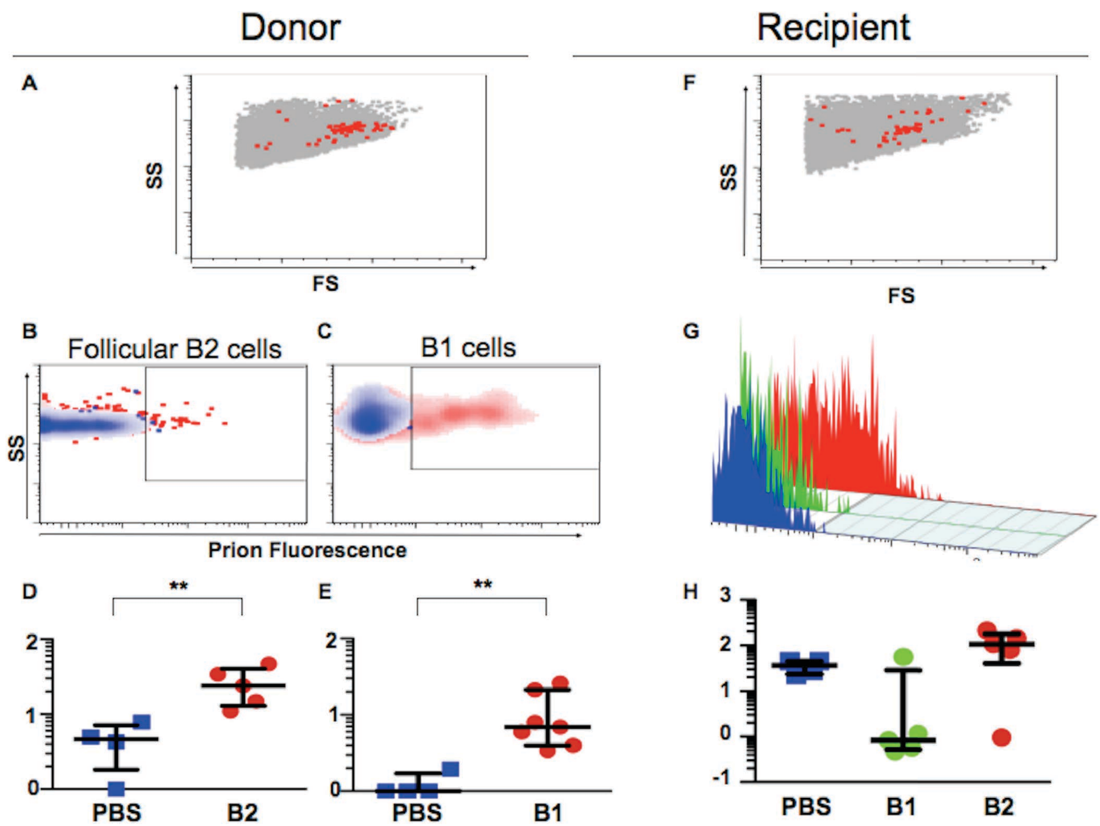

Figure 2.14. Flow cytometric analysis of B cell subsets in transport of prion rods. Adoptive transfer experiment was performed similarly as experiments in Figure 2.13. Prion rods were injected IP into donor mice and six hours later immune cells harvested from the PC were washed and transferred into the PC of recipient mice. MedLN from donor (panels a-e) and recipient mice (panels f-h) were analyzed 6 HPI for prion-bearing B1 and B2 cells. Donor MedLN cells were analyzed for $SSC^{lo}CD21^{+}B220^{+}CD5^{-}CD11b\text{-}CD23^{+}$ follicular B2 cells (b and d) and $SSC^{lo}B220^{-}$ $CD21^{-}CD23^{-}CD11b^{+}CD5^{+}$ B-1 cells (c and e) bearing prion rods. Recipient MedLNs were also analyzed for prion uptake by B2 cells (red peak (g) and dots (h)) and B1 cells (green). B cell subsets were compared to cells in MedLN from PBS inoculated control mice (blue). Cell counts in graphs are shown as $\log_{10}$ per 10^5 total cells (d and e) or per 10^4 B cells (h).

The role of Complement in prionophil uptake and trafficking of prions 2 HPI

Complement facilitates prion pathogenesis, replication and uptake by FDCs and conventional DCs [13-15]. To examine the interplay of complement with prions in early inflammatory events involving the MPS, we inoculated mice deficient in complement components C1q or C3 with prions IP and analyzed immune cells from the PC and MedLN for prion retention 2 HPI.

Impaired ability of DCs from Complement deficient mice to capture prions from the PC

While *C1q*$^{-/-}$ and *C3*$^{-/-}$ mice possessed similar numbers of total prionophils in the PC, they exhibited altered prionophil proportions compared to controls (figure 2.15, panels f, k, p, and u). We detected fewer *pr*DCs from *C1q*$^{-/-}$ (panels n and x, median=390; IQR=184 to 1077 n=11, p=0.01) or *C3*$^{-/-}$ mice (panel s and x, median=913; IQR=165 to 1492 n=7, p=0.01) than from wt mice (panels i and x, median= 3089; IQR=982 to 33614 n=17, p=0.001). Concomitantly, we observed increases in *pr*Neuts from *C1q*$^{-/-}$ (panels m and w, median 4006; IQR=296 to 8508 n=11, p=0.01) and *C3*$^{-/-}$ (panels r and w, median 2420; IQR=1383 to 10098 n=7, p=0.05) mice compared to wt mice (panels h and w, median 93; IQR=42 to 6669 n=11, p=0.001). Consequently, the proportion of *pr*DCs in the PC decreased 8.4-fold in *C1q*$^{-/-}$ (figure 2.15, pie chart right of panel O, dotted purple wedge) and two-fold in *C3*$^{-/-}$ mice (dotted green wedge from panel T pie chart) compared to wt (dotted red wedge from Panel J pie chart), while *pr*Neut proportions increased 40.6 and 21-fold for *C1q*$^{-/-}$ and *C3*$^{-/-}$ mice, respectively (compare black wedges in the three pie charts right of j, o and t). We also detected a two-fold decrease in *pr*Monos from *C3*$^{-/-}$ (striped green) but not *C1q*$^{-/-}$ (striped purple) mice compared to wt (striped red). We detected no significant proportional changes in *pr*MΦs (solid colored wedges), which remained the predominant prion scavenger in the PC of wt (j and y), *C1q*$^{-/-}$ (o and y) and *C3*$^{-/-}$ (t and y) mice.

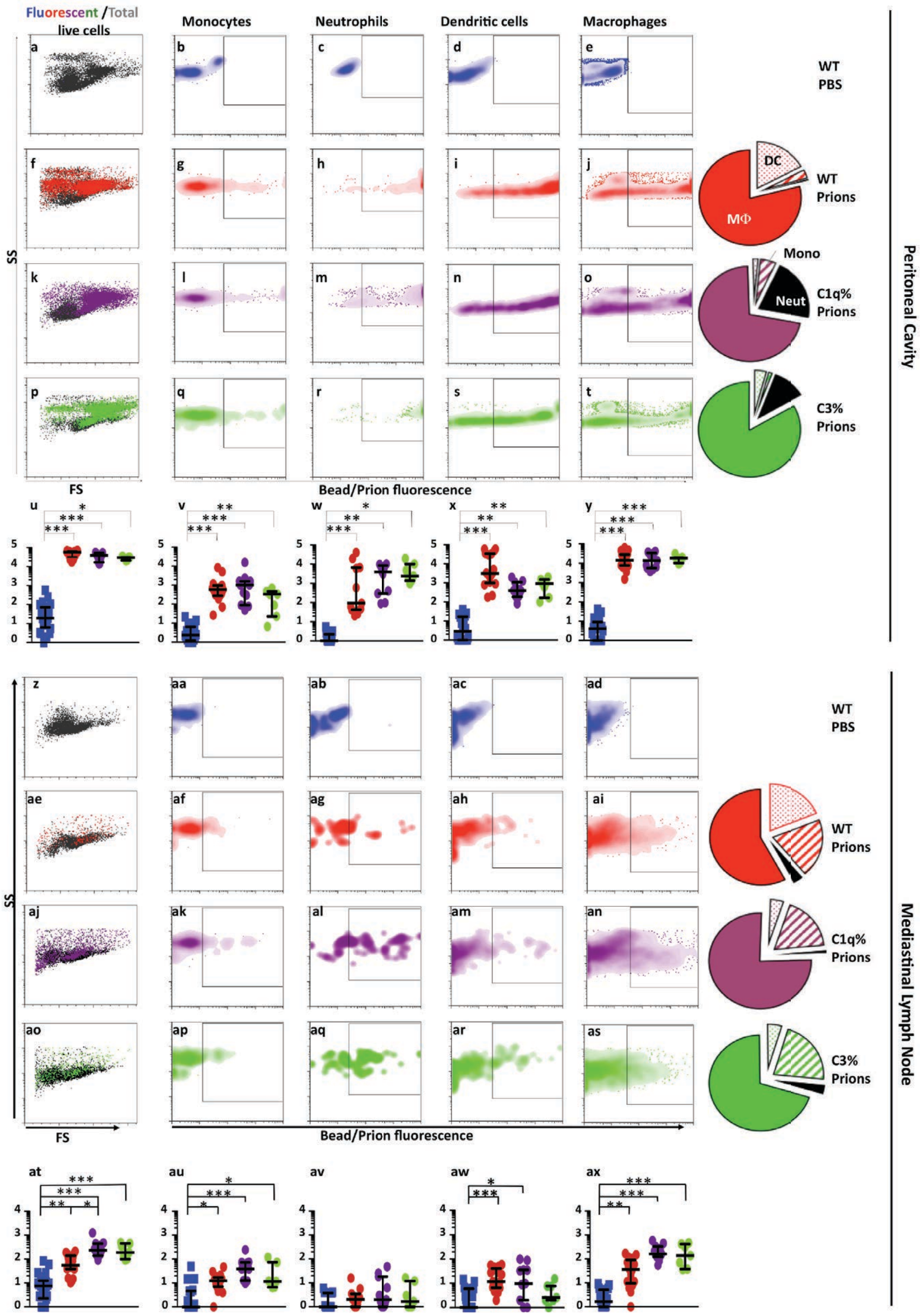

Figure 2.15. Flow cytometric analysis of immune cells trafficking prions in complement deficient mice. Figure panels are arranged similarly as in Figure 4. Pie charts to the right of the flow cytographs of prionophils from wt (f-j), *C1q*$^{-/--}$ (k-o) and *C3*$^{-/-}$ (p-t) mice represent relative frequencies of prionophils. Pie chart wedges depict MΦs from wt (red), *C1q*$^{-/-}$ (purple), and *C3*$^{-/-}$

(green) mice, DCs from wt (dotted red), *C1q*$^{-/-}$ (dotted purple), and *C3*$^{-/-}$ (dotted green) mice, monocytes from wt (striped red), *C1q*$^{-/-}$ (striped purple), and *C3*$^{-/-}$ (striped green) mice, and neutrophils (black) from wt, *C1q*$^{-/-}$, and *C3*$^{-/-}$ mice.

Impaired ability of DCs from Complement deficient mice to capture prions in the MedLN

Surprisingly, we detected more prionophils in MedLNs from both *C1q*$^{-/-}$ (figure 2.15 panels aj and at) and *C3*$^{-/-}$ (ao and at) mice compared to wt mice (panels ae and at). However, consistent with data derived from the PC, we observed an approximately four-fold reduction in the proportion of *prDCs* in both *C1q*$^{-/-}$ (dotted purple wedge from pie chart right of an) and *C3*$^{-/-}$ (dotted green wedge in chart right of as) MedLNs compared to wt (dotted red wedge, chart right of AI).

Also consistent with PC data, *pr*MΦs from wt (ai and ax, median=36; IQR=11 to 90 n=17, p=0.01), *C1q*$^{-/-}$ (an and ax, median=161; IQR=123 to 333 n=11, p=0.001) and *C3*$^{-/-}$ mice (as and ax, median=137; IQR=37 to 419 n=7, p=0.001) constitute the majority of immune cells involved in prion uptake. We observed increases in both raw numbers (ax) and proportions of *pr*MΦs from *C1q*$^{-/-}$ and *C3*$^{-/-}$ mice compared to wt (compare solid colored wedges from the pie charts to the right of panels ai, an and as). Relative proportions of *pr*Monos (striped purple, green and red wedges), *pr*Neuts (black wedges) and *pr*B cells (data not shown) remained similar in *C1q*$^{-/-}$, *C3*$^{-/-}$ and wt MedLNs.

Discussion

In order to gain insight into incunabular immunological events in prion infection, when the innate immune system initially confronts prions, we used highly enriched, fluorochrome conjugated prions to document prion trafficking and immune cell confrontation hours after initial exposure. We attempted to model prion trafficking as closely to a natural infection as possible using nonsaturating amounts of highly enriched, heterogeneously-sized, bona fide infectious prions. Fluorochrome conjugation of enriched prions eliminated detection using anti-prion protein antibodies, which cross-react with endogenous PrP^C and complicate data interpretation.

Many studies suggest a role for MΦs and $CD11c^+$ DCs in the capture, degradation and/or transport of prions [8,9,16-23]. Consistent with these previous data, *pr*MΦs and *pr*DCs comprised the vast majority of prionophils detected in the PC 2 HPI, while *pr*Monos, *pr*B cells and *pr*Neuts comprised the remaining small fraction. Only DCs and B cells preferentially captured prions over beads, evincing receptor mediated capture by these cells, perhaps by innate immune receptors as previously suggested[7,13,15,24].

Based on current paradigms of cell-mediated trafficking of antigens[10,25-27], including prions[22,24], from infection sites to draining lymph nodes, we expected to find few prionophils in the MedLN before 16 HPI. Instead, we found considerable numbers of *pr*MΦs, *pr*Monos, *pr*DCs and, strikingly, huge increases in *pr*B cell proportions well before then. These data raise the strong possibility that a considerable portion of prions that we injected IP passively traveled through lymphatics draining the PC, arriving in MedLNs via afferent lymphatics and captured by resident immune cells, as has been observed for other free antigens[10,26,28]. We substantiated this possibility for prions by identifying significant numbers of prionophilic resident DCs, SCS MΦs, innate B1 and follicular B2 cells in MedLNs 2 to 6 HPI. Adoptive transfer experiments revealed a small number of monocytes and B2 cells, but not migratory DCs, MΦs and B1 cells, pre-loaded with prions from donor mice, present in MedLNs of recipient mice at these times. We assert that the very small number of monocytes are not likely to transport the large amount of prions to MedLNs and transfer them to very large numbers of SC MΦs there. These data compellingly support a mechanism of cell autonomous movement of smaller prion aggregates from the infection site to draining lymph nodes.

Data supporting a cell autonomous route of lymphotropic prion trafficking also lends insight into intranodal prion movement. The incredible proportion of *pr*B cells in MedLNs at early time points indicates that B cells are most likely receiving prions from other immune cells, probably SCS MΦs and resident DCs within the lymph nodes, consistent with current models of intranodal antigen trafficking[26,29]. B cells are likely not the only cells receiving prions from other cells in the LN. FDCs, which trap and replicate prions in germinal centers, originate from stromal cells and are sessile, permanent residents in LNs[30,31]. Thus, they must receive prions intranodally from another source, perhaps *pr*B cells or by directly capturing small prion aggregates arriving in the LN through follicular conduits. We also reproducibly observed a considerable proportion of *pr*T cells in MedLNs but not in the PC, at all time points, further supporting intranodal, intercellular prion transfer. Future experiments documenting intranodal prion trafficking in real time using multiphoton intravital microscopy will confirm this hypothesis.

Numerous studies corroborate the facilitative role of Complement in peripheral prion pathogenesis. In this study we found that fewer DCs captured prions without C1q or C3 and fewer monocytes captured prions without C3, while neutrophil capture dramatically increased in the PC. MΦs predominantly and efficiently captured prions seemingly independent of C1q and C3. We interpret these data to reveal that DCs and monocytes require C1q and/or C3 for optimal prion retention, perhaps through Complement receptors like Mac-1, SIGN-R1 or Calreticulin [7,28]. The neurotoxic prion peptide $PrP_{106\text{-}126}$ has been shown to bind the G protein-coupled receptor, formyl peptide receptor-like 1 (FPRL-1) on, and enhance proinflammatory cytokine production from monocytes[32]. Prions binding FPRL-1 on monocytes could explain this prionophil's apparently reduced dependence on Complement for prion capture.

Based on the data described here, we propose an updated, more detailed model of lymphotropic and intranodal prion trafficking by immune cells (Figure 2.16). Biphasic lymphotropic transport of prions occurs from the initial entry site upon peripheral prion infection. A first wave of smaller prion aggregates passively percolate through interstitia, and collect into and quickly travel through the lymphatic system to draining lymph nodes. A small number of monocytes also rapidly and actively transport larger prion aggregates. SCS MΦs capture free prions as they emerge from afferent lymphatic vessels, while resident DCs extend processes into follicular conduits and extract free prions. MΦs at the site of infection capture large and small aggregates with or without Complement, perhaps by scavenger or other phagocytic receptors, or even macropinocytosis. These peripheral MΦs more likely degrade and/or sequester the majority of prions, whereas DCs and monocytes preferentially retain Complement-opsonized prions on their cell surfaces via Complement receptors. These *pr*DCs and *pr*Monos deliver the second wave of prions to draining LNs at least 12 hours later.

Inside LNs, SCS MΦs capture free prions or receive them from incoming *pr*DCs and *pr*Monos. *pr*DCs or SCS *pr*MΦs (which are more prone to present antigen than phagocytic peripheral *pr*MΦs) transfer prions to follicular B2 cells (and perhaps a few T cells), most likely but not necessarily aided by Complement. *pr*B2 cells then shuttle prions from the SCS or follicular conduits to FDCs, which express copious amounts of PrP^{C} that is converted into PrP^{Sc} in this optimized prion bioreactor. Cell autonomous prions not captured by SCS MΦs or resident DCs may encounter follicular B2 cells at follicular conduit termini or travel deep into the follicle where FDCs directly bind them. While prion replication certainly requires PrP^{C}, incunabular prion capture and trafficking does not.

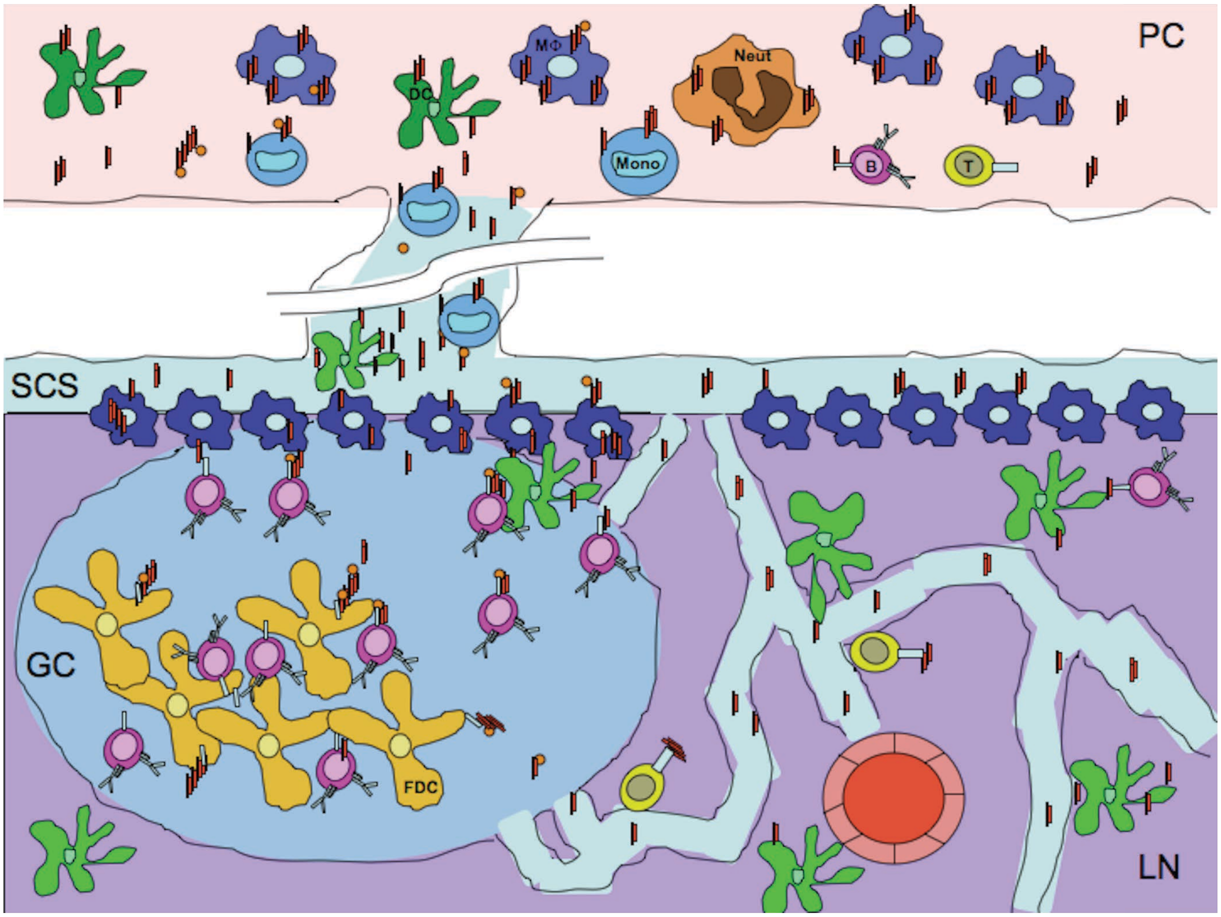

Figure 2.16. Prion Trafficking Model. Immune cells encounter prions in the PC and MedLN. Mφ, DCs, monocytes, neutrophils, B and T cells have all been shown to associate with prions in the PC and MedLN early after infection. Small prion particles traffic passively through the lymphatic system and enter the lymph node through afferent lymphatic vessels where they encounter B cells through follicular conduits. DCs may also access prions through protrusion of their dendrites through tight junctions into follicular condiuts. SCS Mφs trap larger prion or prion-complement immune complexes through scavenger or complement receptor 3 and may present them to underlying follicular B cells. Inflammatory monocytes actively transport prions to SCS Mφs, B cells, or DCs in the draining lymph node. B cells facilitate intrafollicular prion trafficking to FDCs for efficient prion replication.

REFERENCES

1. Prusiner, S. B. Novel proteinaceous infectious particles cause scrapie. *Science* **216**, 136–144 (1982).
2. Büeler, H. R. *et al.* Mice devoid of PrP are resistant to scrapie. *Cell* **73**, 1339–1347 (1993).
3. Brown, K. L. *et al.* Scrapie replication in lymphoid tissues depends on prion protein-expressing follicular dendritic cells. *Nat. Med.* **5**, 1308–1312 (1999).
4. Montrasio, F. *et al.* Impaired prion replication in spleens of mice lacking functional follicular dendritic cells. *Science* **288**, 1257–1259 (2000).
5. Götze, O. & Müller-Eberhard, H. J. The c3-activator system: an alternate pathway of complement activation. *J. Exp. Med.* **134**, 90–108 (1971).
6. Jiang, H., Burdick, D., Glabe, C. G., Cotman, C. W. & Tenner, A. J. beta-Amyloid activates complement by binding to a specific region of the collagen-like domain of the C1q A chain. *J. Immunol.* **152**, 5050–5059 (1994).
7. Sim, R. B., Kishore, U., Villiers, C. L., Marche, P. N. & Mitchell, D. A. C1q binding and complement activation by prions and amyloids. *Immunobiology* **212**, 355–362 (2007).
8. Aucouturier, P. Infected splenic dendritic cells are sufficient for prion transmission to the CNS in mouse scrapie. *J. Clin. Invest.* **108**, 703–708 (2001).
9. Beringue, V. *et al.* Role of spleen macrophages in the clearance of scrapie agent early in pathogenesis. *J. Pathol.* **190**, 495–502 (2000).
10. Manolova, V. *et al.* Nanoparticles target distinct dendritic cell populations according to their size. *Eur. J. Immunol.* **38**, 1404–1413 (2008).
11. Beier, R. & Gebert, A. Kinetics of particle uptake in the domes of Peyer's patches. *Am. J. Physiol.* **275**, G130–G137 (1998).
12. Itano, A. A. *et al.* Distinct dendritic cell populations sequentially present antigen to CD4 T cells and stimulate different aspects of cell-mediated immunity. *Immunity* **19**, 47–57 (2003).
13. Flores-Langarica, A., Sebti, Y., Mitchell, D. A., Sim, R. B. & MacPherson, G. G. Scrapie pathogenesis: the role of complement C1q in scrapie agent uptake by conventional dendritic cells. *J. Immunol.* **182**, 1305 (2009).
14. McCulloch, L. *et al.* Follicular Dendritic Cell-Specific Prion Protein (PrPc) Expression Alone Is Sufficient to Sustain Prion Infection in the Spleen. *PLoS_Pathog.* **7**, e1002402 (2011).
15. Zabel, M. D. *et al.* Stromal complement receptor CD21/35 facilitates lymphoid prion colonization and pathogenesis. *J. Immunol.* **179**, 6144–6152 (2007).
16. Carp, R. I. & Callahan, S. M. In vitro interaction of scrapie agent and mouse peritoneal macrophages. *Intervirology* **16**, 8–13 (1981).
17. Sassa, Y., Inoshima, Y. & Ishiguro, N. Bovine macrophage degradation of scrapie and BSE PrPSc. *Vet. Immunol. Immunopathol.* **133**, 33–39 (2010).
18. Sigurdson, C. J. *et al.* PrP(CWD) lymphoid cell targets in early and advanced chronic wasting disease of mule deer. *J. Gen. Virol.* **83**, 2617–2628 (2002).

19. Zhou, H. *et al.* Induction of macrophage migration by neurotoxic prion protein fragment. *J. Neurosci. Methods* **181**, 1–5 (2009).
20. Cordier-Dirikoc, S. & Chabry, J. Temporary Depletion of CD11c+ Dendritic Cells Delays Lymphoinvasion after Intraperitonal Scrapie Infection. *J. Virol.* **82**, 8933–8936 (2008).
21. Defaweux, V. *et al.* Interfaces between dendritic cells, other immune cells, and nerve fibres in mouse Peyer's patches: potential sites for neuroinvasion in prion diseases. *Microsc. Res. Tech.* **66**, 1–9 (2005).
22. Huang, F. P., Farquhar, C. F., Mabbott, N. A., Bruce, M. E. & MacPherson, G. G. Migrating intestinal dendritic cells transport PrP(Sc) from the gut. *J. Gen. Virol.* **83**, 267–271 (2002).
23. Raymond, C. R., Aucouturier, P. & Mabbott, N. A. In vivo depletion of CD11c+ cells impairs scrapie agent neuroinvasion from the intestine. *J. Immunol.* **179**, 7758–7766 (2007).
24. Mabbott, N. A. The complement system in prion diseases. *Curr. Opin. Immunol.* **16**, 587–593 (2004).
25. Mempel, T. R., Henrickson, S. E. & Andrian, Von, U. H. T-cell priming by dendriticcells in lymph nodes occurs in three distinct phases. *Nature* **427**, 154–159 (2004).
26. Junt, T. *et al.* Subcapsular sinus macrophages in lymph nodes clear lymph-borne viruses and present them to antiviral B cells. *Nature* **450**, 110–114 (2007).
27. Gonzalez, S. F. *et al.* Trafficking of B Cell Antigen in Lymph Nodes. *Annu. Rev. Immunol.* **29**, 215–233 (2011).
28. Gonzalez, S. F. *et al.* Capture of influenza by medullary dendritic cells via SIGN-R1 is essential for humoral immunity in draining lymph nodes. *Nat. Immunol.* **11**, 427–434 (2010).
29. Carrasco, Y. R. & Batista, F. D. B cells acquire particulate antigen in a macrophage-rich area at the boundary between the follicle and the subcapsular sinus of the lymph node. *Immunity* **27**, 160–171 (2007).
30. Li, L. & Choi, Y. S. Follicular dendritic cell-signaling molecules required for proliferation and differentiation of GC-B cells. *Semin. Immunol.* **14**, 259–266 (2002).
31. MacLennan, I. C. Germinal centers. *Annu. Rev. Immunol.* **12**, 117–139 (1994).
32. Le, Y. *et al.* Cutting Edge: The Neurotoxic Prion Peptide Fragment PrP(106-126) Is a Chemotactic Agonist for the G Protein-Coupled Receptor Formyl Peptide Receptor-Like 1. *J. Immunol.* **166**, 1448–1451. (2001).
33. Büeler, H. *et al.* Normal development and behaviour of mice lacking the neuronal cell-surface PrP protein. *Nature* **356**, 577–582 (1992).
34. Browning, S. R. *et al.* Browning SH Hoover E Telling GC Transmission of prions from mule deer and elk with chronic wasting disease to transgenic mice expressing cervid PrP JV 2004. *J. Virol.* **78**, 13345–13350 (2004).
35. Botto, M. *et al.* Homozygous C1q deficiency causes glomerulonephritis associated with multiple apoptotic bodies. *Nat. Genet.* **19**, 56–59 (1998).
36. Safar, J. *et al.* Molecular mass, biochemical composition, and physicochemical behavior of the infectious form of the scrapie precursor protein monomer. *Proc. Natl. Acad. Sci. U.S.A.* **87**, 6373–6377 (1990).
37. Johnson, T. E. *et al.* Monitoring Immune Cells Trafficking Fluorescent Prion Rods Hours after Intraperitoneal Infection. *J. Vis. Exp.* (2010).doi:10.3791/2349

38. Nichols, T. A. *et al.* Detection of protease-resistant cervid prion protein in water from a CWD-endemic area. *Prion* **3**, 171–183 (2009).

CHAPTER 3:

GENETIC DEPLETION OF COMPLEMENT RECEPTOR CD21/35 PREVENTS TERMINAL PRION DISEASE IN A MOUSE MODEL OF CHRONIC WASTING DISEASE[2]

Summary

The Complement System has been shown to facilitate peripheral prion pathogenesis. Mice lacking Complement receptors CD21/35 partially resist terminal prion disease when infected intraperitoneally with mouse-adapted scrapie prions. Chronic wasting disease (CWD) is an emerging prion disease of captive and free-ranging cervid populations that, like scrapie, has been shown to involve the immune system, which probably contributes to their relatively facile horizontal and environmental transmission. Here we show that mice overexpressing the cervid prion protein and susceptible to CWD (Tg(cerPrP)5037 mice) but lack CD21/35 expression completely resist clinical CWD upon peripheral infection. CD21/35 deficient Tg5037 mice exhibit greatly impaired splenic prion accumulation and replication throughout disease, similar to CD21/35 deficient murine PrP mice infected with mouse scrapie. TgA5037;CD21/35$^{-/-}$ mice exhibited little or no neuropathology and deposition of misfolded, protease-resistant PrP associated with CWD. CD21/35 translocates to lipid rafts and mediates a strong germinal center response to prion infection that we propose provides the optimal environment for prion

---

[2] Previously published as: Michel, B. *et al.* Genetic Depletion of Complement Receptors CD21/35 Prevents Terminal Prion Disease in a Mouse Model of Chronic Wasting Disease. *J Immunol.* (2012). http://www.jimmunol.org/content/early/2012/09/21/jimmunol.1201579.full.pdf

accumulation and replication. We further propose a potential role for CD21/35 in selecting prion quasi-species present in prion strains that may exhibit differential zoonotic potential compared to the parental strains.

Introduction

Chronic Wasting Disease (CWD) is the only recognized naturally occurring transmissible spongiform encephalopathy (TSE), affecting captive and free-ranging cervids [1] in North America and captive cervids in South Korea. Similar to other TSEs, CWD is caused by prions, unusual infectious agents devoid of instructional nucleic acid [2] and characterized by the accumulation of PrPRES, a proteinase K (PK) resistant form of the normal cellular prion protein, PrPc. CWD and the sheep TSE Scrapie can be transmitted relatively efficiently compared to other TSEs, probably contributing to their higher prevalences [3,4]. Prions have been detected in nervous and lymphoid tissue, muscle, blood, saliva, urine and feces [5-13]. Of particular interest are lymphoid tissues because they contain prions often before the central nervous system, implicating the lymphoid system as an initial site of extracerebral prion accumulation and replication. Lymphoid follicles or inflammatory foci accumulate and replicate prions primarily on follicular dendritic cells (FDCs) that express relatively large amounts of PrP^{C} [14-18]. FDCs originate from perivascular precursor cells [19] and trap immune complexes on their elaborate projections and present them to B cells, which can be positively selected, activated, undergo immunoglobulin affinity maturation and become plasma cells. FDCs may retain Ag on their cell surfaces for prolonged periods, maximizing presentation to B cells and consequently affecting the humoral immune response.

FDC depletion significantly impairs prion replication and FDC specific PrPc expression has been shown to be essential for optimal peripheral prion infection [14,17,18,20]. B cells, while replicating little prion, also play an essential role in peripheral prion pathogenesis [21,22]. This requirement presumably relates to B cells' ability to supply FDCs with critical cytokines important in FDC maturation and maintenance, but may also be involved in lymphotropic and/or intranodal prion trafficking.

Substantial evidence supports a significant role for the Complement system in expediting peripheral prion disease by mediating prion interaction with FDCs and B cells. Complement activation leads to asymmetrical cleavage of both C3 and C4 bound to pathogens. Complement receptors CD21/35 expressed on B cells and FDCs trap opsonized pathogens by binding cleaved C3 and C4 opsonins. Mice express CD21 and CD35 only on B cells and FDCs from alternatively spliced transcripts generated from a single gene, while humans express them on more cell types from separate genes [23,24]. While Complement mediated antigen trapping enhances both innate and adaptive immune responses to microbial pathogens, it actually exacerbates prion pathogenesis. Elimination of complement receptors CD21/35 reduced prion trapping, replication and disease [17]. Interestingly, depletion of CD21/35 has a greater impact on disease progression than deleting their ligand sources, C3 and C4, alluding to a role for CD21/35 in peripheral prion pathogenesis independent of their endogenous ligands. Genetic depletion of C1q also delays prion disease at high doses and prevents disease at low doses after intraperitoneal (I.P.) infection [25,26], and C1q has been shown to bind prions in vitro [27,28].

In this study, we show that complete elimination of the complement receptor CD21/35 in transgenic mice susceptible to CWD significantly delays splenic prion accumulation and blocks progression to terminal disease upon inoculation with CWD prions. To assess the kinetics of prion accumulation in the spleen we developed a semiquantitative prion amplification scoring system based on protein misfolding cyclic amplification (PMCA), which allowed us to evaluate prion replication and/or accumulation at 15, 30, 70, and 140 days post inoculation (DPI). Mice deficient in CD21/35 show a significant impairment in prion retention and replication compared to CD21/35 sufficient mice. We also observed significant germinal center formation during scrapie prion infection that was dependent on CD21/35 and PrPc expression on FDCs. Lipid raft flotation experiments show movement of CD21/35 into lipid rafts on B cells upon prion infection. Overall, these data demonstrate that CD21/35 mediated prion trapping on FDCs and possibly B cells marks an important event in lymphoid prion pathogenesis that promotes terminal prion disease in these mouse models.

Material and Methods

Mice

*Prnp*o/oCD21/35-/-, C3/C4-/-, Tg5037 and TgA20 mice were made as previously described [17,29,30]. *Prnp*o/oCD21/35-/- were crossed with TgA20 or Tg5037 mice to produce TgA20;*Prnp*o/oCD21/35-/- (TgA20;CD21/35-/-) and Tg5037;*Prnp*o/oCD21/35-/- (Tg5037;CD21/35-/-) mice. All mice were bred and maintained at Lab Animal Resources, accredited by the Association for Assessment and Accreditation of Lab Animal Care International, in accordance with protocols approved by the Institutional Animal Care and Use Committee at Colorado State University. Bone marrow chimeric mice were produced as previously described [17].

Preparation of inoculum

10% brain homogenates were prepared in PMCA buffer (4mM EDTA, 150 mM NaCl in PBS) from E2 homogenates derived from a terminally diseased elk brain. RML5 prions were prepared as previously described [17]. 10% homogenates were diluted 1:10 (E2 and RML5) or 1:1000 (RML5) in 320 mM sucrose supplemented with 100 units/mL Penicillin and 100 µg/mL Streptomycin (Gibco) in PBS immediately prior to inoculation.

Inoculations, Clinical scoring and Dissections

Mice were inoculated intraperitoneallly with 100 µl of inoculum using a 28G Insulin syringe. Mice were monitored for clinical symptoms of prion disease, including tail rigidity, impaired 95extensor reflex, akinesia, tremors, ataxia and weight loss. Mice with any four of these symptoms or paralysis were scored terminally sick and euthanized.

Mice were inoculated with inocula described above and euthanized at indicated time points by CO2 inhalation. Brains and spleens were collected and divided sagittally. One brain hemisphere and half a spleen was fixed in 4% paraformaldehyde in PBS for histology and one was homogenized and used for NaPTA precipitation, PMCA or PK digestion.

Sodium phosphotungstic (NaPTA) Precipitation of PrPRES

NaPTA precipitation was performed exactly as described previously [17]. Briefly, Gross cellular debris was removed by centrifugation at 80 x g and 500 µl of supernatant mixed 1:1 with 4% sarkosyl in PBS. Samples were incubated for 15 min at 37°C with constant agitation, then incubated with 50 U/ml benzonase and 12.75 mM MgCl2 for 30 min at 37°C with constant agitation. Prewarmed NaPTA stock solution (pH 7.4) was added to a final concentration of 0.3% and the sample was incubated at 37°C for 30 min with constant agitation and centrifuged at 37°C for 30 min at maximum speed in an Eppendorf microcentrifuge. The pellet was resuspended in 30 µl of 0.1% sarkosyl in PBS and digested with 20 µg/ml PK for 30 min at 37°C.

Protein misfolding cyclic amplification (PMCA), PK digestion and Western blotting (WB)

PMCA was performed and quantified as previously described [13] with slight modifications. Samples were sonicated at 70–85% maximum power for 40 s in a microplate horn sonicator (Qsonic, Framingham), followed by a 30-minute incubation at 37 °C repeated for 24 hours per round for up to five rounds total. PK digestion and WB was performed as previously described [31], except that spleen homogenates were digested with 10 μg/mL PK. PrP was detected using HRP-conjugated Bar244 antibody (Bertin Pharma, Paris).

Histochemistry and Immunohistochemistry

Slides were prepared and stained as previously described [31]. Briefly, 10 μm sections were cut from paraffin-embedded spleen tissue and mounted onto glass slides. Splenic follicles were stained with rat anti-mouse IgM (02031D, Pharmingen) followed by goat anti-rat IgG (H+L) followed by AP-conjugated donkey anti-goat IgG (705-055-147, Jackson) and visualized with Fast Blue (Polysciences, Warrington, PA). Germinal centers were stained with Biotin-conjugated peanut agglutinin (PNA) ABComplex/horseradish peroxidase (ABC/HRP, Dako) and visualized with 3-Amino-9-Ethylcarbazole (AEC, A5754, Sigma).

Splenocyte isolation and flotation assays

Individual whole spleens from at least five mice per group were ground through a nylon mesh to release lymphocytes into single cell suspensions, which were then centrifuged 5 min at 200g and washed twice with ice cold PBS. The remaining splenic tissue was digested for 20 min at 37oC in 1 mg/mL Collagenase, 0.5 mg/mL Dispase and 40μg/mL DNase I (Roche, Mannheim, Germany) with agitation. Supernatants were collected and the remaining tissue digested for another twenty minutes. The samples were pooled and centrifuged 5 min at 200 x g. Cell pellets were washed twice with ice cold PBS, combined with corresponding lymphocyte pellets and incubated 30 min on ice in 400µl 1% Triton X-100 in TNE buffer (25mM Tris-HCl ph7.4, 150mM NaCl, 5mM EDTA 5mM dithiotheitol (DTT)) containing protease inhibitors (Complete Mini tablet, Roche). Samples were centrifuged 10 min at 1000 x g at 4°C to pellet debris and supernatants transferred to new tubes. 133 µl of lysates were mixed with 267 µl 60% (w/v) Optiprep solution (Axis-Shield, Oslo, Norway) and pipetted to the bottom of 13 x 51 mm UltraClear centrifuge tubes (Beckman-Coulter, Palo Alto, CA, USA). 200 µl aliquots of 35%, 30%, 25%, and 20% Optiprep were gently layered on top of the lysates. Tubes were centrifuged 12 h at 4°C in a S55S Sorvall M150SE rotor at 120,000 x g. Two hundred microliter fractions were collected from the top of the tube. SDS-PAGE loading buffer was added to aliquots of each fraction with or without PK digestion (20µg/mL for 30 min) and subjected to 4-12% gradient PAGE.

Germinal Center counting, statistical and phylogenetic analyses.

Follicles were counted in three non-consecutive sections from five distinct areas from at least five spleens as IgM+ B cells forming characteristic follicular foci. Germinal centers were counted as PNA+ B cells (brown stain) within follicles (IgM+ blue stain). We derived percentages of follicles containing GCs (%GCs) by dividing the number of GCs by the number of follicles and multiplying by 100. Statistical analyses were performed using Excel (Microsoft) and Prism software (GraphPad). CD21 sequence alignment and phylogenetic anyalysis was performed using Geneious (BioMatters, Auckland, New Zealand).

Results

Absence of CD21/35 protects mice from CWD

To create a mouse deficient in complement receptors CD21/35 and susceptible to CWD prions, mice deficient in both CD21/35 (CD21/35$^{-/-}$) and mouse PrP^{C} (Prnp$^{o/o}$) were crossed to

Tg (cerPrP) 5037 mice that express high levels of elk, but no mouse, PrP^{C}. Offspring were then screened and resulting Tg5037;CD21/35$^{-/-}$ and Tg5037 littermates inoculated with 100 µg brain homogenate from an elk terminally infected with CWD prions (E2). Tg5037;CD21/35$^{-/-}$ mice showed complete resistance to CWD prions, with no mice showing any clinic signs at the end of the study, while infected Tg5037 mice died from CWD at a median time of 301 DPI (Figure 3.1A). We next examined terminally sick Tg5037 and DPI matched Tg5037;CD21/35$^{-/-}$ mice for characteristic signs of CWD neuropathology (Figure 3.1B-G). Minimal astrogliosis and vacuolization with no PrP^{RES} deposition was observed in nonclinical Tg5037;CD21/35$^{-/-}$ mice at 285 DPI (Figure 3.1B, D and F). However, significant vacuolization, astrogliosis, and PrP^{RES} deposition were observed in terminally sick Tg5037 mice at 285 DPI (Figure 3.1C, E and G). Western blot and densitometric analyses revealed PrP^{RES} in only 3 of 11 brains from Tg5037;CD21/35$^{-/-}$ mice, significantly less than in brains from terminally sick Tg5037 mouse, all of which contained PrP^{RES} and, when compiled together, contained 3.5-fold more PrP^{RES} (Figure 3.1H and I).

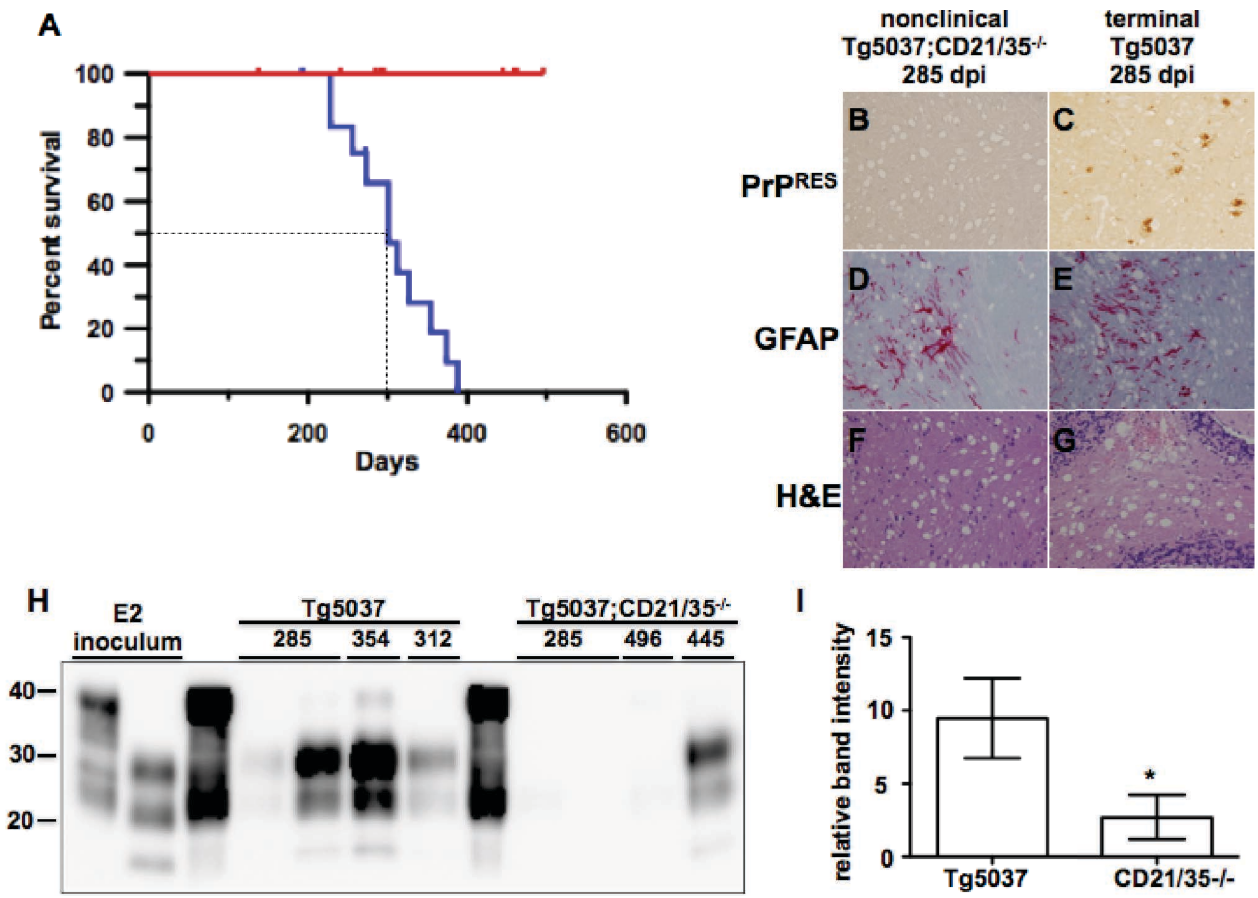

Figure 3.1. Mice deficient in CD21/35 show resistance to CWD prion infection. (A) Tg5037 (blue line, n=8) and Tg5037;CD21/35$^{-/-}$ (red line, n=11) mice were inoculated with 100 μg of brain homogenate from an elk terminally infected with CWD and monitored for terminal disease. Tg5037 mice show a median survival time of 301 dpi, compared to Tg5037;CD21/35$^{-/-}$ mice, all of which remained nonclinical to the end of the study (>500 DPI). (B) IHC of brain sections from nonclinical Tg5037;CD21/35$^{-/-}$ mice 285 dpi (B, D and F) exhibited minimal vacuolization, prion deposition and astogliosis compared to DPI-matched Tg5037 mice (C,E and G). (H) Western blot (WB) analysis of PrP^{RES} content from Tg5037 and Tg5037;CD21/35$^{-/-}$ mice. All samples contain 100 μg of protease digested brain homogenate except lanes 1,3 and 8, which contain 20 μg of undigested brain homogenate (Tg5037 mice (lanes 3 and 8) express five-fold more PrP than cervids (E2, lane 1)). (I) Densitometric analyses of protease resistant bands in the western blot confirm that the brains from terminal Tg5037 mice contain significantly higher PrP^{RES} content compared to Tg5037;CD21/35$^{-/-}$ mice.

Absence of CD21/35 delays prion propagation in the spleen

We next used a semiquantitative prion amplification assay to estimate prion loads in spleens of CWD infected Tg5037 and Tg5037;CD21/35$^{-/-}$ mice. PMCA, a technique used to amplify prions in vitro, takes advantage of a prion's ability to self propagate, using seeded protein fibrilization (Figure 3.2A). We employed PMCA to amplify and quantify minute amounts of PrP^{RES} from spleen homogenates from mice at various intervals after infection. Tg5037 mice at 15 DPI show a significant difference in the amount of splenic PrP^{RES} (Figure 3.2B and C, 75.49 ± 4.43 rpu) compared to Tg5037;CD21/35$^{-/-}$ mice (25.56 ± 4.24 rpu). Using our standard curve for this assay generated previously, we estimate that splenic PrP^{RES} load in Tg5037 mice approximates 20,000 pg/g of spleen tissue (Figure 3.2C). The PMCA score for Tg5037;CD21/35$^{-/-}$ mice falls just out of the dynamic range of our assay (29 rpu), so we can only estimate the load to be < 100 pg/g. We detected much less PrP^{RES} in spleens from Tg5037 mice at 30 DPI (17.17 ± 0.16 rpu) while Tg5037;CD21/35$^{-/-}$ spleens showed only a slight decrease in PrP^{RES} load (21.88 ± 0.15 rpu). Both scores fall just below the range of the PMCA score standard curve. Accumulation of PrP^{RES} differed drastically between the two groups after 30 DPI. PrP^{RES} load increased significantly more in Tg5037 mice from 70 (37.50 ± 0.15 rpu, 250 pg/g) to 140 DPI (55.56 ± 0.11 rpu, 2000 pg/g) to terminal disease (71.00 ± 0.2 rpu, 10,000 pg/g). We detected significantly less PrP^{RES} in spleens from nonclinical Tg5037;CD21/35$^{-/-}$ at 70 (20.00 ± 0.14 rpu, <100 pg/g) and 140 DPI (41 ± 0.16 rpu, 500 pg/g) and at DPIs matched to sick Tg5037 mice (47.00 ± 0.50rpu, 900 pg/g).

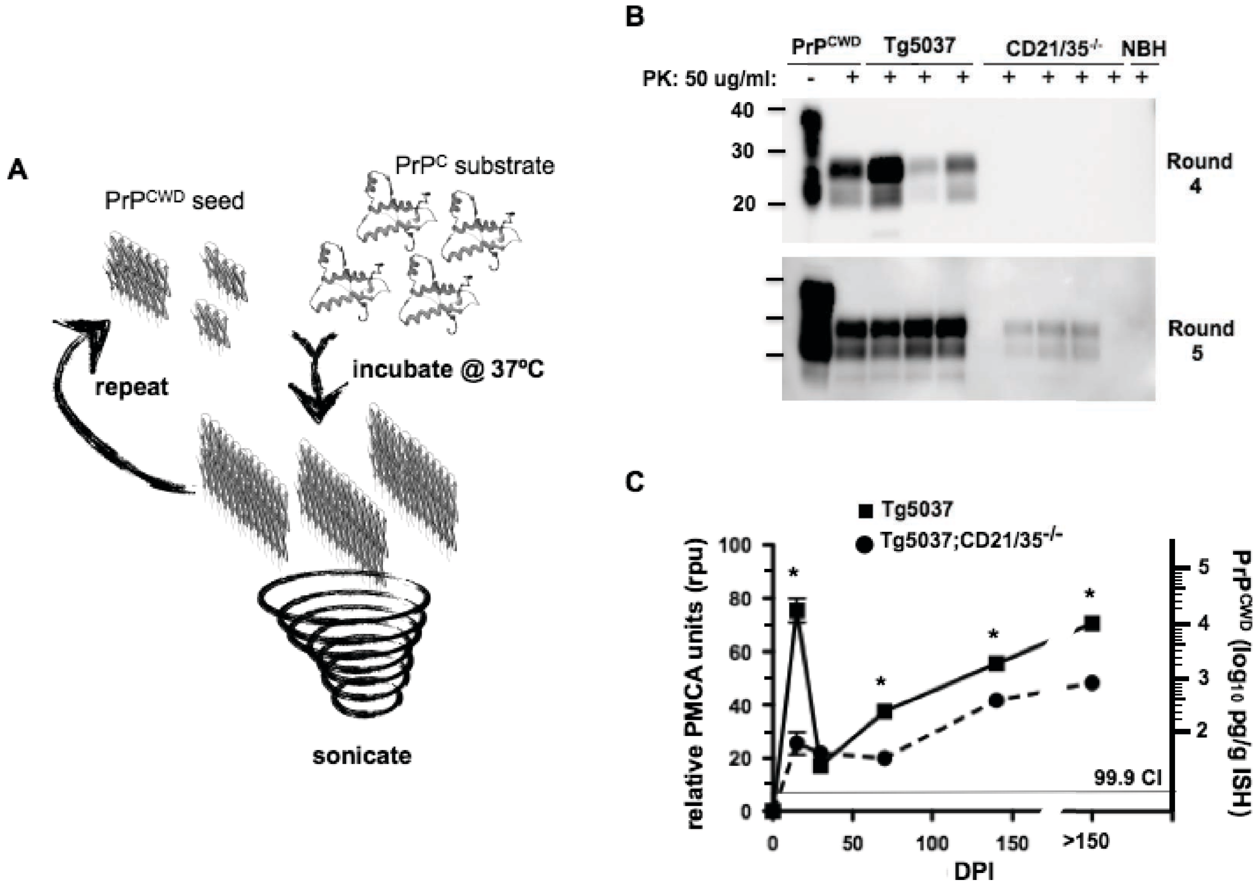

FIGURE 3.2. Tg5037;CD21/35$^{-/-}$ mice show delayed prion accumulation in the spleen. (A) Schematic representation of PMCA. Alternating cycles of incubation and sonication of cellular PrP seeded with PrP^{RES} with substrate followed by Proteinase K (PK) digestion and western blotting (WB) amplify and detect minute quanttites of prions. (B) Representative WB showing PMCA results from round four and five of spleen samples from both Tg5037 and Tg5037;CD21/35$^{-/-}$ mice ($n \geq 5$). All samples contain 100 μg of protease digested PMCA sample except lane 1, which contains 20 μg of undigested sample. We detected PrP^{RES} in Tg5037 spleen samples in round 4 and in Tg5037; CD21/35$^{-/-}$ spleen samples in round 5, indicating a higher CWD prion concentration in mice that express CD21/35. (C) Tg5037 mice accumulate significantly more CWD prions in the spleen at 15, 70, 140 DPI and terminal disease compared to Tg5037;CD21/35$^{-/-}$ mice. Left axis shows PMCA score in relative PMCA units (rpu). Right axis shows PrP^{RES} load in pg/g of infected spleen homogenate. At least five replicates of each sample was assayed ($n \geq 8$, $*p<0.01$).

CD21/35 mediates a strong germinal center response during prion infection

Increased PrP^{RES} retention could be mediated via formation of germinal centers (GCs). Antigen trapping by Fcγ receptors and CD21/35 on FDCs, and concomitant B cell signaling through the B cell receptor (BCR) and the CD21/CD19/CD81 coreceptor stimulates lymphoid follicles to generate GCs [32-35] containing arborized FDCs. Prolonged antigen presentation by FDCs and additional signals (CD40-CD40L) activates B cells to become plasma or memory B cells [36,37]. CD21/35$^{-/-}$ and C3$^{-/-}$ mice have reduced size and numbers of germinal centers before antigenic stimulation [38,39] but high doses of antigen increase GCs to near wt levels. We observed a similar phenomenon in spleens of mice overexpressing PrP^{C} (TgA20, Tg5037, TgA20;CD21/35$^{-/-}$ and Tg5037;CD21/35$^{-/-}$ mice), which exhibited significant GC formation during prion infection independent of CD21/35 expression (data not shown). This most likely occurred because increased PrP^{C} expression increases prion replication and concomitant antigenic stimulation of GC formation, just as high doses of microbial antigens can.

In mouse models expressing normal physiological levels of PrP^{C} and CD21/35, scrapie prion infection causes abnormal GC reactions characterized by hypertrophic FDC dendrites, PrP^{RES} accumulation, and increased maturation and numbers of B cells [40]. We therefore investigated the role of CD21/35 in this process by analyzing GC formation in mice expressing normal wild type mouse PrP^{C} levels, with or without CD21/35 expression, after infecting them with RML5 mouse adapted scrapie prions. We discovered that intraperitoneal inoculation of high and low doses of prions, but not uninfected (mock) brain homogenate, stimulated significant GC formation in spleens of wt, but not CD21/35$^{-/-}$ mice (Figures 3.3A-D and Table 3.1, $n \geq 5$). Interestingly, prion infection, but not 10^8 colony forming units (cfu) of heat-killed *E. coli* or DNP-KLH (data not shown), induced GC formation in C3/4$^{-/-}$ mice, suggesting that CD21/35 can mediate prion-induced GC reactions independent of its endogenous ligands. Moreover, we detected significant amounts of CD21/35 in PrP^{RES} preparations enriched by

NaPTA precipitation from spleen homogenates of infected mice 60 DPI, but very little CD21/35 from NaPTA precipitates from mock infected spleens (Figure 3.3E). We recovered far less PrP^{RES} from $CD21/35^{-/-}$ spleens, consistent with our PMCA data from $Tg5037;CD21/35^{-/-}$ spleens.

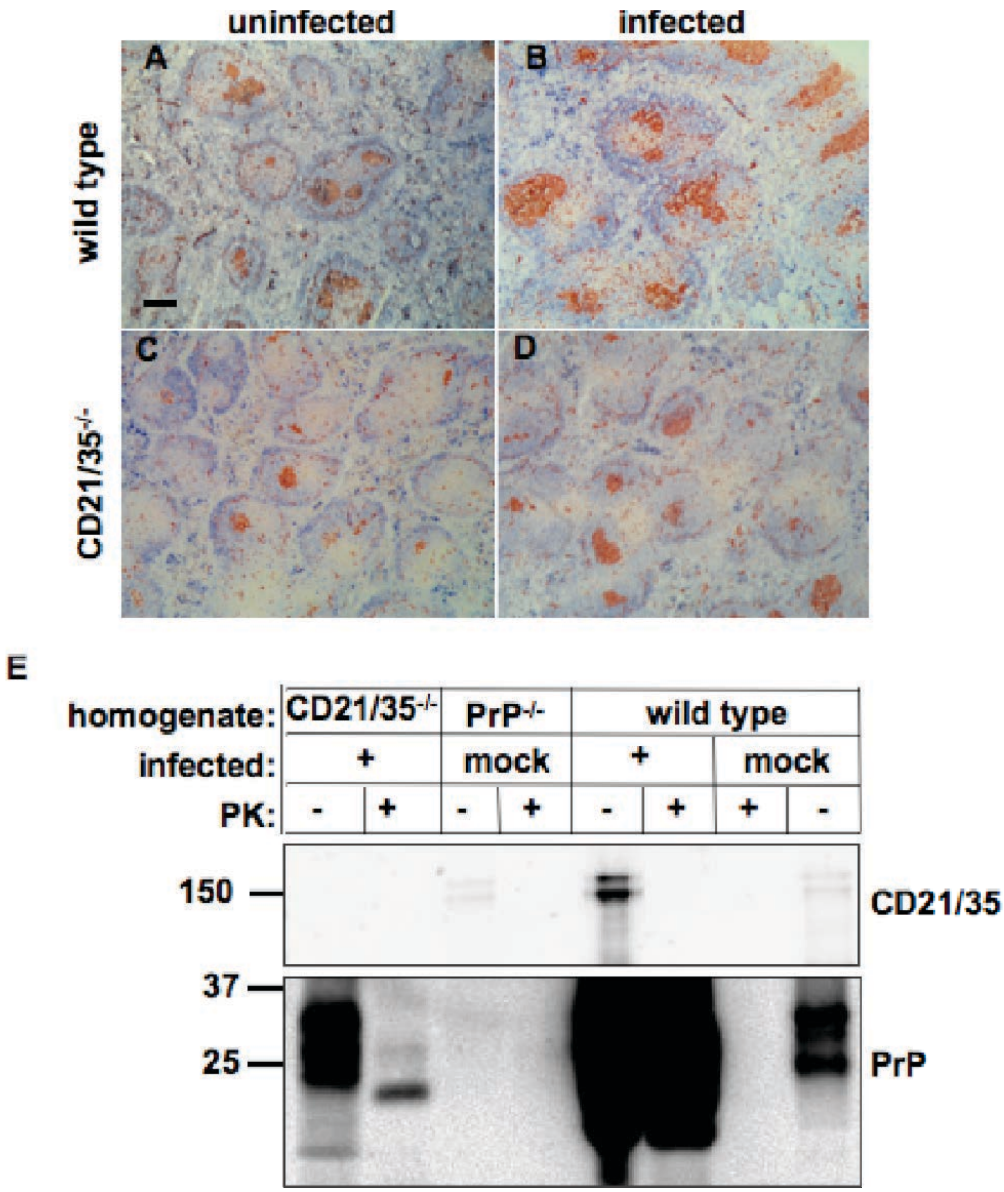

Figure 3.3. Prion infection stimulates germinal center (GC) formation and increases CD21/35 presence in prion-enriched spleen preparations. (A-E) Mice ($n \geq 10$) were inoculated i.p. with 0.1%, prion-infected brain homogenate, sacrificed 60 DPI and frozen spleen sections stained with IgM (blue stain) and PNA (brown) that reveal GCs in splenic follicles from uninfected wt (A) mice that increased in size and number upon prion infection (B), Spleens from CD21/35$^{-/-}$ mice contain relatively few, small GCs (C) that were only nominally increased and less than wt spleens upon prion infection (D). (E) CD21/35 is greatly enriched in NaPTA precipitated PrP^{RES} preparations from spleens of terminally sick mice compared to PrP$^{-/-}$ and mock-infected wt mice. PrP^{RES} was precipitated from 500 μg of total spleen homogenate and equal volumes loaded into each lane.

Table 3.1. *Germinal Center Formation in Peripheral Prion Disease*

Inoculum	DPI[b]	%GC+[a] WT	CD21/35$^{-/-}$	C3/4$^{-/-}$
1% NBH[c]	120	34 ± 5	14 ± 3[d]	15 ± 4[d]
0.1% IBH[e]	30	33 ± 8	25 ± 3	20 ± 3
	60	44 ± 14	17 ± 5[d]	37 ± 7
	90	55 ± 6	21 ± 4[d]	51 ± 5
	term[f]	67 ± 4	23 ± 3[d]	62 ± 6
1% IBH	term[f]	96 ± 16	27 ± 5[d]	72 ± 14
10^8 *E. coli*	7	83 ± 8	19 ± 6	17 ± 4

[a]number of germinal centers/number of follicles
[b]DPI, days post inoculation
[c]NBH, normal brain homogenate
[d] $p<0.01$
[e]IBH, infected brain homogenate
[f]DPI ranged from 280-385 days

CD21/35 translocates to lipid rafts on B cells upon prion infection

GC formation by the traditional primary immune response requires CD21/35 expression on B cells but not FDCs [35]. Closer examination of GC formation in BM chimeric mice infected with prions divulged a pattern of GC formation predominantly dependent on both CD21/35 and PrP^C expression on FDCs (Table 3.2, $n \geq 5$), suggesting that CD21/35 antigen presentation is more important than CD21/35 signaling to mediate this reaction. To resolve this discrepancy in GC formation we assessed whether prion infection alters localization of CD21/35 on the plasma membrane. In a typical primary immune response, C3d or C4d-opsonized antigen binds to specific short consensus repeats (SCRs) of CD21/35, inducing CD19-mediated palmitoylation of the tetraspanin CD81 [41,42] that moves the entire complex into lipid rafts, cholesterol- and sphingolipid-rich microdomains of the plasma membrane [43]. This offers an attractive model of prion replication because PrP^{C} resides in lipid rafts via its glycerophosphatidylinositol (GPI) anchor, and translocation of CD21/35 to the same rafts upon prion infection could effectively bring PrP^{RES} to PrP^{C}. We therefore monitored CD21/35 translocation to lipid rafts on splenocytes from infected mice by lysing them in cold Triton X-100 and subjecting the cleared lysate to density gradient centrifugation. CD21/35 resides predominantly outside lipid rafts on splenocytes from mock-infected wild type mice, as indicated by its presence in detergent soluble fractions (Figure 3.4A). In contrast, PrP was detected in detergent insoluble fractions containing lipid rafts that float to the top of the density gradient and colocalize with the raft marker flotillin. Upon prion infection, a significant amount of CD21/35 moved into detergent insoluble fractions (Figure 3.4B). CD21/35 was present in the same fractions as flotillin and PK-resistant PrP^{RES}, but not the immunoglobulin heavy chain (IgH), indicating that CD21/35 translocation occurred independent of the BCR. Furthermore, while a T cell-dependent antigen failed to stimulate CD21/35 translocation to lipid rafts in $C3/4^{-/-}$ mice (Figure 3.4C), prion infection induced a significant amount of CD21/35 translocation (figure 3.4D). These data strongly suggest that CD21/35 can interact with prions independent of its endogenous ligands, which could explain why $CD21/35^{-/-}$ mice exhibit a more significant delay in disease progression than $C3/4^{-/-}$ mice. While the lack of CD21/35 expression does not completely prevent PrP^{RES} accumulation in lipid rafts, it significantly decreases PrP^{RES} load (Figure 3.4E). Flotation assays on spleens from BM chimeric mice revealed that FDCs appear to express only the short form of the Complement receptor, CD21, and that prion infection fails to translocate CD21 to lipid rafts on FDCs (Figure

3.4F). Thus, prion infection provokes CD21/35 translocation on B cells, which express all members of the CD21/CD19/CD81 coreceptor complex, but not on FDCs, which only express CD21.

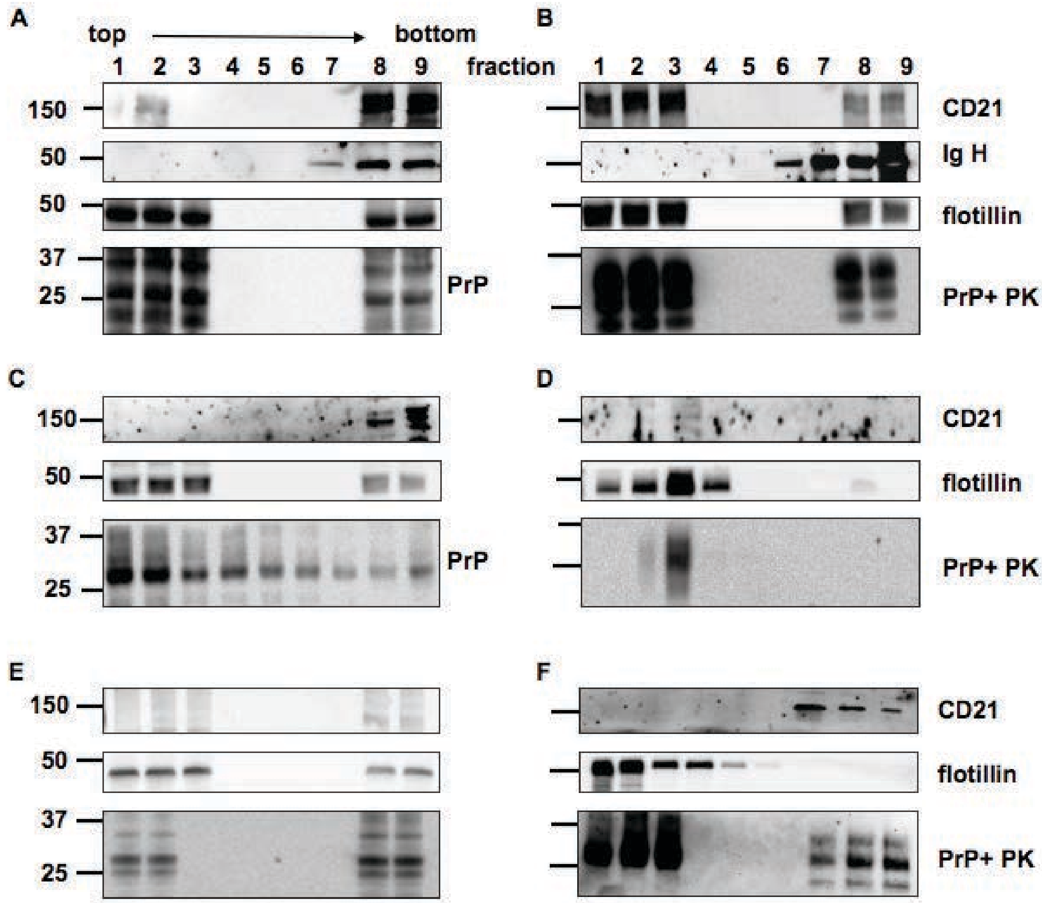

Figure 3.4. Prion infection stimulates CD21/35 translocation to lipid rafts on B cells in CD21/35-expressing mice. 2 x 10^7 splenocytes were lysed in ice-cold Triton X-100 and cleared lysates were centrifuged at the bottom of a density gradient (see Methods). (A) CD21/35 and the B cell receptor (BCR) immunoglobulin heavy chain (IgH) reside outside lipid rafts on mock-infected wt splenocytes. (B) CD21/35, but not IgH, translocates to lipid rafts and colocalizes with PrP^{RES} and the raft marker flotillin on prion-infected wt splenocytes. (C) CD21/35 resides outside lipid rafts on $C3/4^{-/-}$ splenocytes from mice inoculated i.p with 10^8 cfu of heat killed *E. coli*. (D) Upon prion infection, CD21/35 moves into lipid rafts independent of its endogenous ligands in $C3/4^{-/-}$ mice. (E) Infected $CD21/35^{-/-}$ splenocytes retain less PrP^{RES} than infected wt splenocytes (compare to B). (F) Irradiated wt mice reconstituted with $CD21/35^{-/-}$ bone marrow express CD21 only on FDCs. Upon prion infection, CD21 remains outside lipid rafts, indicating that prion-stimulated CD21/35 translocation occurs only on B cells. Data are representative of at least five independent experiments.

Table 3.2. *Germinal Center Formation in Bone Marrow Chimeric Mice Infected with Prions*

Donor BM[a]	Host genotype[b]	CD21/35 expression[c]	PrP^c expression[c]	% GC+[d]
wt	wt	both	both	72 ± 12
wt	$CD21/35^{-/-}$	B cells	both	22 ± 4[e]
$CD21/35^{-/-}$	wt	FDCs	both	78 ± 13
$CD21/35^{-/-}$	$CD21/35^{-/-}$	neither	both	23 ± 3[e]
wt	$PrP^{-/-}$	both	B cells	15 ± 11[e]
$CD21/35^{-/-}$	$PrP^{-/-}$	FDCs	B cells	11 ± 7[e]
$PrP^{-/-}$	wt	both	FDCs	73 ± 9
$PrP^{-/-}$	$CD21/35^{-/-}$	B cells	FDCs	21 ± 2[e]
$PrP^{-/-}$	$PrP^{-/-}$	both	neither	14 ± 4[e]
$PrP^{-/-}$ $CD21/35^{-/-}$	wt	FDCs	FDCs	75 ± 9
$PrP^{-/-}$ $CD21/35^{-/-}$	$CD21/35^{-/-}$	neither	FDCs	19 ± 2[e]
$PrP^{-/-}$ $CD21/35^{-/-}$	$PrP^{-/-}$	FDCs	neither	14 ± 5[e]
wt	$PrP^{-/-}$ $CD21/35^{-/-}$	B cells	B cells	13 ± 6[e]
$PrP^{-/-}$	$PrP^{-/-}$ $CD21/35^{-/-}$	B cells	neither	10 ± 4[e]
$CD21/35^{-/-}$	$PrP^{-/-}$ $CD21/35^{-/-}$	neither	B cells	12 ± 2[e]
$PrP^{-/-}$ $CD21/35^{-/-}$	$PrP^{-/-}$ $CD21/35^{-/-}$	neither	neither	13 ± 4[e]

Table 3.2. *Germinal Center Formation in Bone Marrow Chimeric Mice Infected with Prions*

[a]BM was isolated from mice of the indicated genotype.
[b] Hemopoietic systems of sublethally irradiated mice of the indicated genotypes were reconstituted with donor BM.
[c] CD21/35/35 or PrP expression was restricted to the indicated cell types for each reconstitution group.
[d]Mice inoculated with 1% IBH analyzed 90 DPI
[e] $p<0.01$

Discussion

We investigated the role of the complement receptor CD21/35 in CWD prion accumulation, replication, and disease progression. We observed a complete rescue from terminal CWD of Tg5037 mice lacking CD21/35. Just 3/11 nonclinical Tg5037;CD21/35-/- mice displayed detectable, yet reduced, prion neuropathology and PrP^{RES} deposition in their brains. These results reveal a more dramatic outcome than earlier studies showing only a partial rescue of CD21/35 deficient mice from scrapie infection, despite those mice expressing only wild type (i.e., five-fold less) PrP^{C} levels. This could reflect differences between mouse and cervid CD21 expression, as are apparent between mouse and human CD21. However, little is known about cervid CD21. The gene has yet to be cloned, so comparative analyses with murine CD21/35 are impossible to date. We can, however, compare CD21 sequence homology and phylogeny among other species that are susceptible to TSEs. For example, sheep, which are susceptible to scrapie, a TSE that closely resembles CWD in transmission efficiency and lymphotropism, express a CD21 molecule that shares 65% sequence identity with murine CD21/35, including their ligand binding domains (figure 3.5A). This may explain the similar lymphotropic characteristics of murine and ovine scrapie. Ovine CD21 also shares 65% identity with human CD21/35. Overall, CD21/35 from these three species share 52% identity and 64% similarity. In contrast, bovine CD21, which is 40% larger than the other three CD21/35 molecules (~1400 aa compared to ~1000 aa, respectively), shares less than 20% similarity to the other three CD21/35 molecules. Phylogenetic analysis reveals a clustering of murine, ovine and human CD21/35 proteins, with bovine CD21 much more distantly related (figure 3.5B). Interestingly, BSE has been shown to have little or no lymphotropic characteristics [44-47], perhaps due to the vastly different CD21 molecule that bovines express.

A

```
                1        10        20        30        40        50        60
                |        |         |         |         |         |         |
  Bos taurus    MGAAGPIWVFLTLLAPGVLGQCKFLPRYPFAKPKIQSDQSEFAVGKTWEYECLPGYFKKS
Homo sapiens    mgaagllgvflalvapgvlgi-----------------------s---------------
Mus musculus    MGSLGSLWVFFTLITPGVLEI-----------------------S---------------
  Ovis aries    MTYIWIFYLNLNLIFMISVTT-----------------------YFL------------S

  Bos taurus    FFVTCLKTSNWSNAQQFCKRKSCTVPRELLHGSV-HTPQGIMFGATITFSCDRGYRLIGD
Homo sapiens    ------c----------------gspppilngrisyystpiavgtviryscsgtfrlige
Mus musculus    ------C----------------DPPPEVKNARKPYYSLPIVPGTVLRYTCSPSYRLIGE
  Ovis aries    YFAGIFC----------------DPPPSIKNGRSGYHSGPVALNAVVTYSCASAFRLIGE

  Bos taurus    TSATCLISDNT-VTWDKDLPLCESIPCE---PPPAISNGDFQSSNRDYFYYGTVVTYQCH
Homo sapiens    ksllcitkdkvdgtwdkpapkceyfnkysscpepivpggykirgs-tpyrhgdsvtfack
Mus musculus    KAIFCISENQVHATWDKAPPICESVNKTISCSDPIVPGGFMNKGSKAPFRHGDSVTFTCK
  Ovis aries    RRLFCISKDNVNGIWDKAPPICEYYNRNSVCSEPIIPGGYRTKTSRPPFRHGDAVTFSCN

  Bos taurus    VGQNGKKLFDLLGEKSIYCTSKDNQVGIWNSPPPQCIPVVKCP-IPEVENGAMESGFRRS
Homo sapiens    tn------fsmngnksvwcqa-nnmwgptrlptcvsvfplecpalpmihnghhtsenvgs
Mus musculus    AN------FTMKGSKTVWCQA-NEMWGPTALPVCESDFPLECPSLPTIHNGHHTGQHVDQ
  Ovis aries    AN------FTMKGNKTVWCQA-NRKWGPTPLPICESDTPLECPSLPTIANGHHTGESVAS
```

B

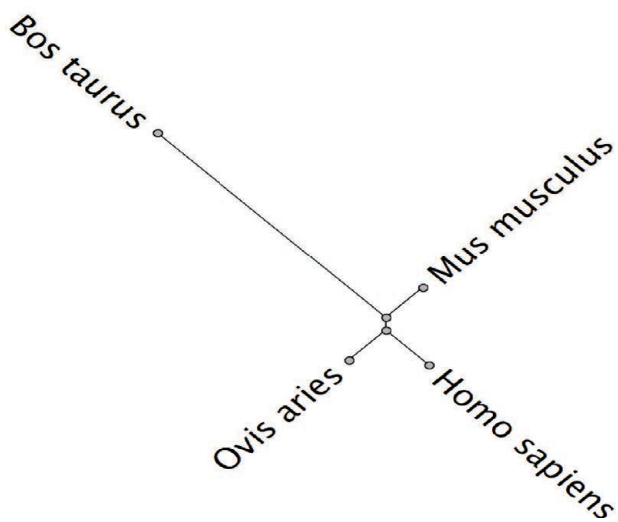

Figure 3.5. Sequence and phylogenetic analyses of CD21/35. A. Sequence alignment of ligand binding domains of bovine, human, mouse and sheep CD21. B. Phylogenetic tree showing relative relatedness of bovine, human, mouse and sheep CD21.

These results indicate a significant role in prion pathogenesis for CD21/35, the importance of which may vary by prion strain. Complement components C1q and C3 have recently been shown to exhibit similar strain preferences in vitro and in vivo [48]. We are currently investigating other prion strains to determine the contribution of CD21/35 to prion pathogenesis in those infection models. Interestingly, cross-species prion transmission was recently shown to result in a higher infection rate of the lymphoreticular system than the central nervous system in the xenohost [49]. This cross-species infection resulted in distinct lymphotropic and neurotropic strains with differential host ranges. These strains may result from tissue-specific strain selection or mutation. The higher efficiency of prion infection in the spleen (which harbor CD21/35 expressing FDCs and B cells) compared to the brain (which lacks them) alludes to a critical role for CD21/35 in prion retention, replication, and possibly strain selection in trans-species prion infection. The lack of CD21/35 that delays peripheral prion accumulation might further limit the lymphoid replication of neurotropic prion strains, resulting in delayed or abrogated disease progression. If so, this would have profound implications for prion xenotransmission and possible therapeutic approaches aimed at CD21/35. For example, targeting CD21/35 to slow the spread of neurotropic prions could be an attractive alternative to most prion disease therapeutics developed to date that target the central nervous system, which can complicate drug delivery. Interfering with CD21/35 mediated prion strain selection could also mitigate emergence of new prion strains with expanded host ranges and prevent a breach of the species barrier like the one that likely caused the BSE and subsequent new-variant CJD outbreak fifteen years ago in the United Kingdom.

To study the kinetics of extraneural CWD prion accumulation, we amplified PrP^{RES} from spleens of CWD prion infected Tg5037 and Tg5037;CD21/35-/- mice at various time points throughout infection. At 15, 70, 140 DPI and terminal disease prion accumulation was significantly lower in CD21/35 deficient mice. The extremely high prion load detected at 15 DPI most likely reflects increased retention of prion inocula early after infection. This delay in extraneural prion accumulation strongly correlates with abrogation of prion neuropathology and terminal disease. These results coincide with our previous data from scrapie mouse models (17), further strengthening evidence that CD21/35 plays an integral part in prion accumulation in peripheral lymphoid organs that ultimately facilitates neuroinvasion.

Furthermore, we show that CD21/35 is present in prion preparations enriched from spleen homogenates by NaPTA precipitation. We also demonstrate germinal center formation in spleens during prion infection primarily dependent on CD21/35 and PrP^C expression on FDCs. It may seem surprising that CD21/35 expression on FDCs, rather than B cells, correlates with prion-induced GC formation, since CD21/CD19/CD81 B cell coreceptor (BCCR) ligation helps activate B cells to form GCs. However, maximal B cell activation and GC formation requires signaling from both the BCR and BCCR [32,33]. Here we show that although prion infection stimulates CD21/35 translocation to lipid rafts on B cells, signaling appears to be suboptimal for GC formation in the absence of concomitant BCR translocation. We observed a strong dependence on both PrP and CD21/35 expression on FDCs for a strong GC response. Paradoxically, CD21/35 translocation did not occur on FDCs, which are the major prion trappers and replicators, but lack other BCCR components required for CD21/35 movement. One could therefore argue that GC formation represents an artifact, rather than a driver of splenic prion replication. Elimination of GCs had no effect on peripheral prion replication and disease progression in mice infected i.p. with RML5 [50], supporting this interpretation. However, GC-deficient mice infected intracranially with 139A mouse adapted scrapie prions exhibited a significant delay to terminal disease [51]. Thus, distinct prion strains may differentially influence GC formation and subsequent prion pathogenesis. Additionally, this discrepancy further highlights potential preferences of distinct tissues for different prion strains. CD21/35 expressing cells within GCs may facilitate this selection process in the lymphoid system. Increased retention of prions on FDCs could induce a persistent state of prion presentation to adjacent B cells sufficient to cause an atypical germinal center response [40]. FDCs may coax B cells to linger there, providing increased Lymphotoxin signaling to FDCs that may promote formation of hypertrophic dendrites that efficiently retain and replicate prions. Consistent with their role as long-lived, long-term antigen presenting cells, FDCs may also present prions to neighboring PrP^{C}-expressing B cells that could induce CD21/35 translocation and move prions proximal to Prp^{C} in lipid rafts and promote further prion replication and GC formation.

Taken together, these data support a principal role of CD21/35 in peripheral prion pathogenesis by trapping PrP^{RES} on both B cells and FDCs. CD21/35 expression on FDCs remains of paramount importance in this process, with B cells playing a lesser, but still important role. We have recently shown that few prion-bearing B cells transport prions from infection sites to draining lymph nodes, but their presence increased dramatically within lymph nodes, indicating a prominent role for B cells in intranodal prion trafficking [52]. We propose that CD21/35 mediates this and other crucial processes in lymph node prion trapping and replication and are currently testing this hypothesis.

REFERENCES

1. Williams, E. S. & Young, S. Spongiform encephalopathy of Rocky Mountain elk. *J. Wildl. Dis.* **18**, 465–471 (1982).
2. Prusiner, S. B. Novel proteinaceous infectious particles cause scrapie. *Science* **216**, 136–144 (1982).
3. Miller, M. W. & Williams, E. S. Prion disease: horizontal prion transmission in mule deer. *Nature* (2003).
4. Ryder, S., Dexter, G., Bellworthy, S. & Tongue, S. Demonstration of lateral transmission of scrapie between sheep kept under natural conditions using lymphoid tissue biopsy. *Res. Vet. Sci.* **76**, 211–217 (2004).
5. Gajdusek, D. C., Gibbs, C. J., Jr & Alpers, M. Transmission and passage of experimental 'kuru'to chimpanzees. *Science* **155**, 212–214 (1967).
6. Mould, D. L., Dawson, A. M. & Rennie, J. C. Very early replication of scrapie in lymphocytic tissue. *Nature* **228**, 779 - 780 (1970).
7. Bosque, P. J., Ryou, C. & Telling, G. Prions in skeletal muscle. *Proc. Natl. Acad. Sci. U.S.A.* **99,** 3812-3817 (2002).
8. Angers, R. C. Prions in Skeletal Muscles of Deer with Chronic Wasting Disease. *Science* **311**, 1117–1117 (2006).
9. Mathiason, C. K. *et al.* Infectious Prions in the Saliva and Blood of Deer with Chronic Wasting Disease. *Science* **314**, 133–136 (2006).
10. Seeger, H. *et al.* Coincident scrapie infection and nephritis lead to urinary prion excretion. *Science* **310**, 324–326 (2005).
11. Haley, N. J. *et al.* Detection of Chronic Wasting Disease Prions in Salivary, Urinary, and Intestinal Tissues of Deer: Potential Mechanisms of Prion Shedding and Transmission. *J. Virol.* **85**, 6309–6318 (2011).
12. Tamgüney, G. *et al.* Asymptomatic deer excrete infectious prions in faeces. *Nature* **461**, 529–532 (2009).
13. Pulford, B., Spraker, T. R., Wyckoff, A. C. & Meyerett, C. Detection of PrPCWD in feces from naturally exposed Rocky Mountain elk (Cervus elaphus nelsoni) using protein misfolding cyclic amplification. *J. Wildl. Dis.* **48,** 425-434 (2012).
14. Montrasio, F. *et al.* Impaired prion replication in spleens of mice lacking functional follicular dendritic cells. *Science* **288**, 1257–1259 (2000).
15. Brown, K. L. *et al.* Scrapie replication in lymphoid tissues depends on prion protein-expressing follicular dendritic cells. *Nat. Med.* **5**, 1308–1312 (1999).
16. Heikenwalder, M. *et al.* Chronic lymphocytic inflammation specifies the organ tropism of prions. *Science* **307**, 1107–1110 (2005).
17. Zabel, M. D. *et al.* Stromal complement receptor CD21/35 facilitates lymphoid prion colonization and pathogenesis. *J. Immunol.* **179**, 6144–6152 (2007).
18. McCulloch, L. *et al.* Follicular Dendritic Cell-Specific Prion Protein (PrPc) Expression Alone Is Sufficient to Sustain Prion Infection in the Spleen. *PLoS Pathog.* **7**, e1002402 (2011).
19. Krautler, N. J. *et al.* Follicular dendritic cells emerge from ubiquitous perivascular precursors. *Cell* **150**, 194–206 (2012).
20. Prinz, M. *et al.* Positioning of follicular dendritic cells within the spleen controls prion neuroinvasion. *Nature* **425**, 957–962 (2003).

21. Klein, M. A. *et al.* A crucial role for B cells in neuroinvasive scrapie. *Nature* **390**, 687–690 (1997).
22. Klein, M. A. M. *et al.* PrP expression in B lymphocytes is not required for prion neuroinvasion. *Nat. Med.* **4**, 1429–1433 (1998).
23. Zabel, M. D. & Weis, J. H. Cell-specific regulation of the CD21 gene. *Int. Immunopharmacol.* **3,** 483-493. (2001).
24. Roozendaal, R. & Carroll, M. C. Complement receptors CD21 and CD35 in humoral immunity. *Immunol. Rev.* (2007).
25. Klein, M. A. *et al.* Complement facilitates early prion pathogenesis. *Nat. Med.* **7**, 488–492 (2001).
26. Mabbott, N. A., Bruce, M. E., Botto, M., Walport, M. J. & Pepys, M. B. Temporary depletion of complement component C3 or genetic deficiency of C1q significantly delays onset of scrapie. *Nat. Med.* **7**, 485–487 (2001).
27. Mitchell, D. A., Kirby, L., Paulin, S. M., Villiers, C. L. & Sim, R. B. Prion protein activates and fixes complement directly via the classical pathway: Implications for the mechanism of scrapie agent propagation in lymphoid tissue. *Mol. Immunol.* **44**, 2997–3004 (2007).
28. Sim, R. B., Kishore, U., Villiers, C. L., Marche, P. N. & Mitchell, D. A. C1q binding and complement activation by prions and amyloids. *Immunobiology* **212**, 355–362 (2007).
29. Fischer, M. *et al.* Prion protein (PrP) with amino-proximal deletions restoring susceptibility of PrP knockout mice to scrapie. *EMBO. J.* **15**, 1255–1264 (1996).
30. Angers, R. C., Seward, T. S., Napier, D. & Green, M. Chronic wasting disease prions in elk antler velvet. *Emerg. Infect. Dis.* **5,** 696-703 (2009).
31. Meyerett, C. *et al.* In vitro strain adaptation of CWD prions by serial protein misfolding cyclic amplification. *Virology* **382**, 267–276 (2008).
32. Fang, Y., Xu, C., Fu, Y. X. & Holers, V. M. Expression of complement receptors 1 and 2 on follicular dendritic cells is necessary for the generation of a strong antigen-specific IgG response. *J. Immunol.* **11,** 5273-5279 (1998).
33. Fischer, M. B., Goerg, S., Shen, L. M. & Prodeus, A. P. Dependence of germinal center B cells on expression of CD21/CD35 for survival. *Science* **280,** 582-585 (1998).
34. Aydar, Y. Y., Balogh, P. P., Tew, J. G. J. & Szakal, A. K. A. Altered regulation of Fc gamma RII on aged follicular dendritic cells correlates with immunoreceptor tyrosine-based inhibition motif signaling in B cells and reduced germinal center formation. *J. Immunol.* **171**, 5975–5987 (2003).
35. Croix, D. A. *et al.* Antibody response to a T-dependent antigen requires B cell expression of complement receptors. *J Exp Med.* **183**, 1857–1864 (1996).
36. Kawabe, T. *et al.* The immune responses in CD40-deficient mice: impaired immunoglobulin class switching and germinal center formation. *Immunity* **1**, 167–178 (1994).
37. Xu, J., Foy, T. M., Laman, J. D., Elliott, E. A. & Dunn, J. J. Mice deficient for the CD40 ligand. *Immunity* **1,** 423–431 (1994).
38. Haas, K. M. K. *et al.* Complement receptors CD21/35 link innate and protective immunity during Streptococcus pneumoniae infection by regulating IgG3 antibody responses. *Immunity* **17**, 713–723 (2002).

39. Fischer, M. B., Ma, M., Goerg, S., Zhou, X. & Xia, J. Regulation of the B cell response to T-dependent antigens by classical pathway complement. *J. Immunol.* **157**, 549–556 (1996).
40. McGovern, G., Brown, K. L., Bruce, M. E. & Jeffrey, M. Murine Scrapie Infection Causes an Abnormal Germinal Centre Reaction in the Spleen. *J. Comp. Pathol.* **130**, 181–194 (2004).
41. Cherukuri, A., Carter, R. H., Brooks, S. & Bornmann, W. B cell signaling is regulated by induced palmitoylation of CD81. *J. Biol. Chem.* **279**, 31973–31982 (2004).
42. Cherukuri, A. A. *et al.* The tetraspanin CD81 is necessary for partitioning of coligated CD19/CD21-B cell antigen receptor complexes into signaling-active lipid rafts. *J. Immunol.* **172**, 370–380 (2004).
43. Cherukuri, A. A., Dykstra, M. M. & Pierce, S. K. S. Floating the raft hypothesis: lipid rafts play a role in immune cell activation. *Immunity* **14**, 657–660 (2001).
44. Bradley, R. BSE transmission studies with particular reference to blood. *Dev. Biol. Stand.* **99**, 35–40 (1999).
45. Iwata, N. *et al.* Distribution of PrP(Sc) in cattle with bovine spongiform encephalopathy slaughtered at abattoirs in Japan. *Jpn. J. Infect. Dis.* **59**, 100–107 (2006).
46. Middleton, D. J. D. & Barlow, R. M. R. Failure to transmit bovine spongiform encephalopathy to mice by feeding them with extraneural tissues of affected cattle. *Vet. Rec.* **132**, 545–547 (1993).
47. Terry, L. A. *et al.* Detection of disease-specific PrP in the distal ileum of cattle exposed orally to the agent of bovine spongiform encephalopathy. *Vet. Rec.* **152**, 387–392 (2003).
48. Hasebe, R., Raymond, G. J., Horiuchi, M. & Caughey, B. Reaction of complement factors varies with prion strains in vitro and in vivo. *Virology* **423**, 205–213 (2012).
49. Beringue, V. *et al.* Facilitated Cross-Species Transmission of Prions in Extraneural Tissue. *Science* **335**, 472–475 (2012).
50. Heikenwalder, M. *et al.* Germinal center B cells are dispensable in prion transport and neuroinvasion. *J. Neuroimmunol.* **192**, 113–123 (2007).
51. Burwinkel, M. *et al.* Rapid disease development in scrapie-infected mice deficient for CD40 ligand. *EMBO. Rep.* **5**, 527–531 (2004).
52. Michel, B. *et al.* Incunabular immunological events in prion trafficking. *Sci. Rep.* **2**, 440 (2012).

CHAPTER 4:

COMPLEMENT PROTEIN C3 EXACERBATES DISEASE IN A MOUSE MODEL OF CHRONIC WASTING DISEASE.

Summary

Accumulating evidence shows a critical role of the complement system in facilitating attachment of prions to both B cells and FDCs and assisting in prion replication. Complement activation intensifies disease in prion-infected animals, and elimination of complement components inhibits prion accumulation, replication, and pathogenesis. Chronic wasting disease is a highly infectious prion disease of captive and fee-ranging cervid populations that has utilized the complement system for efficient peripheral prion replication and most likely efficient horizontal transmission. Here we show that complete genetic or transient pharmacological depletion of C3 prolongs incubation times and significantly delays splenic accumulation in a CWD transgenic mouse model. Using a semiquantitative prion amplification scoring system we show that C3 impacts disease progression in the early stages of disease by slowing the kinetic rate of accumulation and/or replication of PrP^{RES}. The delayed kinetics in PrP^{RES} replication correlates with delayed disease kinetics in mice deficient in C3. Taken together, these data support a critical role of C3 in peripheral CWD prion pathogenesis.

Introduction

Chronic Wasting Disease (CWD) is a highly contagious prion disease of unknown origin affecting both wild and farmed raised deer, moose and elk [1,2]. First described as a disease entity by E.S. Williams and colleagues in the 1970s [1], CWD has become the most contagious and puzzling prion disease to date. Similar to other prion diseases, CWD is characterized by the accumulation PrP^{RES}, a proteinase K (PK) resistant form of the cellular prion protein, PrP^{C} [3]. According to the Prion hypothesis, PrP^{RES} is the non-genomic pathogen that causes prion diseases. CWD seems to be unique among prion diseases in its prevalence in both wild (≤ 45% [4]) and captive (≤ 90% [5]) animal populations.

Prions have been found in lymphoid and nervous tissue, muscle, blood, feces, urine and saliva [6-11]. Much research has focused on lymphoid tissues, as peripheral prion accumulation and replication has been documented there. Prion accumulation and replication occur on follicular dendritic cells (FDCs) within lymphoid follicles of secondary lymphoid organs (SLOs) [12,13]. FDCs differentiate from perivascular precursors and display antigenic immune complexes on their dendritic processes to B cells to promote survival, Immunoglobulin affinity maturation and activation to plasma cells [14].

FDCs and B cells are both important for optimal peripheral prion pathogenesis [15-18]. Accumulating evidence shows a critical role of the complement system in facilitating attachment of prions to both B cells and FDCs and assisting in prion replication [19,20]. The complement system plays a vital role in immune-mediated defense against pathogens. Multiple pathways activate the complement system, all converging at C3 activation [21]. C3 is the most abundant complement protein, present in the blood at mean physiological concentrations of 1.2 mg/ml [22]. C3 convertases asymmetrically cleave C3, revealing a thioester bond on the large fragment, C3b, that reacts with carbohydrates on microbial surfaces. Covalently bound C3b molecules opsonize microbial pathogens and mark them for phagocytosis by innate immune cells or lysis by the membrane attack complex. Murine Complement receptors CR2(CD21)/ CR1 (CD35) expressed on B cells and FDCs trap pathogens coated with C3 cleavage products and mediate appropriate immune responses. Opsonization is critical for eliminating invading pathogens. However, many pathogens manipulate complement regulatory components to avoid being eliminated [23] or promote their attachment to or infection of the host [24,25]. Complement activation exacerbates disease in prion-infected animals, and elimination of CD21/35 inhibits prion accumulation, replication, and pathogenesis [35, 36].

In this study, we show that complete genetic or transient pharmacological depletion of C3 prolongs incubation times and significantly delays splenic accumulation in a CWD transgenic mouse model. Using a semiquantitative prion amplification scoring system we show that C3 impacts disease progression in the early stages of disease by slowing the kinetic rate of accumulation and/or replication of PrP^{RES}. The dilatory kinetics in PrP^{RES} replication correlates with dilatory disease kinetics in mice deficient in C3.

Materials and Methods

Mice

$C3^{-/-}$ were purchased from Charles River (Wilmington, MA), $Prnp^{o/o}$ and Tg5037 mice were made as previously described [26,27]. $Prnp^{o/o}$ and $C3^{-/-}$mice were bred to produce $Prnp^{o/o}C3^{-/-}$ mice, which were crossed with Tg5037 mice to produce Tg5037;$Prnp^{o/o}C3^{-/-}$ (Tg5037;$C3^{-/-}$) mice. All mice were bred and maintained at Lab Animal Resources, accredited by the Association for Assessment and Accreditation of Lab Animal Care International, in accordance with protocols approved by the Institutional Animal Care and Use Committee at Colorado State University.

Preparation and inoculation of cobra venom factor

Cobra venom factor (CVF) is a C3b homologue that forms a C3 convertase with Factor Bb, but is resistant to inactivation by Complement regulatory proteins CR1 and Factor I, resulting in rapid and near complete temporarily depletion of C3. At least one intraperitoneal injection of 100 µl of 900 µg/ml of CVF (Sigma) in PBS or PBS alone as a control, was given 24 h before inoculation with CWD. Following CWD infection, additional injections of CVF at 5, 10, and 15 dpi were given. C3 concentration was assayed by enzyme-linked immunosorbent assay (ELISA).

ELISA

Double antibody sandwich ELISAs were performed as outlined by the manufacturer (Immunology Consultant Laboratory, Inc). Briefly, serum collected from mice were diluted 1/50000 and 100 μl of this serum transferred into an anti-C3 ELISA microtiter plate and incubated for 20 minutes. Following incubation the contents were aspirated and wells washed four times with diluted wash solution. Next, 100 μl of enzyme antibody conjugate was added and the samples incubated in the dark for 20 minutes. The solution was aspirated and wells washed four times. 100 μl of TMB substrate was added into each well and allowed to incubate in the dark for 20 minutes. After incubation 100 ul of stop solution was added to each well. Fully-developed plates were read at 405 nm by an *Opsys* MR plate reader.

Preparation of inoculum

10% elk and deer brain homogenates infected with CWD prions were prepared in PMCA buffer (4mM EDTA, 150 mM NaCl in PBS). These 10% homogenates were diluted 1:10 in 320 mM sucrose supplemented with 100 units/mL Penicillin and 100 µg/mL Streptomycin (Gibco) in PBS immediately prior to inoculation.

Inoculations, Clinical scoring and Dissections

Mice were inoculated intraperitoneallly with 100 µl of CWD infected brain homogenate using a 28G Insulin syringe. Mice were observed throughout the study for clinical signs of prion disease, including tail rigidity, impaired extensor reflex, akinesia, tremors, ataxia and weight loss. Mice displaying any four of these signs or paralysis were scored terminally ill and sacrificed.

Inoculated mice were sacrificed at distinct time points by CO_2 inhalation. Spleens and brains collected from these mice were divided sagittally. One brain hemisphere and half a spleen were fixed in 4% paraformaldehyde in PBS for 5 days before histology. The other brain hemisphere and half spleen was homogenized and used for PK digestion, western blot analysis, and PMCA.

Histology and Immunocytochemistry

Slides were prepared and stained as previously described [28].

PMCA, PK digest and WB

PMCA on spleen samples was performed and semiquantified as previously described [29]. Briefly, spleen samples were sonicated at 70–85% maximum power for 40 s in a microplate horn sonicator (Qsonic, Framingham, MA), followed by a 30-minute incubation at 37 °C repeated for 24 hours per round for up to five rounds total. PK digestion and WB was performed as previously described [28], except that spleen homogenates were digested with 10 μg/mL PK.

We weighted sample scores according to the PMCA round at which they first appeared positive by WB and set a detection threshold distinguishing positive from negative PMCA samples based on the 99.9% confidence interval for designating NBH samples as negative, calculated from the mean PMCA score of 73 NBH control samples using the Student’s t-table. We estimated cervid PrP^{RES} (PrP^{CWD}) loads in spleens by first generating a standard curve by plotting serial dilutions of known concentration of PrP^{CWD} titrated into uninfected spleen homogenates versus their PMCA scores generated after prion amplification. We then quantified

PrP^{CWD} loads (y) by substituting PMCA scores (x) into the nonlinear equation $y = -0.6626x^{0.3771}+17.87x^{0.1845}$ (r^2=0.88).

Results

Genetic or pharmacological depletion of C3 results in significant delays in CWD pathogenesis.

We tested whether Complement protein C3 is important early in or throughout peripheral prion infection, or both. To create mice deficient in C3 and susceptible to CWD prions, mice deficient in both C3 ($C3^{-/-}$) and mouse PrP^C ($Prnp^{o/o}$) were crossed to Tg5037 mice that express high levels of elk, but no mouse, PrP. Offspring from breeding pairs were then screened for Tg5037;$C3^{-/-}$ mice. To temporarily deplete C3, Tg5037 were inoculated with either 100 µl of 900 µg/ml of the C3 convertase-activating CVF (Sigma) or PBS at least 24 hours prior to and 5, 10, and 15 days post inoculation (dpi) of 100 µg brain homogenate from an elk terminally infected with CWD prions (Figure 4.1A). At all time points tested there was a significant decrease in C3 concentration in the serum of CVF treatedTg5037 mice compared to PBS treated Tg5037 mice. Although serum C3 concentrations were significantly different at 15 DPI, C3 concentrations of CVF treated mice rose above normal physiological levels (~1mg/ml) indicating a probable antibody response against CVF that limited its effectiveness after the third administration. We estimate that C3 levels remained at or below 50% of PBS-treated mice for 7-10 DPI.

Both Tg5037;$C3^{-/-}$ and CVF treated Tg5037 mice showed a median survival time of 513 and 441 dpi, respectively. These median survival times were significantly longer than Tg5037control mice, which showed a median survival time of 312 dpi (Figure 4.1B). Terminally ill Tg5037;$C3^{-/-}$ mice, CVF treated Tg5037 mice, and control PBS treated Tg5037 mice exhibited vacuolization, PrP^{Sc} deposition, and severe astrogloisis (D-I). Western blot and densitometric analyses revealed PrP^{RES} in all brains from terminally ill Tg5037;C3$^{-/-}$, CVF and PBS treated Tg5037 mice.

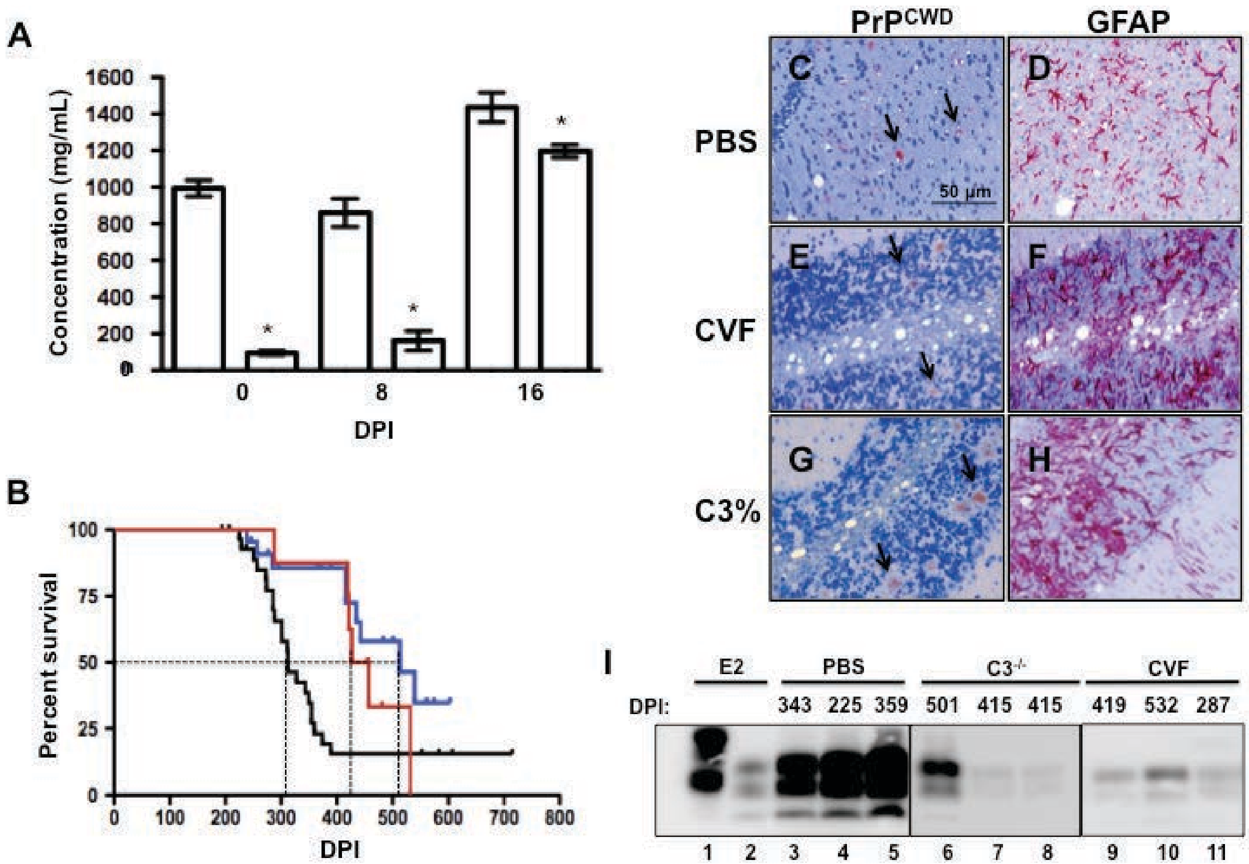

FIGURE 4.1. Mice genetically and pharmacologically deficient in C3 show delays in CWD prion infection. Tg5037 mice were inoculated with either CVF (n=8) or PBS (n=5) at least 24 hours prior to i.p. inoculation (0 hpi) of 100 µg of CWD infected brain homogenate. After infection with CWD prions, additional CVF inoculations at 5, 10, and 15 days post infection were administered to maintain transient C3 depletion (A). At 0 hpi, 8, and 16 dpi there was a significant depletion of C3 in mice treated with CVF. (B) CVF treated Tg5037 (red) and Tg5037;C3$^{-/-}$mice (blue) show a median survival time of 441 and 513 dpi respectively compared to PBS and non PBS treated Tg5037 mice (black), which show a median survival time of 312 dpi (p value=0.0064). (C) IHC of brain sections from PBS (C-D), CVF (E-F), and C3$^{-/-}$ (G-H) mice. (J) Western blot (WB) analysis of PrP^{Sc} content from PBS, Tg5037;C3$^{-/-}$, and CVF mice.

Absence of C3 delays prion propagation in the spleen.

We next used PMCA to evaluate the prion loads in the spleens of CWD infected Tg5037, Tg5037;C3$^{-/-}$, and CVF mice. These semiquantitative prion amplification assay takes advantages of a prion's ability to self propagate, using seeded protein fibrilization. This diagnostic technique is employed to amplify diminutive amounts of infectious protease-resistant forms of PrP (PrP^{RES}) to detectable levels by stimulating its conversion from PrP^{C} [30]. We utilized PMCA to amplify and semi-quantify small amounts of PrP^{RES} from spleen homogenates from mice at distinct intervals after CWD prion infection. Tg5037 mice at 15 dpi showed a significant difference in the amount of splenic PrP^{RES} (Figure 4.2, 63.49 ± 8.160 rpu) compared to Tg5037;C3$^{-/-}$ mice (11.36 ± 9.15 rpu). Using our previously generated standard curve for this assay [29], we show that splenic PrP^{RES} load in bothTg5037 to be approximately 5,500 pg/g of spleen tissue (figure 4.2). The PMCA score for tg5037;C3$^{-/-}$ mice fall out of the dynamic range of our assay, so we can only estimate the load to be <100pg/g. Tg5037 mice at 30 DPI showed no significant difference in prion load (22.920 ± 6.540 rpu, <100pg/g) compared to Tg5037;C3$^{-/-}$ mice (20.00 ± 9.72 rpu, <100 pg/g). PrP^{RES} increased significantly at 70 DPI (38.930 ± 6.9, 350 pg/g) and 140DPI (42.8 ± 6.33, 500 pg/g) in Tg5037 mice. We detected significantly less PrP^{RES} in the spleens of TG5037;C3-/- mice at 70 DPI (0± 0, <100 pg/g) and 140 DPI (22.50 ± 10.17, <100 pg/g).

In addition to genetically depleting C3, we temporarily depleted C3 with CVF and checked for PrP^{RES} accumulation in the spleen of Tg5037 mice. One dose of CVF was administered one and five dpi. Although not significantly different, CVF treated mice at 45 (0±0, <100 pg/g), 70 (23.33±9.55 rpu, <100 pg/g), and 151 (20.00 ± 11.95, <100 pg/g) dpi exhibited consistently lower mean prion loads compared to TG g5037 mice.

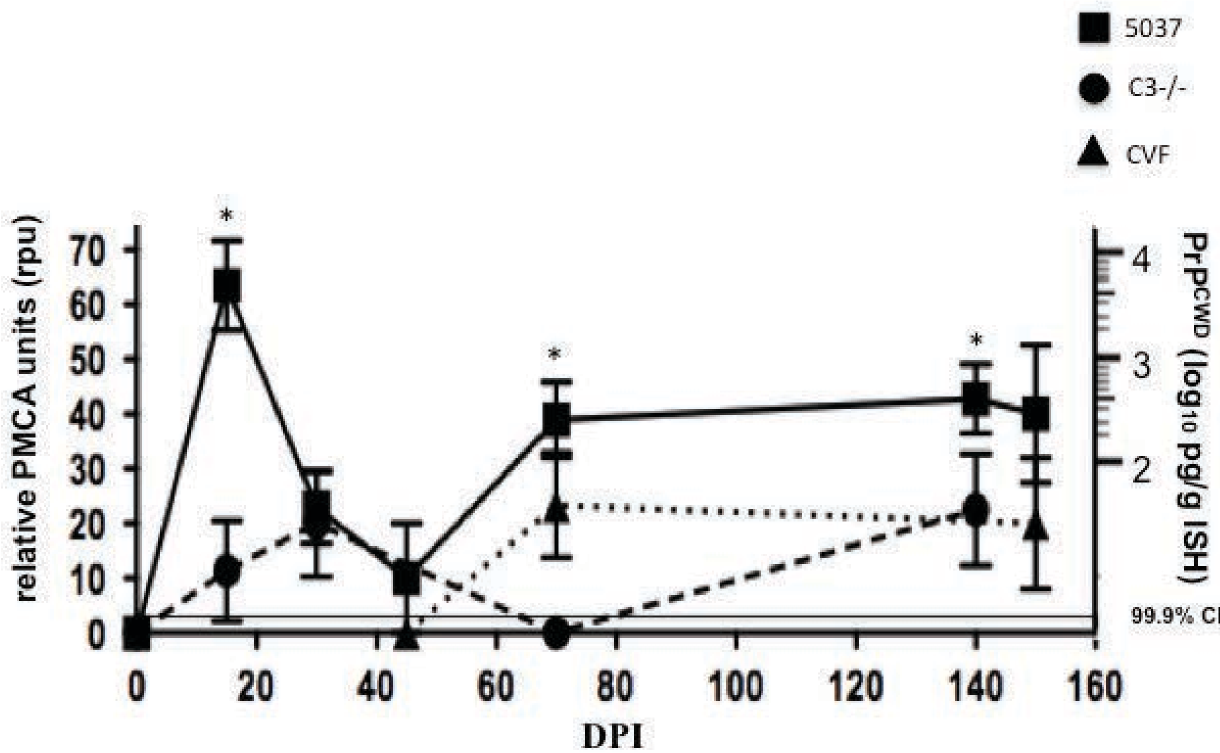

FIGURE 4.2. C3-deficient mice showed delayed prion accumulation in the spleen at early time points. Tg5037 mice (n=83) accumulated significantly more CWD prions in the spleen at 15, 70 and 140 dpi compared to Tg5037;C3$^{-/-}$ mice (15, 70, and 140 dpi $p<0.05$ n=41). There was no significant difference in prion accumulation between PBS treated (n=24) Tg5037 mice and CVF treated Tg5037 mice (n=18) at 45, 70 and 151 dpi.

Discussion

We investigated the role of complement protein C3 in CWD prion accumulation, replication, and disease progression. CWD development in mice with genetic or pharmacological depletion of C3 showed significant delays in disease development. In Tg5037;C3$^{-/-}$ mice the median survival time was longer than that seen in CVF treated mice. This difference may be attributed to both transient depletion and incomplete knockdown of C3. The delays in disease development in CWD infected Tg5037;C3$^{-/-}$ mice were more drastic than previous studies of C3 deficient mice infected with scrapie [19, 37], even though these mice expressed five-fold less PrP^{C}. Complement components C1q and C3 have recently been shown to display similar strain preferences in vitro and in vivo [31]. These results point to a vital role in prion pathogenesis for C3, the importance of which may differ by prion strain. Interestingly, in CWD and scrapie prion infections, depleting CD21/35 impacts disease progression significantly more than depleting its endogenous ligands, C3 and C4. Furthermore, CD21/35 was greatly enriched in NaPTA precipitated PrP^{RES} preparations from spleens of terminally sick mice [19.] These Data strongly suggests a role of C21/35 in peripheral prion pathogenesis independent of its endogenous ligands. Recently, prion transmission barriers were shown to be more readily breached in the lymphoreticular system than in the nervous system [32]. These cross-species infections resulted in distinct lymphotropic and neurotropic strains with differential host ranges. We hypothesized that this phenomenon may be due to the peripheral expression of CD21/35 by FDCs and B lymphocytes. This expression of CD21/35 may play an important role in propagation, replication and strain selection in the spleen. In light of our current findings, we extend our recent hypothesis to include C3. As with CD21/35, lack of C3 may inhibit the efficiency of selection, propagation, and replication of neurotropic prion strains. If true, this would have serious implications for cross-species transmission, subclinical infections, and possible therapeutic approaches aimed at both complement proteins and their respective receptors.

To study the kinetics of splenic CWD prion accumulation, we amplified PrP^{RES} from spleens of CWD prion infected Tg5037, Tg503;$C3^{-/-}$, and CVF treated mice at various time points throughout infection. At 15, 70, 140 dpi, Tg5037;$C3^{-/-}$ mice showed significantly less PrP^{RES} than Tg5037 mice, whereas, no significant difference in splenic PrP^{RES} could be detected in CVF-treated mice at any of the time points tested. We hypothesize that the incomplete transient knockdown of C3 in CVF treated mice may contribute to higher concentrations PrP^{RES} compared to Tg5037;$C3^{-/-}$ mice. Although PrP^{RES} was not significantly different between

Tg5037 and CVF treated mice at the time points tested, CVF treated mice showed a significant delay in disease development compared toTg5037 mice. This indicates that similar to Tg5037;C3$^{-/-}$ mice, CVF treated mice most likely showed a significant decrease in PrP^{RES} accumulation before 45 dpi. This points to a more pronounced role of C3 in the earlier stages of disease. This delay in splenic prion replication and/or accumulation strongly corresponds with a delay in terminal disease.

While C3 exerts most of its effect early in prion disease; complete, sustained C3 depletion results in less severe prion pathogenesis and longer delays in incubation times than incomplete, transient depletion. This result is most likely due to insufficient depletion of C3 with CVF, resulting in not only residual endogenous ligands for CD21/35 early during infection, but also normal levels of C3 throughout most of the infection. Consequently, this transient, incomplete depletion of C3 may lead to higher kinetic rates of accumulation and/or replication in the spleen later in infection. C3 may help to recapture newly synthesized prions from FDCs in SLOs, as well as prions emanating from the CNS in centrifugal movement back to SLOs. This may increase the rate of prionogenesis, resulting in higher prion titers and shorter incubation times in mice replete with C3 at later stages of disease. This result could also be attributed to C3 expression in the central nervous system (CNS) [33,34]. Unlike Tg5037;C3$^{-/-}$ mice, CVF treated mice likely express C3 in the CNS after transient depletion with CVF, which may exacerbate disease in the later stages of CWD.

Taken together, these data support a critical role of C3 in peripheral CWD pathogenesis. C3 opsonization of PrP^{CWD} may facilitate trapping by B lymphocytes and FDCs optimizing intranodal trafficking or peripheral prion replication. Recently, we have shown that B lymphocytes within lymph nodes trap large amounts of prions hours after infection, indicating a important role for this lymphocyte in intranodal trafficking. We have also shown that depleting C3 in these mice affects prion capture by APCs. We suspect that, similar to DCs and monocytes, C3 depletion may also affect prion uptake by CD21/35 positive follicular B cells. This may in turn delay transport of prions to FDCs, consequently leading to delays in prion accumulation, replication, and perpheral prion pathogenesis. We are currently investigating the potential role of C3 in this process.

REFERENCES

1. Williams, E. S. & Young, S. Chronic wasting disease of captive mule deer: a spongiform encephalopathy. *J. Wildl. Dis.* **16**, 89–98 (1980).
2. Williams, E. S. & Young, S. Spongiform encephalopathy of Rocky Mountain elk. *J. Wildl. Dis.* **18**, 465–471 (1982).
3. Prusiner, S. B. Novel proteinaceous infectious particles cause scrapie. *Science* **216**, 136–144 (1982).
4. Miller, M. W. & Conner, M. M. Epidemiology of chronic wasting disease in free-ranging mule deer: spatial, temporal, and demographic influences on observed prevalence patterns. *J. Wildl. Dis.* **41**, 275–290 (2005).
5. Williams, E. S. Chronic wasting disease. *Vet. Pathol.* **42**, 530–549 (2005).
6. Gonzalez-Romero, D., Barria, M. A., Leon, P., Morales, R. & Soto, C. Detection of infectious prions in urine. *FEBS Lett.* **582**, 3161–3166 (2008).
7. Haley, N. J. *et al.* Detection of Chronic Wasting Disease Prions in Salivary, Urinary, and Intestinal Tissues of Deer: Potential Mechanisms of Prion Shedding and Transmission. *J. Virol.* **85**, 6309–6318 (2011).
8. Angers, R. C. Prions in Skeletal Muscles of Deer with Chronic Wasting Disease. *Science* **311**, 1117–1117 (2006).
9. Mathiason, C. K. *et al.* B Cells and Platelets Harbor Prion Infectivity in the Blood of Deer Infected with Chronic Wasting Disease. *J. Virol.* **84**, 5097–5107 (2010).
10. O'Rourke, K. I. *et al.* Abundant PrPCWD in Tonsil from Mule Deer with Preclinical Chronic Wasting Disease. *J. Vet. Diagn. Invest.* **15**, 320–323 (2003).
11. Gajdusek, D. C., Gibbs, C. J., Jr & Alpers, M. Transmission and passage of experimental ‘kuru’to chimpanzees. *Science* **155**, 212–214 (1967).
12. Kitamoto, T., Muramoto, T., Mohri, S., Doh-ura, K. & Tateishi, J. Abnormal isoform of prion protein accumulates in follicular dendritic cells in mice with Creutzfeldt-Jakob disease. *J. Virol.***65**, 6292–6295 (1991).
13. Brown, K. L. *et al.* Scrapie replication in lymphoid tissues depends on prion protein-expressing follicular dendritic cells. *Nat. Med.* **5**, 1308–1312 (1999).
14. Krautler, N. J. *et al.* Follicular dendritic cells emerge from ubiquitous perivascular precursors. *Cell* **150**, 194–206 (2012).
15. Montrasio, F. *et al.* Impaired prion replication in spleens of mice lacking functional follicular dendritic cells. *Science* **288**, 1257–1259 (2000).
16. McCulloch, L. *et al.* Follicular Dendritic Cell-Specific Prion Protein (PrPc) Expression Alone Is Sufficient to Sustain Prion Infection in the Spleen. *PLoS Pathog.* **7**, e1002402 (2011).
17. Klein, M. A. *et al.* A crucial role for B cells in neuroinvasive scrapie. *Nature* **390**, 687–690 (1997).
18. Mabbott, N. A., Young, J., McConnell, I. & Bruce, M. E. Follicular dendritic cell dedifferentiation by treatment with an inhibitor of the lymphotoxin pathway dramatically reduces scrapie susceptibility. *J. Virol.* **77**, 6845–6854 (2003).
19. Zabel, M. D. *et al.* Stromal complement receptor CD21/35 facilitates lymphoid prion colonization and pathogenesis. *J. Immunol.* **179**, 6144–6152 (2007).
20. Michel, B. *et al.* Incunabular immunological events in prion trafficking. *Sci. Rep.* **2**, 440 (2012).

21. Ricklin, D., Hajishengallis, G., Yang, K. & Lambris, J. D. Complement: a key system for immune surveillance and homeostasis. *Nat. Immunol.* **11**, 785–797 (2010).
22. Lambris, J. D. & Muller-Eberhard, H. J. The multifunctional role of C3: structural analysis of its interactions with physiological ligands. *Mol. Immunol.* **23**, 1237–1242 (1986).
23. Lambris, J. D., Ricklin, D. & Geisbrecht, B. V. Complement evasion by human pathogens. *Nat. Rev. Micro.* **6**, 132–142 (2008).
24. Oliva, C., Turnbough, C. L. & Kearney, J. F. CD14-Mac-1 interactions in Bacillus anthracis spore internalization by macrophages. *Proc. Natl Acad. Sci.* **106**, 13957–13962 (2009).
25. Wang, M. *et al.* Fimbrial proteins of porphyromonas gingivalis mediate in vivo virulence and exploit TLR2 and complement receptor 3 to persist in macrophages. *J. Immunol.* **179**, 2349–2358 (2007).
26. Büeler, H. *et al.* Normal development and behaviour of mice lacking the neuronal cell-surface PrP protein. *Nature* **356**, 577–582 (1992).
27. Angers, R. C., Seward, T. S., Napier, D. & Green, M. Chronic wasting disease prions in elk antler velvet. *Emerg. Infect. Dis.* **15,** 696-703 (2009).
28. Meyerett, C. *et al.* In vitro strain adaptation of CWD prions by serial protein misfolding cyclic amplification. *Virology* **382**, 267–276 (2008).
29. Pulford, B. *et al.* Detection of PrPCWD in feces from naturally exposed Rocky Mountain elk (Cervus elaphus nelsoni) using protein misfolding cyclic amplification. *J. Wildl. Dis.* **48**, 425–434 (2012).
30. Saborio, G. P., Permanne, B. & Soto, C. Sensitive detection of pathological prion protein by cyclic amplification of protein misfolding. *Nature* **411**, 810–813 (2001).
31. Hasebe, R., Raymond, G. J., Horiuchi, M. & Caughey, B. Reaction of complement factors varies with prion strains in vitro and in vivo. *Virology* **423**, 205–213 (2012).
32. Beringue, V. *et al.* Facilitated Cross-Species Transmission of Prions in Extraneural Tissue. *Science* **335**, 472–475 (2012).
33. Gasque, P., Thomas, A., Fontaine, M. & Morgan, B. P. Complement activation on human neuroblastoma cell lines in vitro: route of activation and expression of functional complement regulatory proteins. *J. Neuroimmunol* **66**, 29–40 (1996).
34. Beek, J., Elward, K. & Gasque, P. Activation of complement in the central nervous system. *Ann. N.Y. Acad. Sci.* **992**, 56–71 (2003).
35. Klein, M. A. *et al.* Complement facilitates early prion pathogenesis. *Nat. Med.* **7**, 488–492 (2001).
36. Mabbott, N. A., Bruce, M. E., Botto, M., Walport, M. J. & Pepys, M. B. Temporary depletion of complement component C3 or genetic deficiency of C1q significantly delays onset of scrapie. *Nat. Med.* **7**, 485–487 (2001).
37. Michel, B. *et al.* Genetic Depletion of Complement Receptors CD21/35 Prevents Terminal Prion Disease in a Mouse Model of Chronic Wasting Disease. *J Immunol.* (2012).

OVERALL CONCLUSION

CWD is an emerging and highly infectious prion disease of captive and free-ranging cervid populations that, similar to scrapie, has been shown to involve the immune system, perhaps contributing to their relatively facile horizontal and environmental transmission. While prions most likely engage the innate immune system immediately following infection, little is known about this initial confrontation. In the first part of this thesis I investigated incunabular events in lymphotropic and intranodal CWD prion trafficking by following highly enriched, fluorescent prions from infection sites to draining lymph nodes. I detected biphasic lymphotropic transport of prions from the initial entry site upon peripheral prion inoculation. Prions arrived in draining lymph nodes cell autonomously within two hours of intraperitoneal administration, and this process was independent of complement components C1q and C3. A second wave of cells, dominated by monocytes, infiltrated the lymph nodes hours later in a second wave of prion trafficking. Although their role in early prion passive transport was inconsequential, complement was required for optimal prion uptake by DCs. This finding lends support to a receptor-mediated mechanism for prion uptake by DCs. The drastic increase in proportion of prion-bearing B cells in MedLNs at early time points indicates that B cells most likely received prions from resident lymph node immune cells, probably SCS macrophages and paracortical DCs. These data reveal novel, cell autonomous prion lymphotropism, and a prominent role for B cells in intranodal prion movement.

The complement system has been shown to facilitate scrapie peripheral prion accumulation and/or replication and neuroinvasion. In the second part of my thesis, we demonstrate that complete removal of the complement receptor CD21/35 in transgenic mice susceptible to CWD greatly delays splenic prion accumulation and blocks progression to terminal disease upon inoculation with CWD prions. We also observed significant germinal center formation during scrapie prion infection that was dependent on CD21/35 and PrP^{C} expression on FDCs. Lipid raft flotation experiments show movement of CD21/35 into lipid rafts on B cells upon prion infection, and this translocation occurred independent of endogenous ligand C3. Taken together, these data suggest that CD21/35 mediated prion trapping on FDCs, and possibly B cells, marks an important event in lymphoid prion pathogenesis that contributes to terminal prion disease in these mouse models.

C3 is the most abundant complement protein, being found in the blood at physiological concentrations of 1.2 mg/ml. C3 cleavage may occur through any one of the multiple complement pathways and leads to the opsonization of the outer surface of microbial pathogens. CD21/CD35 expressed on B cells and FDCs trap pathogens coated with C3 cleavage products and mediate appropriate immune responses. Here we show that complete genetic or transient pharmacological depletion of C3 increases incubation times and significantly delays splenic accumulation in a CWD transgenic mouse model. Using PMCA we show that C3 affects disease progression in the early stages of disease by slowing the rate of accumulation and/or replication of PrP^{RES}. The delayed kinetics in PrP^{RES} replication corresponds with delayed disease kinetics in mice deficient in C3. Taken together, these data support a critical role of C3 in peripheral CWD prion pathogenesis.

Future Directions

Although intraperitoneal inoculation of prion-infected brain homogenate is very efficient in causing disease, this route of infection does not correspond to what is normally seen in nature.

Many TSEs, including Kuru, variant Creutzfeldt–Jakob disease (vCJD), BSE, scrapie, and CWD, are acquired through an oral route of infection [1-5]. Acquisition of disease through this route involves transcytosis of prions through the intestinal epithelium, replication on FDCs, and infection of the enteric nervous system [6-10]. Despite the fact that considerable data links immune cells to prion diseases post oral exposure, little evidence directly show a role for these cells in the capture and transport of prions hours after initial infection [11-13]. Because pathogen-immune cell interactions often occur within hours of exposure and dictate the outcome of infection, understanding the interactions of prions with the oral mucosa is vital to comprehending incunabular events in a natural prion infection. With this in mind, we will orally inoculate animals to characterize the immune cell types involved in uptake and trafficking of CWD prions.

B cells have been shown to play a critical role in prion neuroinvasion [14]. Although their role in this process relies less on replication and more on the enrichment of FDCs with critical cytokines, B cells and their intimate association with FDCs remains poorly described[15]. We describe in chapter one a model in which B cells receive prions from SCS Mϕ, migrate into lymphoid follicles and deliver prions to FDCs. However, this possible mechanism remains to be proven experimentally. Recently, intravital microscopy (IVM) has resolved the kinetics of intranodal antigen trafficking and physiological processes associated with germinal center formation [16-22]. This powerful technique allows scientists to image biological processes in living animals at microscopic resolution. IVM makes it possible to visualize cellular reactions over time and space, and allows scientists to carry out experiments under conditions that closely resemble those seen in a natural setting [23]. IVM could provide insight into the cellular interactions that exist between SCS macrophages, B cells, and FDCs during a prion infection.

We are pursuing a potential collaboration in an effort to provide quantitative and dynamic insights into prion immunology.

Over the past several years the study of protein dynamics and interactions often employed optical methods. One method, surface plasmon resonance (SPR), has been used to describe a wide variety of biomolecular interactions in real time [24,25]. This method is able to detect binding between two unlabeled biomolecules by tracking changes in light refraction off the interface between an aqueous solution of possible binding ligands and a biosensor surface coupled to bait proteins (potential receptors) [26,27]. We will be using SPR to study the role of CD21/35 as a potential prion receptor, which could further give insight into peripheral prion replication, xenotransmission, strain selection, and possible therapeutic approaches targeted to CD21/35. Targeting CD21/35 to inhibit the spread of neurotropic prions could be an attractive alternative to most prion disease therapeutics developed to date that target the central nervous system, which is a challenging site for drug delivery. Preventing CD21/35 mediated prion strain selection could also diminish emergence of new prion strains with enlarged host ranges and prevent a breach of the species barrier like the one that most likely caused the BSE and subsequent new-variant CJD outbreak fifteen years ago in the United Kingdom.

REFERENCES

1. Seidel, B. *et al.* Scrapie Agent (Strain 263K) can transmit disease via the oral route after persistence in soil over years. *PLoS ONE* **2**, e435 (2007).
2. Anderson, R. M. *et al.* Transmission dynamics and epidemiology of BSE in British cattle. *Nature* **382**, 779–788 (1996).
3. Collinge, J. *et al.* Kuru in the 21st century - an acquired human prion disease with very long incubation periods. *Lancet* **367**, 2068–2074 (2006).
4. Hilton, D. A. Pathogenesis and prevalence of variant Creutzfeldt-Jakob disease. *J. Pathol.* **208**, 134–141 (2006).
5. Sigurdson, C. J. *et al.* Oral transmission and early lymphoid tropism of chronic wasting disease PrPres in mule deer fawns (Odocoileus hemionus). *J. Gen. Virol.* **80**, 2757–2764 (1999).
6. Mabbott, N. A. & MacPherson, G. G. Prions and their lethal journey to the brain. *Nat. Rev. Micro.* **4**, 201–211 (2006).
7. McBride, P. A. *et al.* Early spread of scrapie from the gastrointestinal tract to the central nervous system involves autonomic fibers of the splanchnic and vagus nerves. *J Virol.* **75**, 9320–9327 (2001).
8. Aguzzi, A. & Calella, A. M. Prions: protein aggregation and infectious diseases. *Physiol. Rev.* **89**, 1105–1152 (2009).
9. Beekes, M. & McBride, P. A. Early accumulation of pathological PrP in the enteric nervous system and gut-associated lymphoid tissue of hamsters orally infected with scrapie. *Neurosci. Lett.* **278**, 181–184 (2000).
10. Prinz, M. *et al.* Oral prion infection requires normal numbers of Peyer's patches but not of enteric lymphocytes. *Am. J. Pathol.* **162**, 1103–1111 (2003).
11. Raymond, C. R., Aucouturier, P. & Mabbott, N. A. In vivo depletion of CD11c+ cells impairs scrapie agent neuroinvasion from the intestine. *J. Immunol.* **179**, 7758–7766 (2007).
12. Donaldson, D. S. *et al.* M cell-depletion blocks oral prion disease pathogenesis. *Mucosal Immunol.* **5**, 216–225 (2012).
13. Huang, F. P., Farquhar, C. F., Mabbott, N. A., Bruce, M. E. & MacPherson, G. G. Migrating intestinal dendritic cells transport PrPSc from the gut. *J. Gen. Virol.* **83**, 267–271 (2002).
14. Klein, M. A. *et al.* A crucial role for B cells in neuroinvasive scrapie. *Nature* **390**, 687–690 (1997).
15. Klein, M. A. M. *et al.* PrP expression in B lymphocytes is not required for prion neuroinvasion. *Nat. Med.* **4**, 1429–1433 (1998).
16. Roozendaal, R. *et al.* Conduits mediate transport of low-molecular-weight antigen to lymph node follicles. *Immunity* **30**, 264–276 (2009).
17. Martinez-Pomares, L. & Gordon, S. Antigen presentation the macrophage way. *Cell* **131**, 641–643 (2007).
18. Carrasco, Y. R. & Batista, F. D. B Cells Acquire Particulate Antigen in a Macrophage-Rich Area at the Boundary between the Follicle and the Subcapsular Sinus of the Lymph Node. *Immunity* **27**, 160–171 (2007).
19. Allen, C. D. C., Okada, T. & Cyster, J. G. Germinal-center organization and cellular dynamics. *Immunity* **27**, 190–202 (2007).

20. Hauser, A. E. *et al.* Definition of germinal-center B cell migration in vivo reveals predominant intrazonal circulation patterns. *Immunity* **26**, 655–667 (2007).
21. Schwickert, T. A. *et al.* In vivo imaging of germinal centres reveals a dynamic open structure. *Nature* **446**, 83–87 (2007).
22. Allen, C. D. C., Okada, T., Tang, H. L. & Cyster, J. G. Imaging of germinal center selection events during affinity maturation. *Science* **315**, 528–531 (2007).
23. Pittet, M. J. & Weissleder, R. Intravital Imaging. *Cell* **147**, 983–991 (2011).
24. Das, A., Zhao, J., Schatz, G. C., Sligar, S. G. & Van Duyne, R. P. Screening of type I and II drug binding to human cytochrome P450-3A4 in nanodiscs by localized surface plasmon resonance spectroscopy. *Anal. Chem.* **81**, 3754–3759 (2009).
25. Blanquet-Grossard, F., Thielens, N. M., Vendrely, C., Jamin, M. & Arlaud, G. J. Complement protein C1q recognizes a conformationally modified form of the prion protein. *Biochemistry* **44**, 4349–4356 (2005).
26. Homola, J. Surface plasmon resonance sensors for detection of chemical and biological species. *Chem. Rev.* **108**, 462–493 (2008).
27. Piliarik, M. & Homola, J. Surface plasmon resonance (SPR) sensors: approaching their limits? *Opt. Express* **17**, 16505–16517 (2009).